DISSERTATION

ORGANIC CARBON STORAGE IN MOUNTAIN RIVER VALLEY BOTTOMS OF THE WESTERN UNITED STATES

Submitted by

Daniel N. Scott

Department of Geosciences

In partial fulfillment of the requirements

For the Degree of Doctor of Philosophy

Colorado State University

Fort Collins, Colorado

Summer 2018

Doctoral Committee:

Advisor: Ellen Wohl

Tim Covino
Peter Nelson
Sara Rathburn

ABSTRACT

ORGANIC CARBON STORAGE IN MOUNTAIN RIVER VALLEY BOTTOMS OF THE WESTERN UNITED STATES

Valley bottoms, which include river channels and associated floodplains, are important components of the terrestrial carbon sink. Downed wood and floodplain soil in valley bottoms act as transient pools of organic carbon (OC) that can be stored for up to millennial timescales. This dissertation focuses on quantifying OC storage as downed wood and soil in mountain river valley bottoms in four disparate watersheds that span three mountain ranges across the western United States. Across these four basins, I measured wood load, floodplain OC content, morphologic metrics, and/or vegetation metrics at a total of 178 sites. I find that wood load is a function of metrics that relate to river corridor spatial heterogeneity and wood storage patterns (together determining wood trapping efficiency) at the reach scale and, at a broader spatial scale, wood supply. Wood in an undisturbed basin stores twice as much wood OC as a similar but extensively clearcut basin. In examining floodplain soil OC, I find that much of the variability in OC concentration is due to local factors, such as soil moisture, elevation (a proxy for temperature), and valley bottom geometry. From this, I conclude that local factors likely play a dominant role in regulating OC concentration in valley bottoms, and that inter-basin trends in climate or vegetation characteristics may not translate directly to trends in OC storage. I also use analysis of OC concentration and soil texture by depth to infer that OC is input to floodplain soils mainly by decaying vegetation, not overbank deposition of fine, OC-bearing sediment. Valley bottoms store significant OC stocks in floodplain soil and downed wood (ranging from 0

to 998 Mg C/ha) that vary with valley bottom form and geomorphic processes. Valley bottom morphology, soil retention, and vegetation dynamics determine partitioning of valley bottom OC between soil and wood, implying that modern biogeomorphic process and the legacy of past erosion regulate the modern distribution of OC in river networks. Soil burial is essential to preserving old OC, as measured by an extensive sample of 121 radiocarbon ages of floodplain soil OC. These radiocarbon data indicate a median residence time of floodplain soil OC of 185 yr BP. The age of the floodplain soil OC pool and the distribution of OC between wood and soil imply that OC storage in mountain rivers is sensitive over relatively short timescales to alterations in soil and wood retention, which may have both short- and long-term feedbacks with the distribution of OC between the land and atmosphere. Mountain river valley bottoms act as a high magnitude and moderately long-lasting pool of OC stored on land.

ACKNOWLEDGEMENTS

I thank my adviser, Ellen Wohl, for always being there to support me throughout this and the many side projects we've worked on over the last few years. Ellen's kind words and effective mentorship made this project possible and kept me on track throughout. Fieldwork for this project was long and grueling, but took me to some wonderful places. I am very grateful to Ellen Daugherty for accompanying me in the field and being a steadfast and loving partner. She has accompanied me through all the challenges and celebrations that define a dissertation, and I love her dearly. My father, David Scott, provided a home base for my fieldwork in Washington, and helped to raise me with the outdoor skills and passion for suffering in the jungles of the Northwest necessary to accomplish this fieldwork, for which I will be forever grateful.

Thanks to Katherine Lininger for the hours of discussion about statistics, carbon, and river processes that helped shape the methods and ideas presented here. Thanks to Sara Lowe for her capable handling of the major undertaking that was processing many of my soil samples. Thanks to Derek Schook, Natalie Kramer Anderson, Nick Sutfin, and the rest of the fluvial family for stimulating scientific discussions and providing a supportive working environment.

The Quileute Tribe and Olympic National Park graciously allowed me to perform this research on their lands. This work was generously funded by a National Geographic Society Young Explorer Grant and NSF grant EAR-1562713. The content presented here has benefitted greatly from constructive review by anonymous reviewers, Charles Luce, as well as my committee members Sara Rathburn, Tim Covino, and Peter Nelson.

This dissertation uses "I" and "my" to describe this work. This is solely a formality, and the credit for this work is rightfully shared by myself and Ellen Wohl.

DEDICATION

I dedicate this dissertation to my mother, Andrea Jo Scott, who died on May 29, 2016. Andrea raised me with an unending love of the mountains and wilderness, and that love is at the heart of all my research. I will carry the lessons and love she gave me in all my endeavors.

TABLE OF CONTENTS

LIST OF TABLES

LIST OF FIGURES

Chapter 1 : Introduction

Carbon cycling between the atmosphere, land, ocean, and bedrock is a first-order control on global climate. Understanding carbon partitioning and transport between these reservoirs is essential to constraining estimates of future climate and managing anthropogenic climate change. Approximately half of anthropogenic CO_2 emissions are sequestered in the oceans and on land (Aufdenkampe et al., 2011; Ballantyne et al., 2012), but the spatial distribution and behavior of the land carbon sink in particular remains poorly understood. Freshwater systems that store, transport, and process organic carbon (OC) from the terrestrial biosphere (biospheric OC) may account for much of the land carbon sink (Battin et al., 2008, 2009). Additionally, rivers, lakes, and reservoirs are a major focus of land management, including that aimed at sequestering carbon on land (e.g., Bullinger-Weber et al., 2014).

River systems actively transport, store, and process OC as it moves through the biosphere (Battin et al., 2008; Sutfin et al., 2016). After sequestration on land via primary production, OC enters streams primarily by the input of dead organic matter (e.g., litter, downed wood) or dissolved OC (DOC)-rich exudates (Blair and Leithold, 2014). OC can also enter river systems via the erosion of carbon-rich rock (Hilton et al., 2011). The primary reservoirs of OC within valley bottoms in terms of magnitude and residence time are downed wood and soil (Sutfin et al., 2016). Although OC can also be stored within in-channel or riparian biomass, I focus on OC stored in wood and floodplain soil as the dominant moderate- (10^2 yr) to long-term (10^3 yr) pools of OC in valley bottoms. I define valley bottom as the geomorphic feature consisting of floodplains and associated riparian forests, fluvial terraces that are near the active channel, and

the active channel, with a boundary defined by the transition between either the active channel, floodplains, or terraces and valley walls.

Once OC enters valley bottoms, it can either reside in wood or floodplain soils or move downstream via erosion. At any time, OC can be respired by microbes, returning to the atmosphere. Microbial respiration of OC to the atmosphere is generally suppressed at low temperatures in saturated environments (Falloon et al., 2011; Jobbágy and Jackson, 2000; Sutfin et al., 2016), which therefore favor preservation of OC. If OC is recalcitrant (e.g., bound to mineral grains), it can avoid respiration long enough to reach depositional features either within river systems (Mulholland and Elwood, 1982; Scott and Wohl, 2017) or off-shore (Leithold et al., 2016), where it may reside for long periods and represent a net transfer of carbon from the atmosphere to either the land or ocean. The ratio of OC respiration by microbial activity to delivery to long-term storage zones determines whether and to what degree river systems act as a source or sink of carbon to or from the atmosphere.

A warming climate is predicted to alter hydrology, disturbance regime, soil moisture and temperature dynamics that regulate microbial respiration, and erosion and sedimentation dynamics that regulate the storage and transport of OC in river corridors, especially in mountainous regions (IPCC, 2014). In addition, society continues to expand and develop mountain regions via natural resource extraction and urbanization. These activities are likely to influence the factors that control the substantial OC pool in river corridors (Sutfin et al., 2016; Sutfin and Wohl, 2017; Wohl et al., 2017a). As such, it is imperative to quantify the spatial distribution and controls on OC stored in mountain river valley bottoms to understand how to focus management on especially sensitive portions of river networks, what processes to manage, and how to predict response to climate change.

To address these issues, I quantified the spatial distribution of OC stored in downed wood and soil across the entirety of four watersheds in three disparate mountain ranges of the western United States. I also quantified the residence time of OC stored in soil in these basins to further understand the floodplain soil OC pool. These basins include the Sitkum and South Fork (SF) Calawah, in the Olympic Mountains of Washington, the Middle Fork (MF) Snoqualmie in the Central Cascade Range of Washington, and the Big Sandy in the Wind River Range of Wyoming. These basins represent a continuum of climate, vegetation characteristics, and tectonics. The Olympic Mountains are the wettest of the three ranges, and exhibit the densest vegetation and highest exhumation rates. In contrast, the Wind River Range is semi-arid, with sparse forests and parklands, and low exhumation rates. Between these two extremes, the Cascades exhibit a moderately high exhumation rate and dense forests, but not as much annual precipitation as the Olympics. I use my extensive field dataset from these contrasting basins to draw conclusions about the impact of inter-basin-scale processes on OC storage magnitude, mechanism, and residence time. By modeling OC variability within each basin, I also draw conclusions about the smaller scale, intra-basin processes that control OC dynamics.

In Chapter 2, I focus on wood loads (directly correlated to wood OC storage), and how wood loads vary throughout river networks. I use the Sitkum and SF Calawah as a paired basin study to evaluate the effects of logging on wood loads, because both basins are nearly identical except for the fact that the Sitkum has been extensively clearcut and the SF Calawah has been preserved from direct disturbance by being within Olympic National Park. Comparisons between basins with differing land use within the same climatic region (Sitkum and SF Calawah) and between basins in differing climates (MF Snoqualmie and Big Sandy) combined with multiple linear regression modeling of these data reveal that wood load is a function of metrics that

generally describe river corridor spatial heterogeneity, metrics that describe wood storage patterns, and metrics that relate to wood supply. From this, I generate a conceptual model of controls on wood load. The model suggests that spatial heterogeneity and wood storage pattern together determine wood trapping efficiency. Trapping efficiency in turn regulates how wood supply to the valley bottom determines wood load. I also find that wood in an undisturbed basin stores significant amounts of OC, and that wood load restoration has the potential to restore significant amounts of OC to valley bottoms. This conceptual model of wood load controls could be used as a framework to guide wood load modeling and restoration at multiple scales.

I follow my analysis of wood loads with an analysis of the other dominant OC storage mechanism in rivers, floodplain soil, in Chapter 3. I use my dataset to examine variability in OC concentration between my study basins as well as within them, at multiple spatial scales. I find that although there are some differences between basins, much of the variability in OC concentration is due to local factors, such as soil moisture and valley bottom geometry. From this, I conclude that local factors likely play a dominant role in regulating OC concentration in valley bottoms, and that inter-basin trends in climate or vegetation characteristics may not translate directly to trends in OC storage. I also use analysis of OC concentration and soil texture by depth to infer that OC is input to floodplain soils mainly by decaying vegetation, not overbank deposition of fine, OC-bearing sediment. This chapter concludes by showing how geomorphology and hydrology play strong roles in determining the spatial distribution of soil OC in mountain river corridors.

I then bring together data on OC storage in wood and soil in valley bottoms in Chapter 4 to show how geomorphology and climate interact to control OC stock and age in mountain river valley bottoms. I again compare four disparate mountain river basins to show that mountain river

valley bottoms store substantial OC stocks in floodplain soil and downed wood that vary with valley bottom form and geomorphic processes. I quantify soil OC radiocarbon age to show that soil burial is essential to preserving old OC. Valley bottom morphology, soil retention, and vegetation dynamics determine partitioning of valley bottom OC between soil and wood, implying that modern biogeomorphic process and the legacy of past erosion regulate the modern distribution of OC in river networks. The age of the floodplain soil OC pool and the distribution of OC between wood and soil imply that mountain rivers are highly sensitive to alterations in soil and wood retention, which may have both short- and long-term feedbacks with the distribution of OC between the land and atmosphere.

Finally, in Chapter 5 I conclude by summarizing the results of Chapters 2 through 4. I then discuss the major conclusions of this dissertation and important caveats that establish the limitations of those conclusions. I finish by discussing logical next steps to further my understanding of OC dynamics in river basins. I follow Chapter 5 with a short section (Appendix A) on my attempt to look for a signal of European settlement in soil OC content of floodplains on the Olympic Peninsula. Appendix A details a failed study, but the lessons learned and the data contained in that appendix may be of use in the future.

This dissertation consists of three papers (corresponding to Chapters 2-4) that are currently in revision or review. Chapter 2 is currently in revision at *Water Resources Research*. Chapter 3 is currently in review at *Earth Surface Dynamics*. Chapter 4 is currently in review at *Geophysical Research Letters*. Data for all three manuscripts can be found at the CSU Digital Repository.

Chapter 2 : Natural and Anthropogenic Controls on Wood Loads in River Corridors of the Rocky, Cascade, and Olympic Mountains, USA

2.1 Summary

Wood in rivers creates habitat, shapes the morphology of valley bottoms, and acts as a pool of organic carbon (OC). Effective riverine wood management depends on a robust understanding of the spatial distribution of wood throughout river networks. This motivates the analysis of wood load in relation to both reach- and basin-scale processes. I present wood load data coupled with precipitation, forest stand characteristic, land use, and geomorphic data across four basins in the Rocky, Cascade, and Olympic Mountains of the western USA. Comparisons between basins with differing land use within the same climatic region and between basins in differing climates combined with multiple linear regression modeling of intra-basin wood load variability reveal that wood load is a function of metrics that generally describe river corridor spatial heterogeneity, metrics that describe wood storage patterns, and, at a broader scale, metrics that relate to wood supply. From this, I generate a conceptual model to describe controls on wood load across spatial scales. I use this model to propose that spatial heterogeneity and wood storage pattern together determine reach-scale wood trapping efficiency. Trapping efficiency in turn regulates how wood supply to valley bottoms determines wood load. I also find that wood load restoration has the potential to restore significant amounts of OC to valley bottoms in the form of wood in a disturbed basin. This conceptual model of wood load controls may serve as a framework to guide wood load modeling and restoration at multiple scales.

2.2 Introduction

Wood accumulates in rivers via bank erosion and mass movements from hillsides. Because wood can remain stable in the channel and on floodplains, it plays a foundational role in shaping the ecology and geomorphology of valley bottoms. By providing colonization surfaces for periphyton and macroinvertebrates as well as a source of carbon, wood increases microhabitat diversity and provides energy input to macroinvertebrates (Benke and Wallace, 2003; Wondzell and Bisson, 2003). By shaping the location, abundance, and geometry of pools and altering bed texture (Gomi et al., 2003; Montgomery et al., 1996, 2003), wood can regulate habitat abundance and diversity for fishes (Jones et al., 2014; Nagayama et al., 2012). Wood in rivers also serves as a pool of organic material (Naiman et al., 1987; Osei et al., 2015; Sutfin et al., 2016), providing a source of organic matter as it breaks down and impacting terrestrial organic carbon (OC) cycling (Elosegi et al., 2007; Wohl et al., 2017a). The potentially substantial role of wood in storing OC motivates quantification of wood loads not only in terms of wood volume per unit area, but also as an estimated OC stock (mass per unit area).

Wood loads are a function of channel geometry, land use, bioclimatic regime, and geomorphic processes (Wohl et al., 2017b). Wood volume per unit length of stream or per unit area in the valley bottom typically correlates inversely with channel width and drainage area (Beechie and Sibley, 1997; Bilby and Ward, 1989, 1991; Wohl et al., 2017b), although this correlation has been observed to be direct in some cases and is strongly dependent on bioclimatic region and riparian forest characteristics (Burton et al., 2016; Wohl et al., 2017b). Wood loads have little consistent relation to channel characteristics across bioclimatic regions, but individual regions and watersheds do display significant trends, allowing wood load to be predicted by variables describing geomorphic, ecologic, and anthropogenic conditions (Hough-Snee et al.,

2015; Wohl et al., 2017b). While mechanisms influencing wood transport have been explored in flume environments (Bocchiola et al., 2006; Braudrick et al., 1997; Davidson et al., 2015), there is a lack of mechanistic understanding of the processes that influence wood loads in natural systems. Such a mechanistic understanding is necessary to explain differences between bioclimatic regions and explain wood load spatial distribution across scales. This motivates us to seek a mechanistic understanding of the controls on wood load across spatial scales.

By regulating storage pattern and mobility, wood jams are a potential mechanistic control on wood transport and wood load. Based on their relative rates of mobilization, wood jams are more stable than dispersed wood pieces within a given reach (Dixon and Sear, 2014; Ruiz-Villanueva et al., 2016; Wohl and Goode, 2008). However, wood jams are not uniformly distributed throughout river networks (Benda, 1990; Cadol et al., 2009; Marcus et al., 2002). This implies that the importance of wood jams and their impacts on wood transport vary with network position, likely due to differences in piece mobility, which is strongly regulated by stream size relative to the length of wood pieces (Gurnell et al., 2002; Kramer and Wohl, 2016). This motivates an analysis of the importance of jams in regulating wood loads relative to other variables that might impact wood loads.

Forest management, especially in the form of timber harvest, is one of the most widespread human impacts on forests in mountainous regions. Logging commonly impacts wood in valley bottoms by influencing both recruitment rates and the rate at which mass movements transfer wood from hillslopes to rivers. Logging and associated road-building increase the rate of mass wasting on steep slopes (Guthrie, 2002; Jakob, 2000; Roberts et al., 2004; Sidle et al., 2006; Wolter et al., 2010), potentially increasing the delivery of wood to floodplains and channels. However, the widespread wood removal and streamside harvesting of wood associated

with clearcutting in many regions has a net effect of strongly reducing wood loads and reducing wood trapping ability by reducing in-stream roughness (Hyatt & Naiman, 2001; Ruffing et al., 2015; Wohl, 2014). This loss of roughness can act as a negative feedback on wood storage, leading to high rates of wood export from the system even after riparian corridors have reforested (Bilby, 1984). The impact of logging on in-stream wood has been demonstrated dominantly through the loss of large wood pieces (Bilby and Ward, 1991; Ralph et al., 1994), which could reduce the occurrence of relatively stable wood jams. However, we lack a rigorous analysis of the effects of logging across entire river networks.

2.2.1 Objectives

Here, I seek to move towards a mechanistic and multi-scale understanding of the controls on wood loads by quantifying wood loads across a diverse set of mountain river basins and modeling relationships between those wood loads and the natural and anthropogenic (namely, logging) processes that impact them. To my knowledge, I provide the first field-based quantification of wood load across the entirety of my four study basins, allowing a rigorous examination of the intra-basin trends in wood load from headwaters to basin outlet. By quantifying wood loads and using published data on wood density and OC content, I also seek to apply my examination of wood load variability to variability in wood OC storage.

Previous broad-scale studies of wood load spatial variability (Hough-Snee et al., 2015; Wohl et al., 2017b) generally conclude that wood loads can be conceptualized at either broad (inter-basin) or local (intra-basin) scales by taking into account either bioclimatic or site-specific variables (e.g., land use, channel geometry), respectively. However, a conceptual model to describe wood load spatial distribution that applies at all scales has yet to be developed. I use my

extensive field dataset and statistical analyses to suggest that a single conceptual framework can be used to guide understanding of wood load spatial variability both within (intra-basin) and between (inter-basin) river basins.

I use statistical modeling of field-sampled wood load data from four mountain river basins in three distinct regions across the western USA to determine the dominant controls on wood load both within each basin (intra-basin) and between basins (inter-basins). By taking into account wood supply and mechanistic variables relating to reach-scale wood trapping efficiency, I develop a novel conceptual understanding of wood load spatial variability that applies to multiple scales. This conceptual model explains my results and provides a basis for further testing of multi-scale controls on wood load spatial distribution in river networks.

2.3 Methods

2.3.1 Field Sites

My choice of study basins maximizes variability within the western United States in factors that may influence wood loads (forest stand characteristics, valley morphology, climate, etc.), allowing for a robust analysis of wood load spatial variability. I quantified basin-scale wood load in the Big Sandy basin in the Wind River Range of Wyoming, the Middle Fork (MF) Snoqualmie basin in the central Cascade Mountains of Washington, and the Sitkum and South Fork (SF) Calawah River basins in the Olympic Mountains of Washington (Figure 2-1). These basins represent three distinct bioclimatic and geomorphologic regions, ranging from the semi-arid Middle Rockies to the wet, glacially influenced Cascades and more fluvially dominated basins in the Olympics.

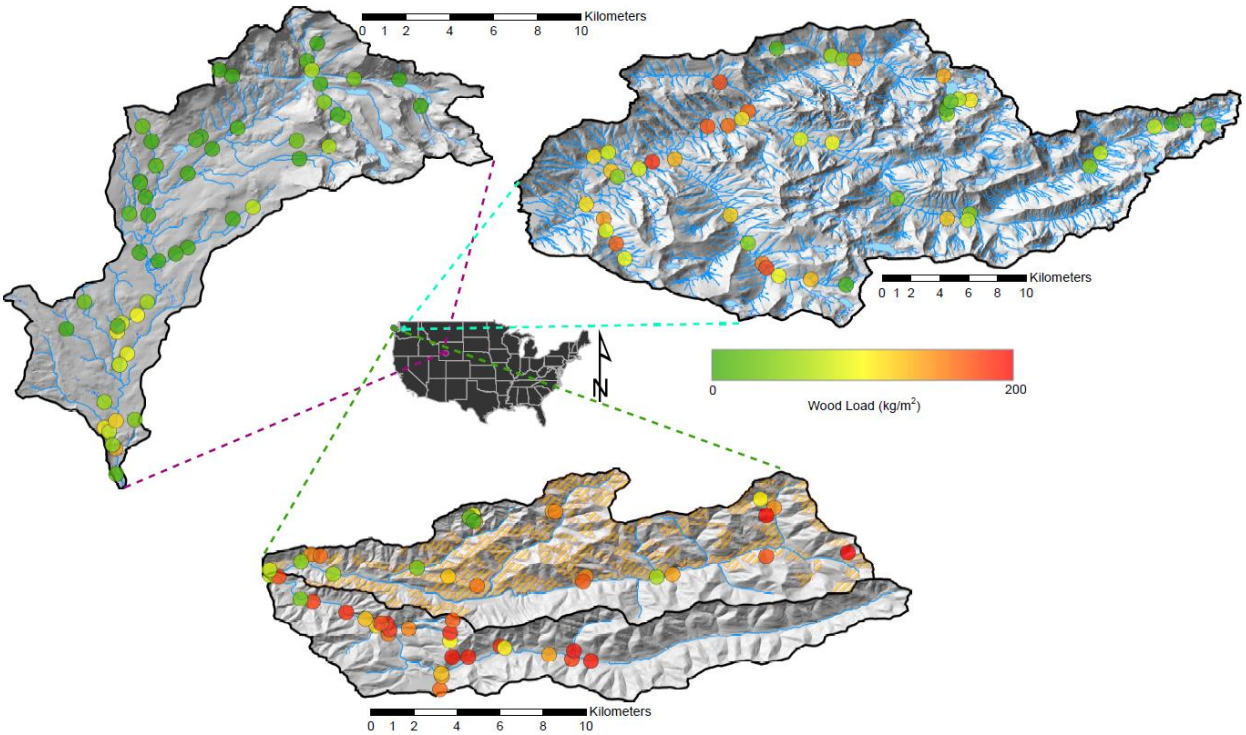

Figure 2-1: Map showing the location, topography, sampling sites, and stream network of the sampled basins. Clockwise, from upper left: Big Sandy watersheds, Wyoming; MF Snoqualmie watersheds, Washington; Sitkum (north) and SF Calawah (south) watersheds, Washington. Circles represent sampling locations at which wood loads were measured. The orange overlay in the Sitkum basin represents areas that have experienced recorded clearcut timber harvest. Sample sites are colored by wood load.

Mean annual precipitation, relief, drainage area, and mean basin slope for each study basin are given in Table 2-1. I performed a paired basin study using the Sitkum and SF Calawah basins to examine the effects of basin-wide clearcut timber harvest. These two basins are of similar network geometry (Figure 2-1) and are both underlain by marine sedimentary rocks (Gerstel & Lingley Jr., 2000). Forests in both basins are dominated by Douglas fir (*Pseudotsuga menziesii*), Sitka spruce (*Picea sitchensis*) and western hemlock (*Tsuga heterophylla*). The SF Calawah lies entirely within the boundary of Olympic National Park and has not experienced forest harvest or road building, in contrast to the Sitkum, which has been clearcut extensively since the 1940s (orange overlay in Figure 2-1). Road building and clearcut timber harvest were

widespread in the Sitkum until the 1990s, with 15 m (50 ft) riparian buffers being implemented on many reaches in 1975. Currently, forests are dominantly being thinned and roads are being decommissioned to enhance forest habitat and reduce mass movement frequency. The result of this land use has been the loss of large trees able to be recruited to streams by bank and hillslope failure (Pacific District Olympic National Forest, 2012). These basins provide a nearly ideal field setting in which to evaluate the effects of basin-wide clearcutting on wood loads.

Table 2-1: Characteristics of study basins. Mean annual precipitation data are from PRISM (Oregon State University, 2004). Relief, drainage area, and mean basin slope are calculated from a 10 m DEM.

Basin	Mean Annual Precipitation (m)	Relief (m)	Drainage Area (km^2)	Mean Basin Slope (%)
Sitkum	3.61	1024	112	49
SF Calawah	3.67	1024	85	45
MF Snoqualmie	3.04	2079	407	60
Big Sandy	0.72	1630	114	25

I also present data from the MF Snoqualmie and Big Sandy Rivers. The MF Snoqualmie exhibits glaciogenic topography, with streams ranging from steep, debris flow dominated headwater channels to lower gradient, wide, laterally unconfined channels in its lower reaches, and has been extensively logged in its lower elevation reaches. The elevation range in the MF Snoqualmie generates a strong vegetation gradient. The talus, active glaciers, and alpine tundra at the highest elevations grade to subalpine forests dominated by mountain hemlock (*Tsuga mertensiana*) (above approximately 1500 m), but also including Pacific silver fir (*Abies amabalis*) and noble fir (*Abies procera*) grading into the montane zone (above approximately 900 m). At lower elevations, uplands and terraces are covered by Douglas fir (*Pseudotsuga menziesii*) and western hemlock (*Tsuga heterophylla*), whereas active riparian zones are dominated by red alder (*Alnus rubra*) and bigleaf maple (*Acer macrophyllum*).

The Big Sandy also exhibits glaciogenic topography, but is much drier than the MF Snoqualmie. While higher elevations (above approximately 3100 m) are characterized by herbaceous alpine tundra, the subalpine zone (approximately 2900 to 3100 m) is characterized by forests of whitebark pine (*Pinus albicaulis*), Engelmann spruce (*Picea engelmannii*), and subalpine fir (*Abies lasiocarpa*). The montane zone (approximately 2600 m to 2900 m) is comprised dominantly of lodgepole pine (*Pinus contorta*). Only a small portion of this basin (approximately 1%) resides below 2500 m, where shrub steppe begins to dominate (Fall, 1994). Forests in this basin are patchy, with substantial grassy parklands and meadows. Comparing this basin to the MF Snoqualmie, SF Calawah, and Sitkum provides bioclimatic contrast that allows us to examine wood load trends across a range of stream morphologies in regions with differing precipitation, forest characteristics, and network structure.

2.3.2 Study Design and Sampling

I sampled basins in summer 2016 (Sitkum, SF Calawah, and Big Sandy) and summer 2017 (MF Snoqualmie). Sampling during the summer ensured that there were no large, wood-transporting floods during sampling, such that my data represent an estimate of the wood load in each basin at a single time. I collected a total of 148 reach-scale (each reach is 100 m or 10 channel widths long, whichever was shorter) samples of valley bottom wood load across all four study basins.

I used stratified random sampling to generate an unbiased sample of wood load measurement sites in each basin. My sampling objective in the Olympics was to sample uniformly across stream orders (Strahler, 1957) in order to sample a relatively even distribution of channel and valley widths. Because of the sparser vegetation in the Big Sandy basin, I found

that I could gather information about the stream network by analyzing satellite imagery. I used a combination of a 10 m DEM and satellite imagery to manually map the extent of the valley bottom along the entire stream network, with the objective of delineating confined and unconfined valley sections. I defined unconfined valley bottoms as those in which channel width occupied no more than half the valley bottom, and confined valley bottoms as those in which channel width occupied greater than half the valley bottom. I then stratified the stream network by five drainage area classes to ensure uniform sampling throughout the basin. This produced two stratifications, one of drainage area and the other of confinement. I stratified the MF Snoqualmie stream network by slope into four strata. I chose to not measure wood loads in parts of the network steeper than 0.30 m/m as classified by a 10 m DEM, although field-based measurements indicated that some study sites were steeper than this threshold. Within each slope strata, I randomly selected ten reaches for sampling wood load.

In all four basins, but especially in the Sitkum and SF Calawah, I was unable to reach all randomly sampled sites due to time constraints. This resulted in the subjective selection of sites that were accessible and that I felt maintained as unbiased a sample as possible. Total numbers of sites and the proportion of sites that were subjectively chosen are listed in Table 2-2.

Table 2-2: Matrix of variables measured in each basin. Variables in italics are relevant response variables for comparisons or models presented in this study. Grey shading indicates the variable was measured, while a blank cell indicates that it was not measured. Basin slope refers to the slope of hillsides and channels upstream of the study reach. Note that for the Sitkum and SF Calawah, valley width is equivalent to bankfull width. Derivative variables (e.g., proportion of wood stored in jams) or those that are used to calculate variables included here (e.g., piece diameter and length) are not shown, but were calculated for all basins for which data were available. Note that 24 samples were measured in the Sitkum and 26 in the SF Calawah.

Basin:		MF Snoqualmie	Big Sandy	Sitkum & SF Calawah
Variables Measured	*Wood Load*			
	Jam Density			
	Confinement			
	Bedform			
	Channel Slope			
	Bed Material			
	Multithread			
	Valley Width			
	Bankfull Width			
	Bankfull Depth			
	Stream Power			
	Elevation			
	Basin Slope			
	Canopy Cover			
	NLCD			
	Drainage Area			
Total Sample Sites:		46	52	50
% Sites Subjectively Chosen:		17	8	32

2.3.3 Reach-Scale Field Measurements

Table 2-2 summarizes which measurements were collected in each basin. Within each reach, I quantified wood volume in wood jams (accumulations of 3 or more pieces touching one another) using a census approach, measuring the length, width, and height of a rectangular prism that best fit the jam (i.e., these geometric measurements did not correspond to flow direction) and visually estimating the porosity. Although this method is not as accurate as dismantling jams to measure every wood piece (e.g., Manners et al., 2007), my consistency in this method (i.e., only a single person made all estimates using consistent methodology) likely minimizes systematic bias. Within each reach, I quantified wood volume in dispersed pieces greater than 10 cm diameter using a combination of two methods, depending on the nature of wood within the reach and channel confinement. For confined valleys with numerous wood pieces dominantly oriented perpendicular to the valley axis, I used an adapted form of a line-intersect sampling strategy (Van Wagner, 1968; Wallace and Benke, 1984) whereby the line was fit to the channel centerline (Warren et al., 2008). I measured the diameter of every wood piece intersected by the line, then calculated wood volume using the formula given by Van Wagner (1968). For unconfined reaches with sufficiently low wood piece abundance, I measured the diameter and length of each wood piece in the reach, calculating piece volume as if each piece was a cylinder. In the MF Snoqualmie, some unconfined floodplains were wide enough that a census of pieces and jams was impractical, so I performed a census within the channel, then performed a single line intersect transect across the floodplain perpendicular to the valley axis to quantify floodplain wood load (Van Wagner, 1968).

I assigned a decay class to each reach that describes all the pieces and jams in each reach using the visual decay classification of Harmon et al. (2011). This allowed us to estimate an

average wood density using the downed dead softwood densities for each decay class listed in Table 5 of Harmon et al. (2011). With an average wood density and volume per reach, I calculated wood mass as the product of density and volume. I used the length of each reach and the valley bottom width to compute a wood mass per unit area of valley bottom.

At each reach, I measured channel geometry and other characteristics using a TruPulse 360 laser rangefinder (Scott et al., 2016), although my measurements were not consistent across all basins because field protocol evolved during the course of the study (Table 2-2). In the MF Snoqualmie, I categorized channels by planform and dominant bedform (Montgomery and Buffington, 1997). I defined planforms as either: straight, where the channel was generally confined and significant lateral migration was not evident; meandering, where lateral migration was evident but only a single channel existed; anastomosing, where vegetated islands separate multiple channels; and anabranching, where a single dominant channel existed with relict channels separated by vegetated islands. For the purposes of statistical modeling, I also classified channels as being either multithread (anastomosing or anabranching) or single thread (straight or meandering). Because logging records are inconsistent and likely inaccurate in the MF Snoqualmie (based on the frequent observation of past logging activity where none was recorded in Forest Service records), I noted whether signs of logging, such as cut stumps, cable, decommissioned roads or railroads, or other logging-associated tools were found near the reach. I also looked for forest stand characteristics that commonly result from clearcut logging: even-aged stands, monocultures, and a lack of undergrowth compared to unlogged forests. These observations, and my resulting classification of reaches as being logged or unlogged, are limited to the forests immediately surrounding the reach.

2.3.4 GIS and Derivative Measurements

A 10 m DEM was utilized for all GIS topographic measurements. I collected the following data for each reach using a GIS platform: elevation, drainage area, land cover classification and canopy cover from the National Land Cover Database (Homer et al., 2015), and the mean slope of the basin upstream of each reach. Utilizing drainage area and field-measured slope at each reach, I calculated an estimated stream power as the product of drainage area, slope, and basin-averaged precipitation.

I calculated a wood jam density to measure the abundance of wood jams in each reach as the number of jams divided by the length of each reach. Following Kramer and Wohl (2016), I calculated a dimensionless maximum piece length for each reach (L^*) as the maximum piece length in the reach divided by the bankfull width, for all reaches except those in the Big Sandy, where bankfull width was not measured. All wood masses were normalized by unit area using the average valley width and length of each reach. For purposes of estimating OC storage in wood, I assumed that half of the measured wood mass was carbon (Lamlom and Savidge, 2003). Variability in wood OC content ranges from 47.21% to 55.2% for conifers (Lamlom and Savidge, 2003), the dominant division of trees present in my study basins. As such, an assumption of 50% OC content is likely a conservative estimate of actual OC content and is a suitable approximation for making first-order estimations of wood OC stock (e.g., Sutfin et al., 2016; Wohl et al., 2012).

2.3.5 Statistical Analyses

All statistical analyses were performed using the R statistical computing software (R Core Team, 2017). Due to differences in variables measured for each region, I conducted

modeling based on model groups with consistent measurements. I modeled wood load in the MF Snoqualmie (sample size, n = 46) and Big Sandy (n = 52) basins individually as well as across both the Sitkum and SF Calawah (n = 50). Because of the lack of variation in hypothesized predictor variables in other basins, I only modeled the proportion of wood in jams in the MF Snoqualmie basin. I note that although this modeling predicts wood load as a mass per unit area, I observe a Pearson correlation coefficient with a 95% confidence interval between 0.98 and 0.99 between wood mass per unit area and wood volume per unit area. I also tested each final model using wood volume as a predictor to ensure that results reported here are equally applicable to wood volume and wood mass.

My modeling strategy starts with univariate analysis between each hypothesized predictor and the response, utilizing mainly comparative Wilcoxon rank-sum tests (Wilcoxon, 1945) or Spearman correlation coefficient statistics. During this filtering, I also view boxplots or scatterplots as appropriate to discern which variables appear to have anything other than a completely random relationship with the response. I then utilize all subsets multiple linear (for wood load) or multiple logistic (for the proportion of wood stored in jams) regression using the corrected Akaike Information Criterion as a model selection criteria (Wagenmakers and Farrell, 2004). I iteratively transform response variables to ensure homoscedasticity of error terms. When selecting a single best model, I utilize both Akaike weight based importance as well as parsimony to select a final, reduced model. I consider sample sizes, p values, and effect magnitudes (odds ratios for logistic regression and slope coefficients for linear regression) in my discussion of variable importance. All other statistical analyses presented here are comparative statistics utilizing Wilcoxon rank-sum tests or pairwise equivalent using a Holm multiple-comparison correction (Holm, 1979) to accommodate generally skewed distributions. Unless

otherwise noted, I present 95% confidence intervals to represent variance on population estimates.

2.4 Results

2.4.1 Controls on Wood Load

Median wood load is significantly different between all study basins except for the MF Snoqualmie and Sitkum basins (Figure 2-2, Table 2-3). Wood load is highest in the SF Calawah, followed by the MF Snoqualmie and Sitkum basins, followed by the Big Sandy basin. Distributions of wood loads are generally right skewed with multiple high wood load outliers, especially in basins in the Olympics. For the entire dataset of wood load in each basin, including decay classes used to estimate wood density, see Scott and Wohl (2018). Trends in wood volume between basins track very similarly to those in wood mass (Figure 2-3).

Table 2-4 shows the variables tested and a summary of results for each model. In general, variables related to wood recruitment and variables related to reach-scale wood trapping efficiency are significant predictors of wood load.

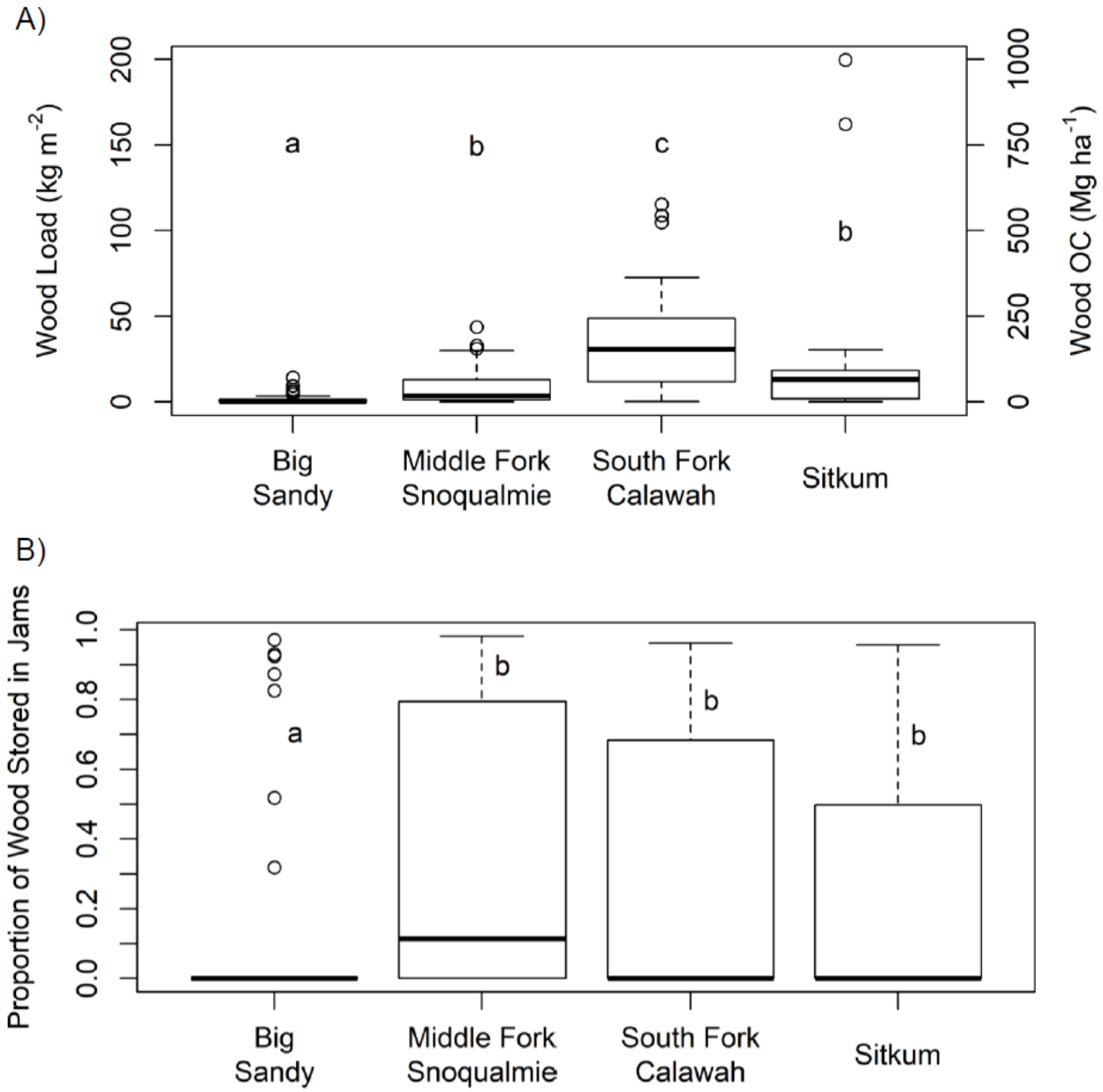

Figure 2-2: Boxplot of wood load and OC storage in wood (A) and the proportion of wood stored in jams (B) by study basin. Bold line represents median. Box top and bottom represent 75th and 25th percentile, respectively. Ends of dashed lines represent 1.5 times the interquartile range. Circles represent outliers. Letters show significantly different groups at a 95% confidence level. Data shown here are summarized in Table 2-3, and translated to wood volume for comparison in Figure 2-3.

Table 2-3: Wood loads and proportion of wood stored in jams for study basins. A) P values for pairwise Wilcoxon rank-sum tests of wood load in each basin (identical for wood OC storage) and the proportion of wood stored in jams. B) P values for pairwise Wilcoxon rank-sum tests of wood load in each basin (identical for wood OC storage) and the proportion of wood stored in jams.

A)

	Big Sandy		Middle Fork Snoqualmie		South Fork Calawah	
	wood load	proportion in jams	wood load	proportion in jams	wood load	proportion in jams
Middle Fork Snoqualmie	< 0.0001	<0.0001				
South Fork Calawah	< 0.0001	0.02	< 0.0001	0.78		
Sitkum	< 0.0001	0.05	0.105	0.58	0.013	0.78

B)

	Big Sandy	**Middle Fork Snoqualmie**	**South Fork Calawah**	**Sitkum**
Median Wood Load ($kg\ m^{-2}$)	0.04 (0.00, 0.50)	3.38 (1.71, 9.23)	30.02 (13.48, 45.91)	13.02 (2.11, 16.14)
Median Wood OC ($Mg\ ha^{-1}$)	0.2 (0.00, 2.52)	16.92 (8.55, 46.13)	152.65 (67.40, 229.54)	65.08 (10.53, 80.68)
Median Proportion of Wood Stored in Jams	0.00 (0.00, 0.00)	0.11 (0.00, 0.56)	0.00 (0.00, 0.68)	0.00 (0.00, 0.48)

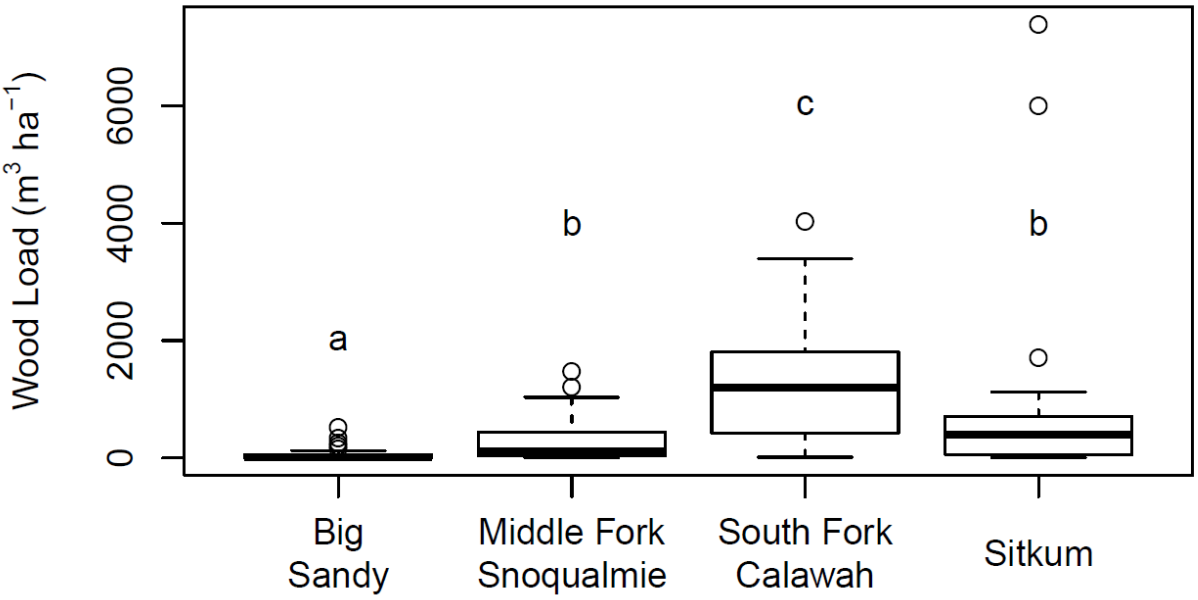

Figure 2-3: Boxplot showing volumetric wood load in each basin. Box top and bottom represent 75th and 25th percentile, respectively. Ends of dashed lines represent 1.5 times the interquartile range. Circles represent outliers. Letters show significantly different groups at a 95% confidence level.

Table 2-4: Matrix of all models presented in text. For each variable and model, grey fill indicates that the variable was included in model selection. A minus (−) indicates that the variable was selected as important in predicting the response, and denotes an indirect correlation, while a plus (+) indicates a direct correlation. In the case of confinement, a negative indicates that unconfined streams display a lower wood load. In the case of multithread channels, a plus indicates that multithread channels were more likely to store wood in jams. NA indicates that the variable is not applicable as a predictor for the model. Note that for the Sitkum and SF Calawah, valley width is equivalent to bankfull width.

Model:		MF Snoqualmie Wood Load	MF Snoqualmie Proportion of Wood in Jams	Big Sandy Wood Load	Sitkum & SF Calawah Wood Load
Variable:	Jam Density	+	NA	+	+
	Confinement	−		−	
	Bedform			NA	NA
	Channel Slope				+
	Bed Material			NA	NA
	Multithread		+	NA	NA
	Valley Width				
	Bankfull Width			NA	NA
	Bankfull Depth		+	NA	NA
	Stream Power				
	Elevation	−		−	
	Basin Slope				
	Canopy Cover				
	NLCD				
	Drainage Area				
	Median Piece Length				
	Median Piece Diameter				
	Max Piece Length				
	Max Piece Diameter				
	L*				
	Logging	NA	NA	NA	−

Multiple linear regression modeling of wood mass per unit area in the MF Snoqualmie study basin reveal jam density (number of jams per meter), elevation, estimated stream power, and confinement to be significant controls on wood load (adjusted $R^2 = 0.40$, $p < 0.0001$). For this model, a cube root transformation (to accommodate 0 values) is found to be appropriate, so all slope coefficients relate to a unit increase in the cube root of wood load. I note that the cube root of wood load, while uninterpretable in itself, is likely analogous to a wood length per unit area, if mass and volume are taken to be highly correlated (which they are in my data, see section 2.2.5) A higher jam density (units of jams/m stream, $\beta = 9.04 \pm 8.16$) and higher estimated stream power (units of m^3, $\beta = 2.13 \text{ X } 10^{-8} \pm 2.06 \text{ X } 10^{-8}$) result in higher wood loads, whereas higher elevations result in lower wood loads (units of m, $\beta = -1.20 \text{ X } 10^{-3} \pm 7.38 \text{ X } 10^{-4}$). Unconfined streams are found to generally store less wood ($\beta = -.48 \pm 0.44$); all other predictors held constant. I note that the effect (β) of stream power on wood load is extremely small, despite its significance in the model. From this, I conclude that although stream power likely has some relation to wood load, its effect is so much smaller than other controls that it is negligible.

Similarly, in the Big Sandy study basin, jam density, elevation, and confinement in addition to median piece length are found to be significant predictors of wood load (adjusted $R^2 = 0.77$, $p < 0.0001$). However, I find that piece length and confinement were strongly related, leading to multicollinearity in any model including both variables. Comparing models similar to the above model but with either confinement (adjusted $R^2 = 0.59$, $p < 0.0001$) or piece length (adjusted $R^2 = 0.71$, $p < 0.0001$) removed, the model that includes confinement explains much more of the variance in wood load. As such, I conclude that confinement is likely the dominant control on wood load over piece length, and eliminate piece length from the final model. Thus, my final model of wood load in the Big Sandy includes only jam density, elevation, and

confinement as significant predictors of the cube root of wood load. Reaches with higher jam densities (units of jams/m, $\beta = 14.38 \pm 6.94$) and lower elevations tend to store more wood (units of m, $\beta = -0.0012 \pm 0.00048$). Like the MF Snoqualmie, unconfined reaches store significantly less wood than confined reaches ($\beta = -0.74 \pm 0.20$).

The Sitkum contains half as much wood as the SF Calawah, likely due to logging (section 3.1.1). After accounting for logging, channel slope and jam density are significant predictors of the cube root of wood load (adjusted $R^2 = 0.34$, $p < 0.0001$) in these basins. Reaches with higher channel slope (units of m/m, $\beta = 2.66 \pm 0.62$) and more jams tend to store more wood (units of jams/m, $\beta = 19.13 \pm 1.63$).

In summary, I find that jam density, elevation, and confinement in the MF Snoqualmie and Big Sandy; and logging, slope, and jam density in the Sitkum and SF Calawah control wood load.

2.4.1.1 Effects of Logging on Wood Loads

Comparing the Sitkum (extensively clearcut) to the SF Calawah (relatively pristine), I find that wood loads are a factor of 2 greater in the SF Calawah (Figure 2, Table S1). Other variables such as bankfull width, slope, wood jam density per unit stream length, median and maximum piece length and diameter do not significantly differ between basins (p values for comparisons are 0.70, 0.24, 0.47, 0.26, 0.19, 0.43, 0.70, respectively). I do note maximum piece diameter may be lower in the Sitkum, and that I may lack the sample size to note this effect. The only factor that is significantly different between basins is elevation, which is significantly higher in the Sitkum ($p < 0.001$). However, I note that elevation was not found, either through univariate analysis ($p = 0.56$) or model selection, to be a meaningful predictor of wood load

when modeling controls on wood load across samples in both the Sitkum and SF Calawah, likely due to the lack of variation in forest stand characteristics with elevation in these basins.

Because historic logging records are largely inaccurate in the MF Snoqualmie, I use my observational mapping of logging to understand logging extent and attempt to understand how variation in logging impacted wood load. I find that with very few exceptions, all sites at low elevations experienced some form of timber harvest, likely within the last century. When considering all sampled reaches in the basin in a univariate analysis, I find that sites with logging apparently contain more wood than sites with no logging nearby ($p = 0.04$). However, I also find that logging is strongly correlated with elevation, such that the median elevation of logged sites ($446\,^{+71}_{-119}$ m) is less than half that of unlogged sites ($989\,^{+173}_{-66}$ m). Elevation is a significant predictor of wood load in this basin due to the high range of elevation and forest types. This suggests that the correlation between local logging activity at a reach and enhanced wood loads in this basin is spurious, and that local impacts of logging cannot be evaluated here.

Smithwick et al. (2002) measured potential carbon stores in forests of the Pacific Northwest, including the Washington Cascades and Olympic Mountains. I utilize measurements of downed log OC mass per unit area from Smithwick et al. (2002) to compare my measured wood loads in Washington to upland downed wood loads so as to examine both how fluvial wood storage compares to upland downed wood storage and how logging affects that comparison (Figure 2-4). I find that the two logged basins likely do not store more wood than their corresponding uplands, whereas the SF Calawah may store more wood than nearby uplands.

In summary, logging has significantly decreased wood loads in the Sitkum compared to the SF Calawah. Although logging has likely had a similar effect on the MF Snoqualmie, I cannot evaluate the local effects of logging on that basin.

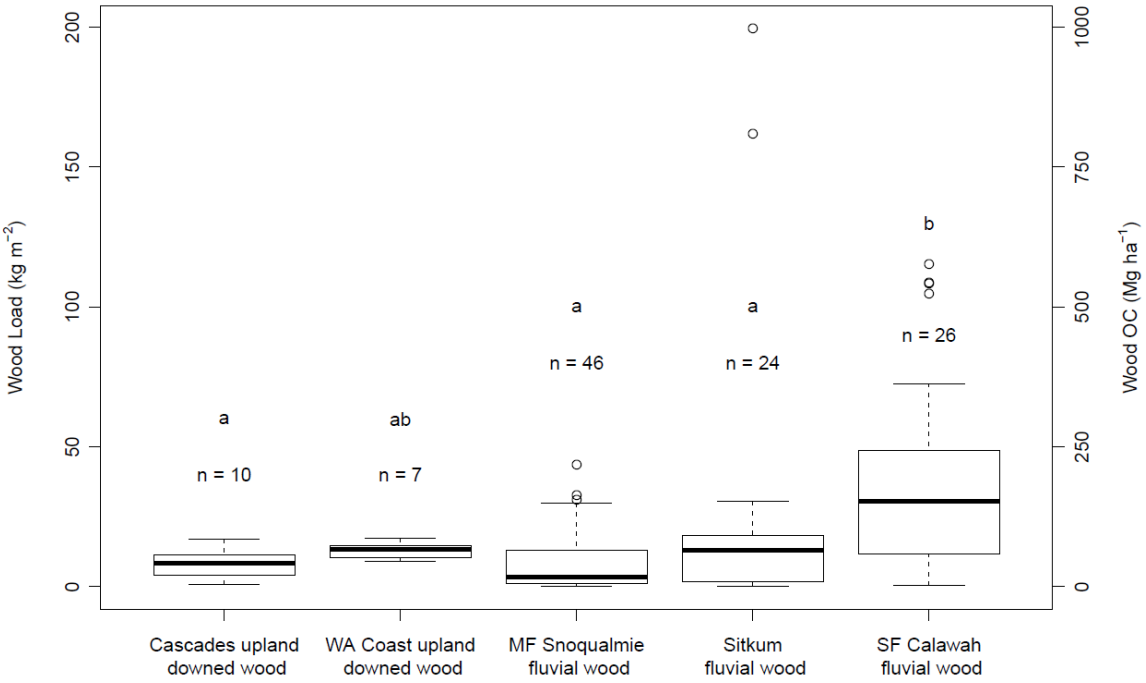

Figure 2-4: Comparison of Pacific Northwest basins valley bottom wood load with upland measurements of coarse downed wood. Box top and bottom represent 75th and 25th percentile, respectively. Ends of dashed lines represent 1.5 times the interquartile range. Circles represent outliers. Letters represent groups that are significantly different at a 95% confidence level, and n values represent sample size.

2.4.2 Controls on the Proportion of Wood Stored in Jams

Despite wood jam density being a significant predictor in models of wood load, median proportions of wood stored in jams for each basin are all well below 50% (Figure 2, Table S1). While some reaches store almost all wood as jams, wood is generally not stored as jams in these dominantly small- to moderate-drainage area study reaches.

Multiple logistic regression modeling in the MF Snoqualmie basin yields bankfull depth and whether the reach is multithread (a measure of spatial heterogeneity) as significant predictors of the proportion of wood in jams. Multithread channels are significantly more likely than single thread channels to store wood as jams (wood is 1.05 to 23.16 times more likely to be stored in a jam if the reach is multithread) and deeper channels tend to store more wood as jams than shallower channels (wood is 0.94 to 6.12 times more likely to be stored in a jam for every 1 m increase in bankfull depth).

In summary, I find that bankfull depth and channel planform control the proportion of wood stored in jams in the MF Snoqualmie.

2.5 Discussion

2.5.1 Basin-Scale Comparisons and the Impacts of Logging on Wood Load

I compare wood loads between basins to examine inter-basin scale influences on wood load such as climate and land use. Differences in wood loads between basins (Figure 2-2 A) can be largely explained by differences in precipitation and land use that result in differing forest stand characteristics. The Big Sandy, with the lowest wood loads, has the correspondingly lowest precipitation and canopy cover ($p < 0.0001$ for comparisons with all other basins). Mean canopy cover in the Big Sandy is 27% ± 4%, whereas mean canopy cover in the MF Snoqualmie, SF Calawah, and Sitkum are 65% ± 5%, 73% ± 6%, and 72% ± 6%, respectively (uncertainty from a 95% confidence interval on the mean). This likely indicates, and field observations support, that forests in the Big Sandy are less dense, trees are smaller, and the resulting supply of wood to the channel is lower.

Although the mean slope of the basin upstream of each reach is not a mechanistic predictor of hillslope instability, the Big Sandy also has, on average, the lowest upstream basin slopes compared to basins in the Pacific Northwest ($p < 0.0001$ for comparisons with all other basins). This indicates that landslides that could deliver large pulses of logs to channels are likely much less frequent in the Big Sandy compared to the Pacific Northwest. This is consistent with estimates of upstream basin mean slope in the Big Sandy being 17° ± 2°, whereas upstream basin slopes in other basins generally hover around 30° (29° ± 1° in the MF Snoqualmie, 31° ± 2° in the Sitkum, and 29° ± 1° in the SF Calawah). Assuming that a hillslope angle of around 30° is a threshold at which landslides become significantly more frequent (Clarke and Burbank, 2010; Larsen and Montgomery, 2012), this indicates that basins in the Pacific Northwest are likely experiencing relatively frequent landslides that potentially input large pulses of logs to valley bottoms (Benda et al., 2003b; Benda and Bigelow, 2014). In addition to the significantly denser forests and larger logs, the likelihood of more pulsed inputs to channels in the Pacific Northwest probably explains higher wood loads. Although the Big Sandy has a lower wood jam density than all other basins ($p = 0.03$ compared to Sitkum, 0.005 for SF Calawah, and <0.0001 for MF Snoqualmie), it is unclear whether jams are simply less likely to form or whether lack of jams is a result of lower wood loads, which is driven more by the lower supply of riparian trees to the channel.

Logging, in addition to climate, acts as an inter-basin scale control on wood load. Comparing the three study basins in the Pacific Northwest, the SF Calawah exhibits a significantly higher wood load than the logged MF Snoqualmie or Sitkum. The MF Snoqualmie exhibits much wider valley bottoms and larger drainage area than basins in the Olympics, potentially confounding comparison. However, even when I restrict this comparison to reaches

with drainage areas lower than the maximum drainage area sampled in the SF Calawah (eliminating reaches with high drainage area and wide valley bottoms from the MF Snoqualmie), the SF Calawah still exhibits significantly higher wood loads than the MF Snoqualmie ($p < 0.0001$) and likely higher wood loads than the Sitkum ($p = 0.06$). This indicates that logging (as opposed to valley morphology) is the dominant cause of reduced wood loads in the MF Snoqualmie and Sitkum, both of which exhibit statistically similar wood loads. Considering the similar precipitation and forest stand characteristics throughout most of the basins (the exception being the subalpine and alpine zones of the MF Snoqualmie), and the observation that both are extensively logged, it seems that wood loads in the Sitkum and MF Snoqualmie are likely lower as a direct result of logging.

I can use comparisons between the three basins in the Pacific Northwest to identify likely mechanisms by which logging has reduced wood loads. Logging impacts the supply of wood to the channel, potentially increasing the probability of landslides that could deliver wood (Guthrie, 2002; Jakob, 2000; Roberts et al., 2004; Sidle et al., 2006; Wolter et al., 2010), but generally reducing the quantity and size of trees available to be recruited to the stream, especially in the absence of riparian buffers (Bilby and Ward, 1991; Ralph et al., 1994). It also impacts in-channel and floodplain roughness if wood is removed or if streams are cleared for tie-drives. This reduction in macro-scale roughness may reduce wood loads by decreasing the ability of a reach to trap wood (Hyatt & Naiman, 2001; Ruffing et al., 2015; Wohl, 2014). Comparing wood sizes in the Sitkum and SF Calawah, there are no significant differences in median ($p = 0.43$) or maximum ($p = 0.70$) piece diameter, or median ($p = 0.26$) or maximum ($p = 0.19$) piece length, all of which could potentially relate to wood trapping efficiency. However, the Sitkum consistently has a lower (albeit insignificantly different) estimated median piece size and the

possibility remains that wood pieces in the Sitkum may be smaller than the SF Calawah. I suspect that the combined effect of clearcut harvesting reducing hillslope wood loads and harvest in the riparian zone reducing the supply of wood to the channel results in lower wood loads. There is no evidence to suggest that log drives occurred in the Sitkum, so logging probably did not directly affect in-channel roughness. Jam density and the proportion of wood stored in jams does not significantly differ between basins, suggesting that logging has not had a direct impact on the storage patterns of wood in these rivers. Compared to a compilation of the impacts of logging on wood loads, my results indicate a similar reduction in wood load to what has previously been observed in northern wet conifer forests (Wohl et al., 2017b). Notably, my study examines the entirety of two otherwise nearly identical basins, lending increased rigor to my comparison relative to past studies.

2.5.2 Controls on Wood Load

My methodology in each basin differed, making generalization of these results difficult. However, I can draw general conclusions across all basins by considering likely explanations for observed intra-basin variability in wood load.

Jam density clearly controls wood load across all basins, despite the proportion of wood stored in jams being significantly less than half in all basins. This indicates that despite their relatively small proportion of storage, wood jams play a disproportionately large role in determining total wood storage within a reach. This may be due to both the structure of wood jams and their impacts on reach-scale wood mobility. Wood jams are hypothesized to have significant effects on the mobility of wood pieces in transport, provided that those pieces are in transport around relatively stable wood jams (Beckman and Wohl, 2014; Kramer and Wohl,

2016). When analyzing the univariate relationship between jam density and wood load in dispersed pieces, only data from the Big Sandy display a positive Spearman correlation ($p = 0.01$, $\rho = 0.34$ with a 95% confidence interval between 0.06 and 0.57), weakly suggesting that the abundance of wood jams plays a role in affecting the piece-trapping capability of a reach. This hypothesized jam-driven trapping may occur such that pieces are more likely to accumulate on jams when more jams are present. I observe a significant positive correlation between jam density and the proportion of wood stored in jams in all basins combined ($p < 0.0001$, $\rho = 0.95$ with a 95% confidence interval between 0.93 and 0.96), as well as in each individual region (all p values < 0.0001, 95% confidence intervals of ρ ranging from 0.74 to 1). This indicates that jams likely increase trapping efficiency by causing more wood to be trapped in jams.

The proportion of wood stored in jams in the MF Snoqualmie is largely controlled by planform and bankfull depth. It is likely that multithread reaches, by having greater spatial heterogeneity in terms of flow depth variance and the presence of bar heads and secondary channels, provide relatively immobile objects to anchor wood jams and allow accumulation of racked pieces. This corroborates the interpretation of Wohl et al. (*In Review)*, who found that the proportion of wood stored in jams is controlled mainly by whether the reach contains multiple channels and Gurnell et al. (2000), who found that geomorphic complexity directly related to wood retention within a reach. The effect of bankfull depth on the proportion of wood stored in jams could be due to channels with greater bankfull depth being able to transport larger logs at a given discharge, making individual pieces more mobile (Iroumé et al., 2015; Kramer and Wohl, 2016). More mobile pieces transported past jams would likely lead to more wood stored in jams. I suspect that wood jam stability is the dominant control on the proportion of wood stored in jams, but wood jam dynamics remain poorly understood. In general, spatial heterogeneity

appears to be a significant factor in determining wood jam dynamics, which in turn strongly influence wood load.

The significance of elevation in determining wood load is likely due to trends in forest type with elevation in the Big Sandy and MF Snoqualmie. Both basins have significant portions of the stream network near and above tree line. As forests become thinner and trees grow more slowly at higher elevations (see section 2.2.1), the supply of wood from hillslopes to the channel via mass movement probably decreases, leading to a decrease in wood load. The homogeneity of forests in the Sitkum and SF Calawah (likely due to the relatively low relief in those basins) probably results in little variation in forest stand characteristics, explaining why elevation has no significant effect on wood load in those basins.

In the Sitkum and SF Calawah, I am surprised that neither bankfull channel width nor dimensionless piece length (L^*) significantly affect wood load, since I tend to observe what appear to be more dense accumulations of wood in smaller, steeper channels (e.g., Figure S3). Slope directly correlates to wood load in these basins and likely also directly correlates to both channel width and the prevalence of large, relatively immobile roughness elements (e.g., boulders) that can trap wood pieces. Higher gradient channels tend to have more cascade or step-pool morphology and large boulders. These are largely absent from the lower gradient portions of the network, which tend to erode either bedrock or gravel to cobble sized substrate. Large clasts can interact with wood to form relatively stable accumulations in steeper streams (Scott et al., 2014). This, combined with the fact that higher gradient reaches tend to have narrower bankfull widths and corresponding valley widths ($p < 0.0001$, $\rho = -0.59$ with a 95% confidence interval between -0.75 and -0.36), probably leads to higher gradient reaches being both able to trap wood in transport more effectively on large, relatively immobile roughness elements and

makes intact trees more likely to be able to span the channel, trapping mobile wood until they begin to break down.

Confinement exerts a consistent and significant control on wood loads in both the MF Snoqualmie and Big Sandy. When wood pieces are able to interact with stable elements of hillslopes such as living trees or stumps, they tend to resist mobilization (Beckman and Wohl, 2014b; Carah et al., 2014, Figure 2-5). Such interaction is only possible if logs within the channel can reach such elements on the hillside, which is more likely when channels are confined by their valley walls. Unconfined reaches, especially those with less vegetated floodplains (observed in montane meadows in the Big Sandy or lower gradient reaches of the MF Snoqualmie with wide gravel bars) may be able to transport wood more readily without the wood being trapped on floodplain or hillslope roughness elements.

Figure 2-5:Pictures of wood stored in valley bottoms of the Sitkum and South Fork Calawah. A) An example of a high-gradient reach in the Sitkum with dense wood storage. Note that wood is pinned on living trees on the valley walls and boulders in the channel. B) An example of a low-gradient reach in the South Fork Calawah with less dense wood storage. Note that wood generally rests on a bar (image taken at low flow), and there are few large, immobile boulders to anchor wood.

It is notable that I am unable to find an effect of L^* on wood load, despite measuring reaches spanning a range of L* values from nearly 0 to 15. However, I find that the presence of

wood jams strongly controls wood loads, and the proportion of wood stored in jams is dominantly a function of channel morphology, according to my modeling. Specifically, the relationship between bankfull depth and the proportion of wood in jams may indicate that wood mobility (regulated in part by bankfull depth) influences wood storage pattern. This indicates that L* alone may be insufficient to predict wood mobility. I find that the factors controlling wood load at the reach scale do not appear to be as scale-dependent with respect to piece length and channel width as has been hypothesized (Kramer and Wohl, 2016), but instead are relatively consistent across the ranges of piece length to channel width examined here.

2.5.3 Conceptual Model of Wood Load in Rivers

I summarize my results and generalize them along with results from previous studies in the form of a conceptual model (Figure 2-6) to describe the dominant controls on valley bottom wood load at multiple spatial scales. While this conceptual model stems directly from my results, I note that it is represents a hypothesis that is explicitly tested by my analyses. I pose this conceptual model to address the lack of a holistic conceptualization of the controls on wood loads that applies to spatial scales from that of a single reach to entire watersheds or regions. While previous work has suggested that quantifying wood load requires site-specific variables, I instead argue that the following conceptual model should allow for these site-specific variables to be viewed in a way that generalizes the processes affecting wood loads, enabling future evaluation of multivariate models that accurately describe wood load in a variety of settings and at multiple scales.

2.5.3.1 Wood Supply

Wood supply refers to the wood flux into the channel from mass movement (Benda & Bigelow, 2014; Martin & Benda, 2001) and riparian recruitment via channel migration (Piégay et al., 2017). The contribution of wood from mass movement depends on forest stand characteristics (i.e., the amount of wood growing on hillsides) and the likelihood of mass movements. Such mass movements are much more common in landscapes where hillslopes reach a threshold mean gradient, proposed to be around 30° (Larsen and Montgomery, 2012), such as those found in the Western Cordillera (Benda et al., 2003a; Benda and Bigelow, 2014). However, mass movement likely contributes only a small proportion of wood flux to channels. Wood likely comes more dominantly from riparian mortality (related to forest stand characteristics and hydroclimatic/disturbance regimes) and bank erosion (Benda and Bigelow, 2014; Piégay et al., 2017). My results indicating relationships between proxies for forest stand density (elevation at an intra-basin scale and climate or logging at an inter-basin scale) and wood load support the idea that land use and hydroclimatic regime determine forest characteristics and resulting wood supply (Hough-Snee et al., 2015).

While my analysis does not directly examine recruitment rate, rates of lateral mobility depend primarily on hydrology, geomorphology, and wood and vegetation dynamics (Brooks et al., 2003; Collins et al., 2012; Richard et al., 2005; Wickert et al., 2013). Broadly, higher degrees of spatial heterogeneity (i.e., multi-thread planforms, active lateral migration) may lead to higher rates of wood supply to channels. At the same time, some forms of spatial heterogeneity (discussed below) and recruitment can be direct results of in-channel and floodplain wood. In this way, spatial heterogeneity, mainly channel morphology dynamics, links a feedback between wood load and wood supply to channels (Figure 2-6).

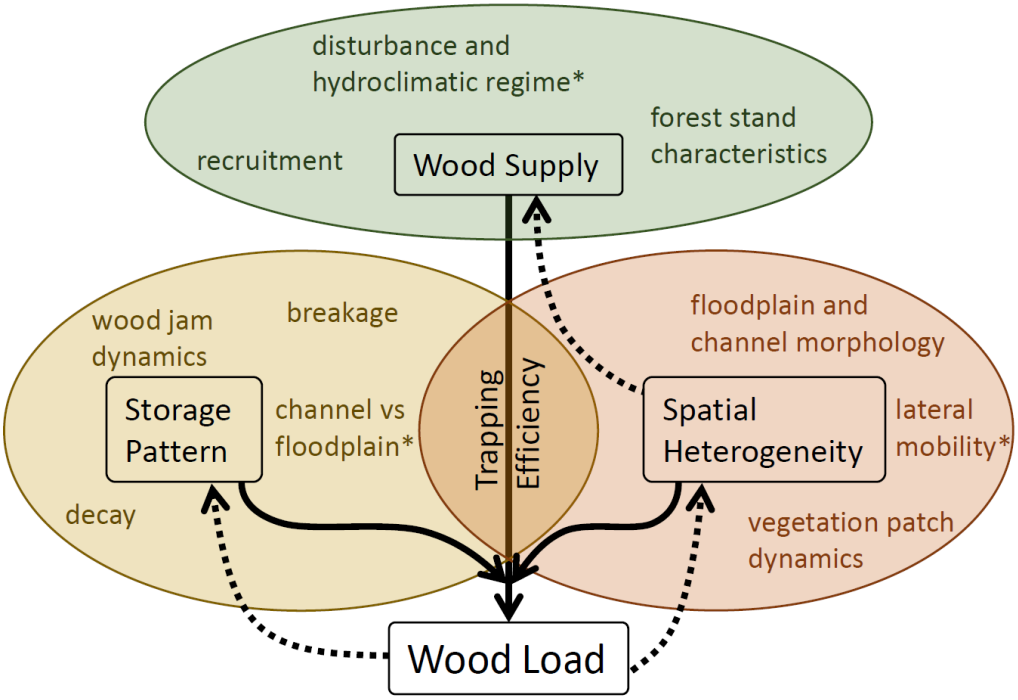

Figure 2-6: Conceptual model of controls on valley bottom wood load. Colored text within the ellipse surrounding each control indicates the processes that regulate that control. Dotted arrows represent feedbacks. Asterisks indicate processes that may regulate other processes within each ellipse. Wood supply regulates wood load through the filter of trapping efficiency. That is, trapping efficiency is the first-order, local control on wood load, whereas wood supply is a broader, basin-scale limit on maximum wood load. This model can be used to explain differences in wood loads between basins (mainly related to wood supply), the effects of anthropogenic activities or changing climate, and variation within a single basin. See text for details.

2.5.3.2 Trapping Efficiency, a Combination of Storage Pattern and Spatial Heterogeneity

My results indicate that jam density is a dominant control on wood load. In my conceptual model, storage pattern refers to how wood is stored in the valley bottom: either on floodplains or in the channel and either as jams or dispersed pieces. In addition, the breakdown of wood by physical breakage or decay also influences how wood is stored, because these processes regulate wood size (Gurnell, 2013). Storage pattern likely plays a strong role in determining the stability of a piece of wood, or how long it will reside within a reach. Wood

stored on the floodplain should be more stable than wood stored in the channel, because mobilization of floodplain wood requires a higher magnitude (and correspondingly less frequent) flow (Wohl et al., 2018). Wood stored in a jam should be, on average, more stable than dispersed pieces (Wohl and Goode, 2008), due to interactions among pieces of wood, sediment, and in-channel and floodplain roughness elements (Bocchiola et al., 2008). Wood load directly feeds back on storage pattern (Figure 2-6), as it is likely that a threshold wood load in channels is required for the formation of jams. More work is needed to understand the mechanism by which jam density relates to wood loads.

Spatial heterogeneity refers to floodplain and channel morphologic complexity and ability to impede wood in transport. Essentially, a smooth, simplified channel with little morphologic variability is less likely to provide features that can retain wood in transport than a morphologically complex channel that exhibits upstream-facing surfaces on which wood can be pinned. Such morphologic complexity can come from a variety of mechanisms. For instance, large, relatively immobile boulders (Braudrick and Grant, 2000), living vegetation both within channels (Dunkerley, 2014; Opperman et al., 2008) and on bars and floodplains, and vegetated islands (Bertoldi et al., 2013; Gurnell et al., 2002) can all act as trapping points for wood in transport. These objects can rack key pieces that can generate wood jams and can act as anchors for dispersed pieces that impact them during transport. Heterogeneity in planform (e.g., bars and pools, meanders) can result in wood deposition in shallower zones of flow in larger channels (Gurnell et al., 2000; Wohl et al., *In Review*). Channel geometry relative to wood length (Kramer and Wohl, 2016; Shields et al., 2006) can determine how likely wood pieces are to span the channel or ramp up on a bank (Wohl, 2013), increasing their resistance to mobilization. While more spatially heterogeneous multithread channels do not significantly store more wood in my

modeling, I do find that multithread channels store higher proportions of wood in jams, which may influence wood load via jam density.

Interpreting my results in the context of similar studies on larger rivers with wider channels relative to log lengths reveals how stream size may influence the nature of spatial heterogeneity. The small to medium streams studied here are generally more confined (i.e., logs interact with banks frequently) and spatial heterogeneity is commonly in the form of bedform variability, large boulders, and bankside vegetation that can trap wood ramped on floodplains and valley walls. Larger streams display spatial heterogeneity dominantly in the form of bars and mid-channel islands that generate shallow flow regions that tend to trap wood (e.g., Gurnell et al., 2000; Wohl et al., *In Review*). My observed positive correlation between slope and wood load in the Sitkum and SF Calawah likely reflects the fact that streams in these basins are uniformly confined by their valley walls, allowing bankside spatial disparities to trap wood, and making large boulders or bedforms the dominant wood trapping mechanisms that can trap wood and maintain jams (Scott et al., 2014). Such morphologic roughness features are likely more common in higher gradient channels in those basins (Aberle and Smart, 2003). For the MF Snoqualmie and Big Sandy, the relationship between slope and wood load is insignificant, likely reflecting the fact that both boulders, bankside disparities, and bedforms as well as planform irregularity, bars, and in-stream vegetation contribute to wood trapping. In those basins, more confined reaches likely allow wood to interact more strongly with bankside heterogeneities, leading to high wood loads.

Vegetation patch dynamics regulate riparian forest stand characteristics (a feedback between spatial heterogeneity and wood supply) as well as the potential for wood to be impeded in transport, especially on bar or floodplain surfaces (Fetherston et al., 1995). Wood in the

channel can determine vegetation patch dynamics by affecting the formation of hard points in the valley bottom (Collins et al., 2012), acting as a feedback between wood load and spatial heterogeneity (Figure 2-6). Lateral mobility is a function of both how effective the river is at eroding its banks and depositing bars as well as the limitations exerted by valley walls or anthropogenic confinement. My observation that confinement is a strong control on wood load, whereby more confined channels have higher wood loads (Wyżga et al., 2017), however, suggests that greater lateral mobility may result in decreased wood trapping efficiency, despite potential increases in recruitment rate. The exception to this may be found in the case of larger rivers (Gurnell et al., 2000; E Wohl et al., *In Review*), where wider reaches may have more bars and islands on which wood can be retained.

With my conceptual model, I propose that wood load is a function of how much wood is deposited within a reach and its residence time, and is controlled by characteristics that affect storage patterns, spatial heterogeneity, and the supply of logs to the channel. Together, spatial heterogeneity and storage pattern determine trapping efficiency, or the wood retentiveness of a reach. This conceptual model relates these characteristics to wood load and facilitates discussion of how wood load feeds back on storage pattern and spatial heterogeneity, which in turn feeds back on supply.

2.5.4 Valley Bottom Wood Contribution to the Riverine OC Pool

A recent compilation of wood OC storage in temperate rivers shows that, with one exception, most past quantifications of wood OC stock are in the range of 1 to 150 Mg C/ha (Sutfin et al., 2016). Comparing the first-order estimates from my study basins to other values from temperate regions contextualizes the impact of logging on the wood OC stock. In the Big

Sandy, a semi-arid basin with much of its area near or above tree line, wood plays a minor role in storing carbon (95% confidence interval on median between 0.0 and 2.5 Mg C/ha). In contrast, study basins in the Pacific Northwest demonstrate substantial OC storage in the form of wood (95% confidence interval on median between 2.7 and 27.9 Mg C/ha). Notably, wood OC storage in the SF Calawah (95% confidence interval on median between 67.4 and 229.5 Mg C/ha) is high compared to most temperate rivers, many of which have been impacted by anthropogenic wood removal or a loss of wood supply (Wohl, 2014; Wohl et al., 2017). The SF Calawah displays higher wood OC stocks than most other measured rivers in the temperate zone (Sutfin et al., 2016), highlighting the potential wood OC storage contribution of undisturbed temperate watersheds. The factor of 2 decrease in wood load between the SF Calawah and the Sitkum in the context of the large extent of anthropogenic disturbances to mountain river basins implies that wood OC storage in mountain river basins has been significantly impacted by anthropogenic disturbance, and that restoration of wood load may have a significant impact on valley bottom OC storage (Lininger et al., 2017).

Understanding the spatial variability in wood residence times is now essential to guide wood load management in the context of climate change and efforts to retain carbon on the landscape. While most wood found in channels is likely less than 50 years old, wood stored in floodplains can reach ages on the order of $10^2 – 10^3$ years (Guyette et al., 2002, 2008; Hyatt and Naiman, 2001; Nanson et al., 1995; Webb and Erskine, 2003). Despite this high variability, wood is likely a significant contribution to the valley bottom carbon pool (Naiman et al., 1987; Sutfin et al., 2016; Wohl et al., 2012). It is important to better quantify how long the substantial riverine wood OC pool resides on the landscape, and its eventual fate after it leaves a watershed (either by export or decay). For example, in the case of the Olympic mountains, it is unknown

whether wood is more recalcitrant in mountain river basins or as driftwood in the near-shore environment (Schwabe et al., 2015; Simenstad et al., 2003).

2.6 Conclusions

I present quantifications of wood load across the entirety of four river basins across the western U.S. to understand intra- and inter-basin variability in wood load spatial distribution. My modeling shows that wood jam density, confinement, elevation, and slope are strong controls on wood loads. Comparing basins with differing land use and those with differing climate reveals the strong impact of wood supply on wood loads.

Interpreting these results in the context of past studies allows us to conceptualize wood load through the interaction of wood supply to the valley bottom and the efficiency of the valley bottom at trapping wood delivered to it (Figure 2-6). I find that differences in wood load between basins and within basins with varying precipitation and forest stand characteristics are likely the result of factors influencing wood supply. Reach-scale variation in wood load is best explained by local geomorphic factors, including how wood is stored and the morphology of the valley bottom. This implies a scale dependence to wood load modeling, but also allows for a holistic framework within which to view wood load variation. Importantly, my results suggest that after accounting for basin-scale variation in variables such as precipitation and forest characteristics (both commonly correlated strongly with elevation), very similar factors control wood load at the reach-scale, namely those that describe spatial heterogeneity and wood storage pattern. I hypothesize that while every basin is slightly different (Hough-Snee et al., 2015), future multivariate predictive models based on this multi-scale conceptualization of wood load controls will likely be able to accommodate inter-basin variability and predict wood load at the reach

scale in a variety of hydroclimatic regions. All factors influencing wood supply and trapping efficiency listed in Figure 2-6 are relatively easy to quantify in both field and flume environments. As such, future statistical analyses, predictive modeling, and experimentation should be able to use the conceptual model I propose as a starting point for determining relevant variables across spatial scales to be used in multivariate modeling of wood load.

In terms of OC storage in valley bottoms, I demonstrate that, especially in wood-rich, undisturbed river networks, wood provides a high magnitude pool of OC. This OC pool may persist for 10^3 years (Guyette et al., 2002; Hyatt and Naiman, 2001), although wood residence time is a major knowledge gap. The factor of two difference between wood loads in the Sitkum and SF Calawah demonstrates the severe impact of clearcut logging with no riparian buffer and provides a clear representation of the potential enhancement of the river corridor that could be achieved by watershed-scale restoration. Restoration actions currently underway in the Sitkum (Pacific District Olympic National Forest, 2012) focus on addressing the wood supply deficiency that likely causes this wood-poor state. However, if my conceptual model is correct, addressing the wood supply impacts of logging at the basin scale will likely only be successful if trapping efficiency is addressed, such that wood is retained within the basin. On a positive note, my comparisons do not suggest that the valley bottom morphology or the density of wood jams differs significantly between these two basins, indicating that the Sitkum may have similar trapping efficiency to the SF Calawah.

2.7 Data Availability

All data supporting the analyses presented here can be found in the CSU Digital Repository (Scott and Wohl, 2018c).

Chapter 3 : Geomorphic regulation of floodplain soil organic carbon concentration in watersheds of the Rocky and Cascade Mountains, USA

3.1 Summary

Mountain rivers have shown the potential for high organic carbon (OC) storage in terms of retaining OC-rich soil. I characterize valley bottom morphology, floodplain soil, and vegetation in two disparate mountain river basins: the Middle Fork Snoqualmie, in the Cascade Mountains, and the Big Sandy, in the Wind River Range of the Rocky Mountains. I use this dataset to examine variability in OC concentration between these basins as well as within them, at multiple spatial scales. I find that although there are some differences between basins, much of the variability in OC concentration is due to local factors, such as soil moisture and valley bottom geometry. From this, I conclude that local factors likely play a dominant role in regulating OC concentration in valley bottoms, and that inter-basin trends in climate or vegetation characteristics may not translate directly to trends in OC storage. I also use analysis of OC concentration and soil texture by depth to infer that OC is input to floodplain soils mainly by decaying vegetation, not overbank deposition of fine, OC-bearing sediment. Geomorphology and hydrology play strong roles in determining the spatial distribution of soil OC in mountain river corridors.

3.2 Introduction

Terrestrial carbon storage plays an important role in regulating the global carbon cycle and the distribution of carbon between oceans, the atmosphere, long-term (10^5 – 10^9 years) storage in rock, and short- to moderate-term storage in the biosphere (10^1 – 10^4 years, including vegetation and soil) (Aufdenkampe et al., 2011; Battin et al., 2009). Soils, in particular, are a

large organic carbon (OC) reservoir with significant spatial variability (Jobbágy and Jackson, 2000; Schmidt et al., 2011), making them difficult to characterize in the context of global carbon cycling. It is essential to quantify the spatial variability of OC stored in the biosphere to constrain the effects of climate change on feedbacks between biospheric and atmospheric carbon storage (Ballantyne et al., 2012). To provide a more complete understanding of how the biospheric carbon pool may change in the future and guide management of soil OC, I seek to provide a better constraint on where carbon is stored in the biosphere and the processes that regulate that storage.

I focus here on river corridors, defined as channels, fluvial deposits, riparian zones, and floodplains (Harvey and Gooseff, 2015), which process, concentrate, transport, and store carbon (Wohl et al., 2017c). In the context of the carbon cycle, floodplains can act as a major component of the biospheric carbon pool (Aufdenkampe et al., 2011; Battin et al., 2009). Floodplain soil can act as a substantial pool of OC, indicating that floodplains may be disproportionately important compared to uplands in terms of carbon storage (D'Elia et al., 2017; Hanberry et al., 2015; Sutfin et al., 2016; Sutfin and Wohl, 2017; Wohl et al., 2012, 2017a). Mountainous regions, due to their high primary productivity (Schimel and Braswell, 2005; Sun et al., 2004), may play a substantial role in the freshwater processing and storage of OC where they retain sediment and water along the river network (Wohl et al., 2017c). Even laterally constrained floodplains in mountainous drainages can store significant quantities of OC that can be mobilized during floods (Rathburn et al., 2017). It is important to understand the spatial distribution of OC to predict its fate during floods and inform management to increase floodplain OC storage (Bullinger-Weber et al., 2014).

Floodplain OC enters river corridor soils via litterfall from vegetation and erosion of OC-bearing bedrock (Hilton et al., 2011; Leithold et al., 2016; Sutfin et al., 2016). OC inputs are either allochthonous, from upstream deposition of soil, particulate, and dissolved OC, or autochthonous, from riparian vegetation (Omengo et al., 2016; Ricker et al., 2013; Sutfin et al., 2016). As such, OC input can be regulated by vegetation dynamics and resulting litter input, hydrologic and sediment transport regimes, and water chemistry.

OC concentration in soil is also regulated by the ability of carbon to sorb to soil particles and the ability of microbes to oxidize soil OC, which can be controlled by rhizosphere dynamics, moisture, and temperature. Sorption of OC to soil particles reduces OC lability and is controlled by grain size and resulting available surface area as well as the availability of calcium, iron, and aluminum (Kaiser and Guggenberger, 2000; Rasmussen et al., 2018). Microbial processing oxidizes OC and represents the primary pathway by which soil OC returns to the atmosphere. In general, low temperatures and frequent saturation inhibit microbial activity and promote OC storage (Falloon et al., 2011; Jobbágy and Jackson, 2000; Sutfin et al., 2016).

At inter-basin scales, hydroclimatic regime controls vegetation dynamics, moisture, and temperature, such that soil OC concentration in disparate regions can be approximately characterized by these predictors (Aufdenkampe et al., 2011; Schimel and Braswell, 2005). However, at the scale of a single watershed, hydrology, ecology, and geomorphology play strong roles in determining soil texture, moisture, and microbial dynamics, in turn controlling OC storage in valley bottoms (Pfeiffer and Wohl, 2018; Scott and Wohl, 2017; Sutfin and Wohl, 2017). As such, a multi-scale approach must be taken to understanding spatial variation in OC concentrations in valley bottoms.

Here, I quantify spatial variations in OC concentration within two disparate river networks. This allows us to examine inter-basin hydroclimatic variation and intra-basin geomorphic and vegetation variation to understand the multi-scale controls on OC concentration.

3.2.1 Objectives and Hypotheses

Across a basin, it is uncertain whether OC concentration follows predictable longitudinal variation, or is controlled by local factors. Similarly, in a vertical floodplain soil profile, it is uncertain whether OC concentration follows a trend similar to uplands, with declining OC concentration with depth, or exhibits vertical heterogeneity as a result of OC-rich layers deposited by floods. It is also unclear whether OC in floodplain soils is dominantly autochthonous or allochthonous. Floodplain soil OC source may be evident from the vertical heterogeneity of OC concentration, whereby dominantly autochthonous OC profiles should decline with depth whereas dominantly allochthonous OC profiles should exhibit vertical heterogeneity, reflecting episodic deposition. My primary objective here is to understand spatial variations in OC concentration both with depth in a soil profile and across a basin. By quantifying these variations, I hope to infer the processes that regulate OC deposition in floodplain soil.

By examining two disparate mountain river basins, I can quantify both inter-basin variation in OC storage as well as variation within each basin. I hypothesize that at an inter-basin scale, hydroclimatic regime and resulting rate of litterfall inputs in the riparian zone (Benfield, 1997) will dominantly regulate OC concentration (H1). I define hydroclimatic regime as the combination of precipitation and temperature dynamics that result in the vegetation characteristics of a basin. At an intra-basin scale, I expect that valley bottom geometry and river

lateral mobility will regulate floodplain sediment characteristics and vegetation dynamics. Thus, I hypothesize that soil OC concentration does not vary along predictable, longitudinal trends within mountain river basins, instead being more dominantly controlled by local fluvial processes and valley bottom form (H2a). I hypothesize that geomorphic process and form determine soil texture and moisture, which in turn set the boundary conditions that regulate the sorption of OC to mineral grains (promoting stabilization) and the potential of OC to be respired by microbes (H2b). In terms of OC inputs to floodplain soils, I hypothesize that the source of OC is dominated by autochthonous vegetation and litter inputs in these basins (H3). As such, I expect OC to dominantly decline with depth, only rarely exhibiting vertical heterogeneity that would represent allochthonous deposition from flooding.

3.3 Methods

This work was done alongside work presented in chapter 1, and hence shares field sites, study design, GIS, and sampling techniques.

3.3.1 Field Sites

I quantified soil organic carbon concentrations to a depth of approximately one meter in the Big Sandy basin in the Wind River Range of Wyoming and the Middle Fork Snoqualmie basin in the central Cascade Mountains of Washington (Figure 3-1). These basins represent distinct bioclimatic and geomorphologic regions, ranging from the wet, glacially influenced Cascades to the semi-arid Middle Rockies.

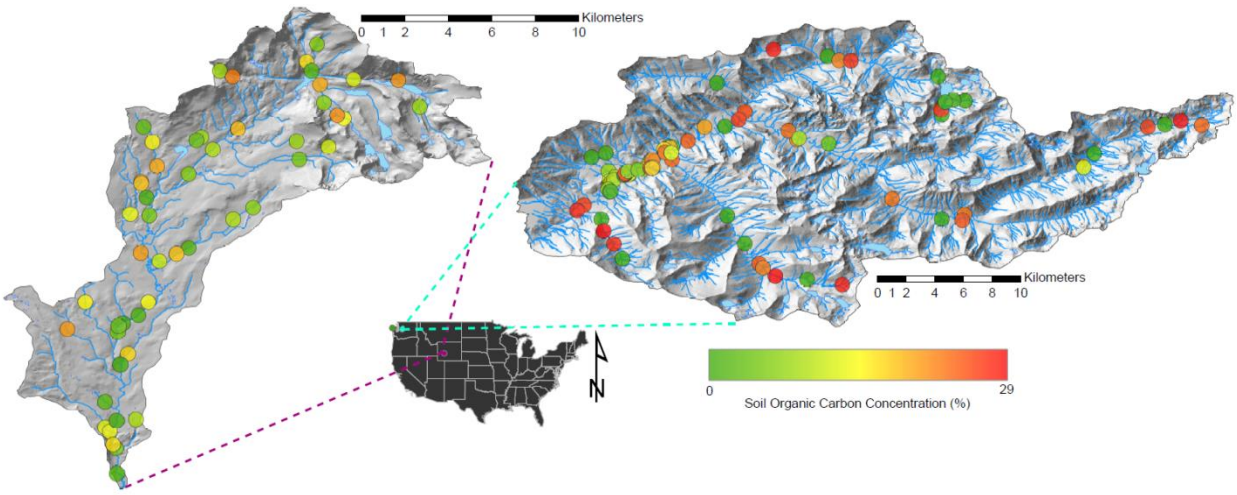

Figure 3-1: Map showing the location, topography, sampling sites, and stream network of the sampled basins. Big Sandy, Wyoming, on left and MF Snoqualmie, Washington, on right. Circles represent sampling locations at which floodplain soil OC was measured. Sample sites are colored by OC concentration.

The MF Snoqualmie has a mean annual precipitation of 3.04 m (Oregon State University, 2004), 2079 m of relief over a 407 km^2 drainage area, and a mean basin slope of 60%. Topography in the MF Snoqualmie is largely glaciogenic, with wide, unconfined valleys at both high and low elevations. Streams range from steep, debris flow dominated headwater channels to lower gradient, wide, laterally unconfined channels in its lower reaches. The lower reaches of the MF Snoqualmie have been clearcut extensively in lower reaches since in the early 1900s, although there is little logging activity today. Vegetation follows an elevation gradient. The talus, active glaciers, and alpine tundra at the highest elevations transition to subalpine forests dominated by mountain hemlock (*Tsuga mertensiana*) (above approximately 1500 m), but also including Pacific silver fir (*Abies amabalis*) and noble fir (*Abies procera*) in the lower subalpine and montane zones (above approximately 900 m). Below the montane zone, uplands and terraces are covered by Douglas fir (*Pseudotsuga menziesii*) and western hemlock (*Tsuga heterophylla*),

whereas active riparian zones are dominated by red alder (*Alnus rubra*) and bigleaf maple (*Acer macrophyllum*).

The Big Sandy is considerably drier than the MF Snoqualmie, but also exhibits broad, glacially carved valleys, especially in headwater reaches. It has a mean annual precipitation of 0.72 m (Oregon State University, 2004), 1630 m of relief over a 114 km^2 drainage area, and a mean basin slope of 25%. Herbaceous alpine tundra dominates higher elevations (above approximately 3100 m), while the subalpine zone (approximately 2900 to 3100 m) is characterized by forests of whitebark pine (*Pinus albicaulis*), Engelmann spruce (*Picea engelmannii*), and subalpine fir (*Abies lasiocarpa*). The montane zone (approximately 2600 m to 2900 m) is comprised dominantly of lodgepole pine (*Pinus contorta*). Only a small portion of this basin (approximately 1%) resides below 2500 m, where shrub steppe begins to dominate (Fall, 1994). Parklands and meadows are abundant in this basin, creating a patchy forest structure. Comparing this basin to the MF Snoqualmie provides bioclimatic contrast that allows us to examine how floodplain soil OC concentrations vary across a range of stream morphologies and floodplain morphologic types in regions with differing precipitation, forest characteristics, and basin morphology.

3.3.2 Study Design and Sampling

I sampled the Big Sandy in summer 2016 and the MF Snoqualmie in summer 2017. During each sampling campaign, no large floods occurred and I observed no floodplain erosion or deposition. Across both basins, I cored a total of 128 floodplain sites to determine soil OC concentration. Cores were collected as a series of individual soil samples at both regular and irregular depth increments.

3.3.2.1 Big Sandy

The sparse vegetation in the Big Sandy basin enabled us to use a combination of a 10 m DEM and satellite imagery to manually map the extent of the valley bottom along the entire stream network and delineate valley bottoms based on confinement. I defined unconfined valley bottoms as those in which channel width occupied no more than half the valley bottom, and confined valley bottoms as those in which channel width occupied greater than half the valley bottom. Within each confinement stratum, I stratified the stream network by five drainage area classes to produce a total of ten strata, ensuring even sampling across the basin. Within each of the resulting ten strata, I randomly selected 5 reaches, producing a total of 50 sample sites throughout the basin. Due to access issues, I sampled 48 out of the 50 randomly located sites. I supplemented these with 4 subjectively located sites that I felt enhanced my ability to capture variation throughout the drainage based on observations in the field, resulting in a total of 52 sampled sites.

3.3.2.2 Middle Fork Snoqualmie

The MF Snoqualmie River basin is larger than the Big Sandy and has extensive, low-gradient floodplains in its downstream reaches. These extensive floodplains display high spatial variability in vegetation, surface water, grain size, and estimated surface age, based on aerial imagery and ground reconnaissance. To ensure an unbiased characterization of these heterogeneous floodplains, I used aerial imagery, a 10 m DEM, and pictures from field reconnaissance to delineate the floodplain into patch categories: fill channels (abandoned channels that have had enough sediment deposited to prevent an oxbow lake from forming), point bars (actively accreting surfaces on the inside of bends), wetlands (areas with standing

water in imagery that are not obviously oxbows), oxbow lakes (abandoned channels dammed at the upstream and downstream ends to form a lake), and general floodplain surfaces (surfaces that cannot be classified into any of the above categories). Within each of these five categories, I randomly selected six points at which to take soil cores.

I also stratified the entire MF Snoqualmie stream network by channel slope into four strata. Within each channel slope strata (hereafter referred to as simply slope strata), I randomly selected ten reaches to collect a single floodplain soil core, resulting in 40 randomly located sample sites.

To supplement randomly sampled sites and accommodate for the infeasibility of accessing two of the randomly sampled sites along the stream network, I also subjectively selected sample sites in places that I felt enhanced the degree to which my sampling captured the variability present among streams in the basin. This resulted in a total of 46 sites stratified by slope, 38 of which were randomly sampled, in addition to 30 sites stratified by floodplain type.

3.3.3 Reach-Scale Field Measurements

At each sampled reach (100 m or 10 channel-widths, whichever was shorter), I measured channel geometry and other characteristics, although my measurements were not consistent across all basins because field protocol evolved during the course of the study. In both basins, I measured confinement, valley bottom width, and channel bed slope. I additionally measured bankfull width and depth in the MF Snoqualmie. I did not measure channel characteristics for sites stratified by floodplain type in the MF Snoqualmie, since they did not correspond to a single reach of channel, as did sites stratified by slope in much more confined valleys.

In the MF Snoqualmie, I also categorized channels by planform and dominant bedform (Montgomery and Buffington, 1997). I defined planforms as either: straight, where the channel was generally confined and significant lateral migration was not evident, meandering, where lateral migration was evident but only a single channel existed, anastomosing, where vegetated islands separated multiple channels, and anabranching, where a single dominant channel existed with relict channels separated by vegetated islands. I further classified channels as being either multithread (anastomosing or anabranching) or single thread (straight or meandering). Because logging records are inconsistent and likely inaccurate in the MF Snoqualmie (based on the frequent observation of past logging activity where none was recorded in Forest Service records), I noted whether signs of logging, such as cut stumps, cable, decommissioned roads or railroads, or other logging-associated tools were found near the reach.

I chose a representative location on the floodplain for each sampled site, based on visual examination of vegetation type, soil surface texture, surface water presence, and elevation relative to the bankfull channel elevation (floodplain sites stratified by type in the MF Snoqualmie were sampled as close to the randomly sampled point as possible). Once a location was chosen, I extracted a 32 mm diameter soil core using an open-sided corer (JMC Large Diameter Sampling Tube). Due to my adaptive methodology, I sampled soil OC slightly differently in the Big Sandy basin versus the MF Snoqualmie. In the Big Sandy, I cored in irregular increments, generally 25-30 cm. After analyzing data from the Big Sandy basin, I realized that sampling in regular increments would make analysis more versatile. As a result, I switched to extracting soil samples at regular, 20 cm increments in the MF Snoqualmie Basin. Cores were taken to refusal (i.e., coarse gravel or other obstructions preventing further soil collection) or a depth of approximately 1 m. Five cores in the Big Sandy, 12 cores in the MF

Snoqualmie sites stratified by slope, and 11 cores in the MF Snoqualmie sites stratified by floodplain type did not reach refusal. When no sand or finer sediment was present in the valley bottom (only occurred in headwater channels of the MF Snoqualmie), I recorded negligible OC concentration. Once soil samples were removed from the ground, they were placed in ziplock bags and frozen within 72 hours (most samples were frozen within 8 hours) and kept frozen until analysis.

3.3.4 Measuring Soil OC and Texture

To measure the concentration of organic carbon in soil samples, I used loss-on-ignition (LOI). I first defrosted samples for 24-48 hours at room temperature. Once defrosted, I thoroughly mixed samples to ensure the most homogenous sample possible. I then subsampled 10-85 g of soil from each sample for analysis. Using crucibles in a muffle furnace, I dried samples in batches of 30 for 24 hours at 105°C to determine moisture content and remove all non-structurally held water. Following the guidelines suggested by Hoogsteen et al. (2015), I then burned samples for 3 hours at 550°C to remove organic matter. By comparing the weight of the burned samples with that of the dried samples, I obtained an LOI weight.

After performing LOI, I used burned samples to perform texture-by-feel to determine the USDA soil texture class and estimated clay content (Thien, 1979). To convert LOI weight to OC concentration, I used the structural water loss correction of Hoogsteen et al. (2015) using clay content estimated from soil texture. This correction considers water held by clay that may not evaporate during drying, but will evaporate during burning. It also estimates the proportion of the LOI weight that is OC.

One potential confounding factor in LOI is carbonates that may burn off during ignition, adding to the LOI weight while not being organic matter. In lithologies where carbonates are rare (e.g., granitoid rocks like those found in the upper MF Snoqualmie and entire Big Sandy basins), this is a relatively negligible issue. However, some of my soil samples came from parts of the MF Snoqualmie basin draining rocks of the western mélange belt, including argillite, graywacke, and marble. I tested samples for the presence of carbonates to determine whether my LOI methods would be sufficient to accurately determine OC concentration. I randomly chose 10 soil samples of a total of 110 that drained rocks that could include carbonates and submitted them to the Colorado State University soil testing laboratory for CHN furnace analysis (Sparks, 1996), which yielded data on the proportion of carbonates by mass in those samples. On average, those samples contained calcium carbonate concentrations of 0.97% (95% confidence interval between 0.96% and 0.97%), and the percentage of the total carbon in those samples comprised of inorganic carbon was, on average, 8.6% (95% confidence interval between 8.51% and 8.78%). From this, I concluded that the amount of carbonate in the samples draining potentially carbonate-bearing rocks was low enough that LOI was likely to still be accurate. Consequently, I analyzed all soil samples using LOI to obtain OC concentration.

3.3.5 GIS and Derivative Measurements

After fieldwork in each basin, I collected the following data for each reach using a GIS platform: elevation, drainage area, land cover classification and canopy cover from the National Land Cover Database (Homer et al., 2015), and the mean slope of the basin draining to each reach (including hillslopes and channels). Utilizing drainage area at each reach and field-measured channel gradient, I calculated an estimated stream power as the product of drainage

area, channel gradient, and basin-averaged precipitation. I utilized a 10 m DEM for all GIS topographic measurements. To estimate clay content for each sample, I used median values for assigned USDA texture classes. To obtain estimated clay content, moisture, and OC for each core, I calculated an average weighted by the percentage of core taken up by each soil sample. For samples stratified by floodplain in the MF Snoqualmie, I categorized floodplain types into those with standing water (wetlands and oxbow lakes) and those with no standing water (all other types).

3.3.6 Statistical Analyses

All statistical analyses were performed using the R statistical computing software (R Core Team, 2017). I conducted all analyses on three modeling groups, based on the variables measured in each group. In the MF Snoqualmie, I grouped observations by stratification type, separating observations stratified by channel slope from observations stratified by floodplain type. I separated these two groups from all observations in the Big Sandy, which were measured consistently. I modeled OC concentration and soil texture with a mixed effects linear regression using individual soil samples (i.e., the individual samples that make up a core) as sample units (n = 103 for MF Snoqualmie stratified by slope, 89 for MF Snoqualmie stratified by floodplain type, and 101 for Big Sandy). I modeled the sampled site as a random effect, acknowledging that individual soil samples within a single core are likely non-independent. I use profiled 95% confidence intervals on effect estimates (β) for fixed effects to evaluate variable importance in mixed effects models.

To gain further insight at the reach-scale, I also modeled average OC concentration and soil moisture at each measured site using multiple linear regression. I modeled soil moisture at

the reach scale because I felt that my single snapshot of moisture conditions was better represented as a site-level average. I first performed univariate analysis between each hypothesized predictor and the response, utilizing mainly comparative Wilcoxon rank-sum tests (Wilcoxon, 1945) or correlational Spearman correlation coefficient statistics. I utilize a Holm multiple-comparison correction (Holm, 1979) for pairwise comparisons. During this filtering, I also view boxplots or scatterplots as appropriate to discern which variables appear to have anything other than a completely random relationship with the response. I then utilize all subsets multiple linear regression using the corrected Akaike Information Criterion as a model selection criteria (Wagenmakers and Farrell, 2004). I iteratively transformed response variables to ensure homoscedasticity of error terms. To select a single best model, I utilized both Akaike weight based importance as well as parsimony to select a final, reduced model. I considered sample sizes, p values, and effect magnitudes in determining variable importance.

I also analyzed each core to determine whether there were buried, high OC concentration layers at depth. I compared each buried soil sample to the sample above it using the criterion that a peak in OC at depth should have an OC concentration 1.5 times that of the overlying sample and be above 0.5% (Appling et al., 2014).

3.4 Results

Model results are presented in Table 3-1. Comparisons between basins and summaries of OC concentration, moisture, and estimated clay content are shown in Figure 3-2.

Table 3-1: Matrix of all models presented in text. Each model is listed by model group, response variable, and scale. Scale refers to the sample unit of the model, where site refers to a core, with the response averaged over all the individual soil samples in the core. For each variable and model, grey fill indicates that the variable was included in either model selection or the full mixed-effects model. A minus (−) indicates that the variable was selected as important in predicting the response, and denotes an indirect correlation, whereas a plus (+) indicates a direct correlation. In the case of confinement, a plus indicates that unconfined streams display a higher magnitude response variable. In the case of bed material, a plus indicates that samples with sand exhibit a higher value of the response. NA indicates that either the variable wasn't measured for that basin or model group or that it is the model response. [1] Depth refers to either the soil sample depth below the ground or the total depth of the core, depending on the sample unit. [2] No significant results were observed for this model. [3] For this model, both valley width and confinement predict texture and can be interpreted interchangeably. However, including both in the same model would yield problems due to multicollinearity.

Model Group	Response	Scale (Sample Unit)	Variables																							
			Confinement	Bedform	Channel Slope	Bed Material	Multithread	Valley Width	Bankfull Width	Bankfull Depth	Stream Power	Floodplain Type	Standing Water	Depth[1]	Clay Content	Moisture	Logging Nearby	Grasses Present	Shrubs Present	Trees Present	Elevation	Basin Slope	Canopy Cover	NLCD	Drainage Area
MF Snoqualmie stratified by slope	OC (%)	Soil Sample										NA	NA	−							+					
	OC (%)	Site	+									NA	NA			+										
	Moisture (%)	Site	+		−							NA	NA			NA					+					
	Texture (%)	Soil Sample	+			+						NA	NA		NA											
MF Snoqualmie stratified by floodplain type	OC (%)	Soil Sample	NA	NA	NA	NA	NA	NA	NA	NA	NA			−												NA
	OC (%)	Site	NA	NA	NA	NA	NA	NA	NA	NA	NA					+							+			NA
	Moisture (%)	Site	NA	NA	NA	NA	NA	NA	NA	NA	NA		+		+	NA										NA
	Texture[2] (%)	Soil Sample	NA	NA	NA	NA	NA	NA	NA	NA	NA				NA											NA
Big Sandy	OC (%)	Soil Sample		NA		NA	NA		NA	NA		NA	NA	−			NA	NA	NA	NA						
	OC (%)	Site		NA		NA	NA		NA	NA		NA	NA	−		+	NA	NA	NA	NA						
	Moisture (%)	Site	+	NA		NA	NA		NA	NA		NA	NA	+		NA	NA	NA	NA	NA	+					
	Texture[3] (%)	Soil Sample	+	NA		NA	NA	+	NA	NA		NA	NA	−	NA		NA	NA	NA	NA						

3.4.1 OC Concentration

Of cores with more than a single sample, I found that 32% (7/22) of cores stratified by slope in the MF Snoqualmie, 32% (8/25) of cores stratified by floodplain type in the MF Snoqualmie, and 6% (2/31) of cores in the Big Sandy exhibited OC concentration peaks at depth. Whether a soil sample was classified as an OC peak had no relation to estimated clay content in sites stratified by floodplain type ($p = 0.28$) or those stratified by slope ($p = 0.89$) in the MF Snoqualmie. In the Big Sandy, soil samples classified as buried OC peaks had significantly higher estimated clay contents ($p = 0.05$) than those that were not classified as peaks.

In general, the floodplain-stratified sites in the MF Snoqualmie stored higher densities of OC than the Big Sandy (Figure 3-2a, b). Figure 3-2a includes zero values (i.e., sites with no OC-bearing sediment, only present in the MF Snoqualmie slope-stratified group), whereas Figure 3-2b does not, because sample units in Figure 3-2b are individual soil samples. Comparing these two groups, it appears that soils in the MF Snoqualmie can exhibit much higher OC concentrations than those in the Big Sandy, but in general, there are many more reaches with no fine sediment available to store OC in the MF Snoqualmie.

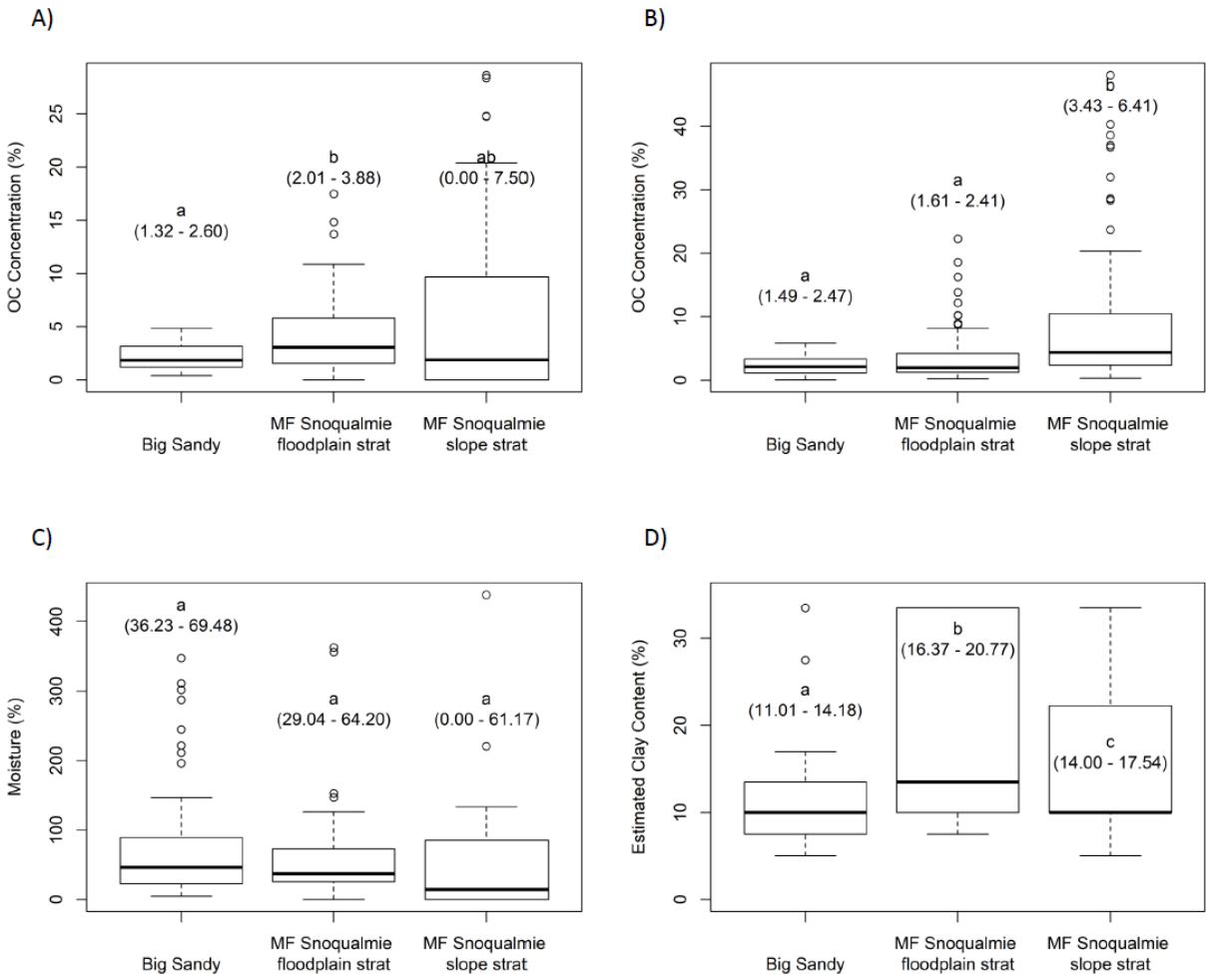

Figure 3-2: Boxplots showing comparisons between model groups of OC concentration at the reach-scale (A), OC concentration at the scale of individual soil samples (B), moisture at the reach-scale (C), and estimated clay content at the scale of individual soil samples (D). Ends of dotted lines represent 1.5 times the inter-quartile range, which is represented by boxes. Bold line represents median. Circles represent outliers. Letters indicate probable differences between groups based on pairwise Wilcoxon (A-C) or t tests (D) with a holm correction. Ranges in parentheses below letters show the 95% confidence interval on the median value for the group (A-C) or the mean value for the group (D) where median confidence intervals were overly constrained due to the categorical nature of my estimated clay content data.

At the scale of individual soil samples, I found that the depth below ground surface was by far the dominant control on OC concentration across all modeling groups. I used a cube root transform for all three mixed effects models of OC concentration. For MF Snoqualmie sites

stratified by slope, deeper soil samples contained less OC ($\beta = -0.0084 \pm 0.0042$), whereas soil samples at higher elevations tended to contain more OC ($\beta = 0.0010 \pm 0.00099$). Depth was the only significant predictor of OC content for both MF Snoqualmie soil samples stratified by floodplain type ($\beta = -0.0084 \pm 0.0042$) and soil samples in the Big Sandy ($\beta = -0.0037 \pm 0.0019$).

Modeling MF Snoqualmie slope-stratified sites at the reach-scale, I found that moisture ($\beta = 0.0078 \pm 0.0031$), and whether the reach was unconfined ($\beta = 0.77 \pm 0.49$) control soil OC (cube root transformation, model adjusted $R^2 = 0.54$, $p < 0.0001$). Modeling MF Snoqualmie floodplain-stratified sites at the site scale, I found that canopy cover ($\beta = 0.012 \pm 0.011$) and moisture ($\beta = 0.0040 \pm 0.0011$) are controls on soil OC (cube root transformation, model adjusted $R^2 = 0.67$, $p < 0.0001$). Modeling Big sandy sites at the reach scale, I found that soil depth ($\beta = -0.012 \pm 0.0071$) and moisture ($\beta = 0.014 \pm 0.0026$) are dominant controls on soil OC concentration (no transformation, model adjusted $R^2 = 0.69$, $p < 0.0001$).

In general, moister, deeper soils store more OC at the reach scale, whereas OC tends to vary dominantly with depth at the scale of individual soil samples. Although estimated clay content did not emerge as a significant predictor of OC concentration, it is used to calculate clay-held water to correct my LOI-based OC concentration measurements, making it important in determining OC for each sample.

3.4.2 Soil Texture

In general, soil texture followed a predictable trend with river size between model groups (Figure 3-2d). Floodplain type-stratified sites in the MF Snoqualmie stored the most clay, followed by slope-stratified sites and then sites in the Big Sandy.

Modeling soil texture at the individual soil sample scale across slope-stratified sites in the MF Snoqualmie, I found whether the reach was confined ($\beta = 5.42 \pm 5.32$), and whether the bed material was dominantly sand ($\beta = 10.47 \pm 6.13$) to be dominant controls on estimated clay content. Modeling soil texture for sites stratified by floodplain type in the MF Snoqualmie yielded no significant trends. In the Big Sandy, I found that either valley width ($\beta = 0.0050 \pm 0.0032$) or whether the stream was unconfined ($\beta = 0.41 \pm 0.33$) as well as depth below ground surface ($\beta = -0.0069 \pm 0.0033$ for model with valley width but not confinement) significantly control soil texture.

To summarize, sites from unconfined, lower energy reaches in the MF Snoqualmie and sites from reaches with wider valley bottoms and at lower depths in the Big Sandy exhibited finer soils.

3.4.3 Soil Moisture

Soil moisture was less variable between basins than either texture or OC concentration (Figure 3-2c). All model groups exhibited similar soil moisture conditions, although there was significant variability within each model group.

Soil moisture at MF Snoqualmie sites stratified by slope is dominantly controlled by channel slope ($\beta = -13.15 \pm 9.11$), elevation ($\beta = 0.0046 \pm 0.0038$), and whether the stream is unconfined ($\beta = 3.89 \pm 2.67$; model adjusted $R^2 = 0.38$, $p < 0.0001$). At MF Snoqualmie sites stratified by floodplain type, estimated clay content ($\beta = 0.060 \pm 0.042$) and whether the floodplain unit had standing water ($\beta = 1.15 \pm 0.71$) significantly controlled soil moisture (model adjusted $R^2 = 0.46$, $p < 0.0001$). In the Big Sandy, soil depth ($\beta = 0.012 \pm 0.012$), elevation ($\beta =$

0.0023 ± 0.0014), and whether the reach was unconfined (β = 0.91 ± 0.75) significantly controlled soil moisture (model adjusted $R^2 = 0.35$, $p < 0.0001$).

3.5 Discussion

3.5.1 Understanding Spatial Variability in OC Concentration in Floodplain Soils (H1 and H2)

Comparing the MF Snoqualmie to the Big Sandy shows that the wetter, higher primary productivity basin is capable of storing greater concentrations of OC in floodplain soils, but that both regions generally store similar OC concentrations in floodplain soils. This result partially agrees with the examination of subalpine lake deltas by Scott and Wohl (2017). In that study, subalpine lake deltas in the MF Snoqualmie were compared to deltas in the drier Colorado Front Range. Subalpine lake deltas displayed similar OC concentrations, likely due to competing but complementary OC stabilization and respiration mechanisms in each region. Those deltas represent a subset of the broader valley bottom soils studied here. This more expansive study points to both geomorphic controls, such as valley bottom geometry, and factors influenced by climate, such as canopy cover, as controls on OC storage in valley bottoms. These results agree with the results of Lininger et al. (2018),which indicate that geomorphic context and vegetation dynamics control OC concentration on floodplain soils along large, lowland rivers in Alaska, USA.

At the reach or site scale, wetter soil profiles consistently yielded higher OC concentrations in all model groups. However, moisture did not differ significantly between model groups (Figure 3-2c), indicating that this alone cannot explain differences between basins. Soils tend to be finer in the MF Snoqualmie, but clay content is not an important predictor of OC concentration in studied soils. Although clay content likely influences OC concentration based

on previous research (Hoffmann et al., 2009), the inclusion of coarse soil material (including particulate organic matter) in my samples may explain the lack of an observed correlation here. Although confinement plays a strong role in determining OC concentration in MF Snoqualmie sites stratified by slope, it doesn't differ significantly between basins (52% of Big Sandy reaches are unconfined compared to 63% of MF Snoqualmie reaches). The major differences between these basins are their hydroclimatic and disturbance regimes. The MF Snoqualmie is at a lower elevation, is wetter, and has denser and higher biomass forests (Smithwick et al., 2002), compared to the drier, sparser parkland forests of the Big Sandy, which likely also experiences more frequent fires based on fire histories of nearby regions (recurrence interval on the order of 10^1 - 10^2 yrs; Houston, 1973; Loope and Gruell, 1973).

Between basins, it is likely that hydroclimatic regime, influencing primary production, plays some role in the MF Snoqualmie's higher maximum OC concentrations in floodplain soils compared to those of the Big Sandy. However, smaller-scale factors such as soil texture and moisture also likely play a role and are not related to drainage area (Table 1), indicating that neither OC concentration nor its controlling factors vary continuously along a river network, and thus supporting H2a and H2b. This also indicates that local factors, set largely by geomorphic and groundwater dynamics, play a significant role in modulating the effect of climate on OC concentrations. If the MF Snoqualmie and Big Sandy displayed significantly different OC concentrations, my first hypothesis regarding the inter-basin controls on OC concentration would be supported. However, I instead find that climate and primary productivity only partially determine OC concentrations, especially when viewed in the context of geomorphic and hydrologic variability. Thus, the results do not support H1.

Each basin (or model group) is slightly different in terms of the controls on soil OC concentration, moisture, and texture. In the MF Snoqualmie sites stratified by slope, higher elevation sites displayed higher OC concentrations. This is contrary to the general trend in primary productivity, which decreases with increasing elevation. However, it is important to note that the headwaters of the MF Snoqualmie are dominated by lakes, deltas, and other depositional features in relatively broad, glacially carved valleys. Subalpine lake deltas have been shown to store high OC concentrations in this basin (Scott and Wohl, 2017), and many of the highest OC concentrations I measured were located in broad, wet meadows, subalpine lake deltas, or other unconfined, high elevation reaches. Such unconfined sites likely have significantly cooler temperatures and tend to have higher soil moisture contents, as shown by my modeling (Table 3-1). As such, although high elevation MF Snoqualmie sites may receive less OC input, they likely have a low rate of OC respiration, resulting in higher OC concentrations on the whole, which agrees with the result of Bao et al. (2017). In the Big Sandy, my modeling suggests that the lower temperatures and higher moisture (Table 3-1) at higher elevations do not compensate for the lower primary productivity, as elevation does not correlate to OC concentration.

In both basins, unconfined reaches contained wetter and finer textured soils, which may result in a higher soil OC capacity. Although confinement only related directly to OC content in MF Snoqualmie sites, it does play a strong role in determining moisture, which plays a role in regulating OC concentration in both basins, likely via inhibiting microbial activity (Howard and Howard, 1993). The relevance of channel slope in determining soil moisture in the MF Snoqualmie but not Big Sandy may reflect the prevalence of high-gradient, debris-flow dominated channels in the MF Snoqualmie that largely exhibited only gravel to boulder substrate, which I assume stores minimal fine sediment, moisture, or OC.

In the Big Sandy, higher soil depths were related to more moisture and finer texture, but less OC concentration. This indicates the trend in OC with depth likely dominates the signal of OC concentration, with deeper sites containing a higher proportion of OC-depleted, deep samples.

3.5.2 Inferring Sources of OC to Floodplain Soils (H3)

OC can be input to floodplain soils by two primary mechanisms. First, dissolved and particulate OC can be deposited on floodplain surfaces by overbank sediment deposition, thus integrating fluvial sedimentary OC into the floodplain soil profile. Second, litter and decomposing vegetation on the floodplain surface, in addition to decomposing wood that may have been deposited by overbank flows, can input OC to floodplain soil.

My modeling of OC concentration yielded results consistent with previous investigations of controls on soil OC storage capacity (Jobbágy and Jackson, 2000; Sutfin and Wohl, 2017). Sites in the heterogeneous floodplain of the MF Snoqualmie displayed a direct correlation between canopy cover and OC concentration, indicating that increased litter inputs lead to increased floodplain soil OC concentration. Sediment inputs likely differ between floodplain depositional units (e.g., coarser sediment may deposit on point bars compared to filled secondary channels), which were not found to be an important predictor of OC concentration. This indicates that vegetation inputs may be more dominant than fluvial sediment inputs at these sites.
The finding that buried OC peaks in the MF Snoqualmie do not have abnormally high clay contents supports the interpretation that wood and litter inputs to soil are the dominant source of OC in the floodplain soils I examined. Buried peaks can be either layers created by overbank deposition and subsequent burial of fine, OC-bearing sediments (Blazejewski et al., 2009; Ricker

et al., 2013), buried pieces of wood (Wohl, 2013), or buried organic horizons that are now capped by sediments that prevent OC respiration. If overbank deposition of fine sediment caused OC peaks, I would expect to see the soil samples classified as peaks exhibiting high clay contents, indicating finer sediment. Instead, my results suggest that in the MF Snoqualmie, buried peaks are likely the result of either buried organic horizons or buried wood. I observed large pieces of decaying, buried wood in floodplain cut banks in the MF Snoqualmie, supporting this inference.

In the Big Sandy, the two cores that exhibited peaks were collected from the same meadow, just downstream of a now-filled former lake that is a potential source of fine sediment. The channels draining this meadow exhibit an anabranching planform, indicating the potential to deposit and bury packets of potentially OC-rich, fine sediments. However, the majority of cores did not exhibit OC peaks, indicating OC input mainly from vegetation at the surface and continuing OC respiration at depth.

OC variation within each core is dominantly a function of depth. I observe a negative correlation between depth below ground surface and OC concentration, which has been observed in other studies, including mountain wetlands and floodplains (Jobbágy and Jackson, 2000; Scott and Wohl, 2017; Sutfin and Wohl, 2017; Zhao et al., 2017). In general, this indicates that OC is enriched at the surface and decomposes with depth. This fits with my finding that the majority of my cores do not exhibit significant OC peaks at depth and supports the dominance of litter and wood OC inputs to floodplain soils. These results support my hypothesis that decaying litter and wood, not overbank sediment deposition, dominates the input of OC to floodplain soils in my study basins (H3). Other basins that experience overbank flows, accompanying deposition of fine sediment, and burial of organic layers exhibit OC storage that is likely dominated by fluvial

deposition (e.g., Blazejewski et al., 2009; D'Elia et al., 2017; Ricker et al., 2013). Thus, it is likely that flow regime, lateral connectivity, and sediment transport dynamics regulate whether floodplain soil OC is dominantly input by overbank deposition of fine material or decaying litter and wood.

3.5.3 Conceptual Model of Soil OC Concentration in Floodplain Soils

I present a conceptual model to summarize my results and place them in the context of recent work examining the controls on OC storage in soils (Figure 3-3). OC is input to floodplains either through the decay of vegetation or the deposition of fine, OC-rich sediment. This input of OC only determines OC concentrations insofar as floodplain soils are capable of storing OC. That storage is effectively determined by a balance between processes that remove OC from floodplains, namely respiration or erosion followed by respiration (Berhe et al., 2007), and processes that regulate OC availability to microbes, namely the capability of the mineral fraction of the soil to sorb OC.

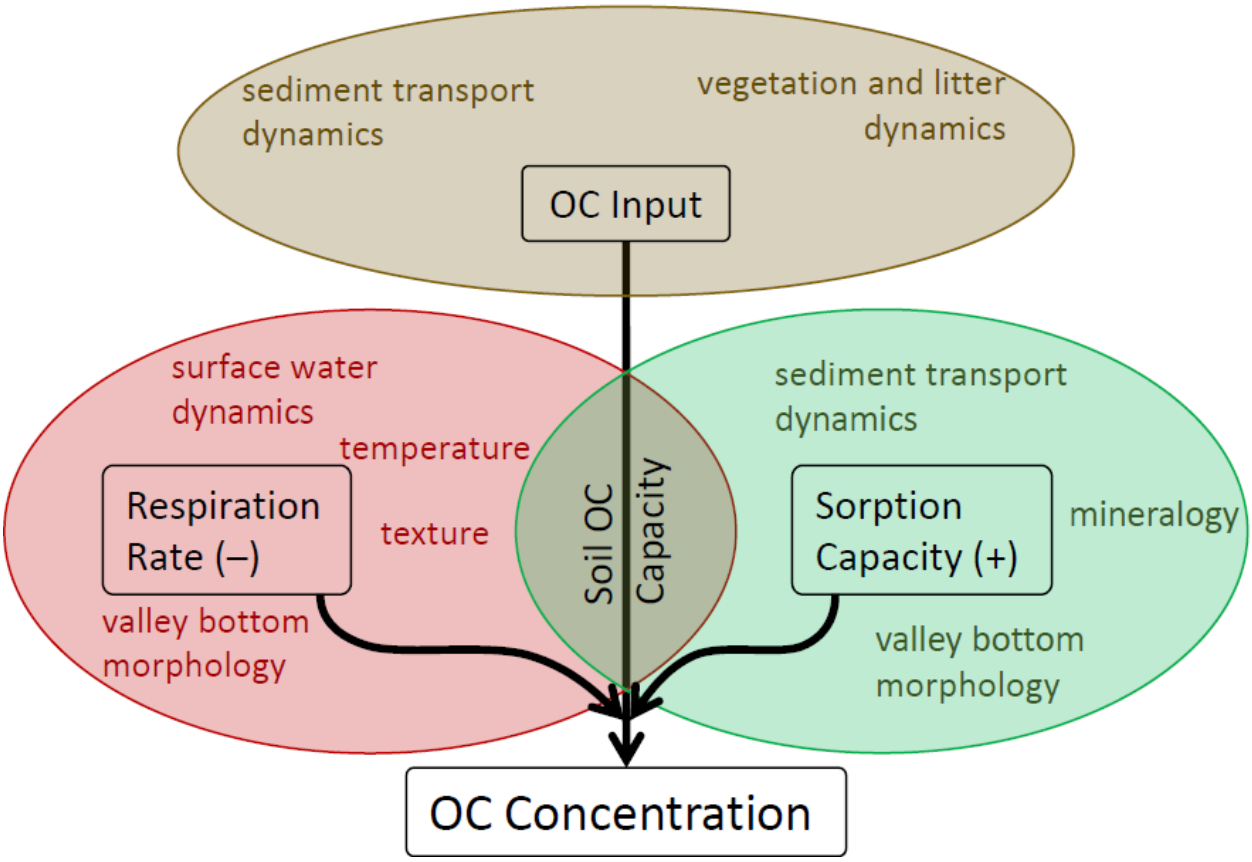

Figure 3-3: Conceptual model of physical processes that influence OC concentration in floodplain soils. Each ellipse corresponds to a major factor that influences OC concentration. Colored text within each ellipse denotes factors that influence OC inputs, sorption capacity, or respiration rate. As sorption capacity increases, so does the OC capacity of the soil. Conversely, as respiration rate (or likelihood) increases, the soil OC capacity decreases. Floodplain soils can only develop high concentrations of OC if there are high rates of OC input. However, the capacity of the soils to store OC regulates that input, and is determined by the competing influences of sorption capacity and respiration rate. See text for further details.

OC sorption capacity reflects a few specific processes. Although soil texture generally relates to the ability of OC to sorb to mineral grains and resulting OC availability, soil chemistry also plays a strong (and potentially dominant) role in regulating OC sorption capacity (Rasmussen et al., 2018). Soil texture is largely determined by valley morphology, according to my modeling (Table 3-1), placing valley morphology and resulting sediment transport dynamics (Gran and Czuba, 2017; Wohl et al., 2017c) as an indirect control on sorption capacity.

Respiration rate is largely determined by microbial activity and the availability of OC to microbes. Erosion can rapidly expose soil OC to microbial respiration (Berhe et al., 2007), whereas soils that reside in largely anoxic conditions can exhibit low rates of microbial respiration (Boye et al., 2017). My results suggesting that moisture controls OC content support the idea that drier soils likely have higher rates of microbial respiration of OC. Moisture is a function of texture, valley bottom morphology, and elevation (a proxy temperature) in my modeling (Table 1). Comparing floodplain types in the MF Snoqualmie, I find that types with standing water exhibit significantly higher soil moisture contents than those without standing water. This indicates spatial variability in moisture content and likely microbial activity (Howard and Howard, 1993). In my modeling, this effect translates to spatial variability in OC concentration within floodplains and across entire basins.

To summarize, I propose that OC inputs are regulated by the capacity of soils to store OC and suppress microbial respiration, allowing OC to accumulate. OC inputs to floodplain soils come from either autochthonous litter accumulation on the floodplain surface, allochthonous wood deposition, or allochthonous deposition of fine, OC-bearing sediments. In these systems, deposition of fine material in overbank flows is rare, leading us to infer that autochthonous litter and allochthonous wood inputs to floodplains dominate OC input. Where soils are more moist, microbial respiration is inhibited and more OC is stored. Although soil texture is likely not a limiting factor on OC concentration in these floodplains, finer textured soils likely have a higher sorption capacity, retaining more of the OC input from decaying plant material.

3.6. Conclusion

I present floodplain soil OC concentration data from two disparate watersheds to compare how inter-basin variability between the two watersheds compares with intra-basin variability in geomorphic and hydrologic characteristics in determining OC concentration. My results indicate that OC concentration in mountain floodplain soils does not vary predictably along a longitudinal gradient, nor does it vary substantially between basins with differing climatic and vegetation characteristics. Instead, geomorphic and hydrologic characteristics, such as valley bottom morphology and soil moisture, dominantly determine floodplain OC concentration.

In my study basins, decaying litter and wood, and not overbank deposition of fine, OC-bearing sediment, is the main source of OC to floodplain soils. It is unclear whether that decaying vegetation is dominated by autochthonous litter inputs from riparian forests or transported downed wood. In comparing my basin to other studied floodplain soils, it seems that vegetation dynamics play a strong role in determining OC concentrations when fine sediment is not regularly deposited on floodplain surfaces. However, I suggest that floodplain soil characteristics, set by geomorphic and hydrologic conditions, regulate how OC inputs translate to the spatial distribution of OC along a river network.

This implies that OC storage in floodplains likely cannot be predicted using consistent, downstream trends, and that management prioritization designed to facilitate floodplain OC storage should be based on local geomorphic and hydrologic process variability within each basin. For instance, management to increase OC sequestration in floodplain soils will likely be more effective where floodplains are unconfined and soils already experience high moisture conditions for much of the year. Along these lines, my results show that modeling the floodplain biospheric OC pool to predict its response to warming and subsequent effects on climate based

on regional factors such as climate and net primary productivity likely misses the substantial inter-basin variability in OC concentration and storage resulting from variability in valley bottom geometry and both geomorphic and hydrologic processes (e.g., Doetterl et al., 2015).

Although my results provide some insights, the question of whether OC stored in floodplain soil comes dominantly from allochthonous versus autochthonous sources remains open. My results imply that more productive, spatially heterogeneous floodplains likely input more OC to soils. Floodplain OC concentration, while mediated largely by moisture dynamics, likely depends mainly on OC inputs from productive riparian forests. This implies that management of OC storage in mountain river floodplains should focus on the restoration of riparian zones to maintain OC input to soil (e.g., Bullinger-Weber et al., 2014). More detailed studies in regions with varying sediment transport and hydrologic regimes are needed to determine what conditions favor autochthonous versus allochthonous OC inputs, but my results suggest that autochthonous sources dominate floodplain OC storage in basins with relatively low rates of vertical accretion and high channel-floodplain connectivity that promotes floodplain wetlands.

3.7 Data Availability

All data supporting the analyses presented here can be found in the CSU Digital Repository (Scott and Wohl, 2018a).

Chapter 4 : Geomorphology and Climate Interact to Control Organic Carbon Stock and Age in Mountain River Valley Bottoms

4.1 Summary

Organic carbon (OC) stored in dead vegetation and soil represents a massive and relatively sensitive pool of carbon whose distribution and residence time affects global climate. Mountain river basins can store large OC stocks. However, the distribution, magnitude, and residence time of OC stored in mountain river valley bottoms remain unquantified on broad scales, hampering understanding of how these regions contribute to terrestrial OC cycling. I compare four disparate mountain river basins to show that mountain river valley bottoms store substantial OC stocks in floodplain soil and downed wood that vary with valley bottom form and geomorphic processes. I quantify soil OC radiocarbon age to show that soil burial is essential to preserving old OC. Valley bottom morphology, soil retention, and vegetation dynamics determine partitioning of valley bottom OC between soil and wood, implying that modern biogeomorphic process and the legacy of past erosion regulate the modern distribution of OC in river networks. The age of the floodplain soil OC pool and the distribution of OC between wood and soil imply that mountain rivers are highly sensitive to alterations in soil and wood retention, which may have both short- and long-term feedbacks with the distribution of OC between the land and atmosphere.

4.2 Introduction

Carbon stored in soil and organic material in freshwater systems is substantial (Aufdenkampe et al., 2011) and varies in both spatial distribution (Battin et al., 2008; Sutfin et

al., 2016; Sutfin and Wohl, 2017; Wohl et al., 2017a) and residence time (Barnes et al., 2018; Omengo et al., 2016). Carbon dynamics in these systems can thus strongly regulate carbon emissions to and sequestration from the atmosphere (Berner, 1990; Stallard, 1998), regulating global climate. While numerous measurements have been made of the radiocarbon age of particulate OC in transport, especially in large river basins (Barnes et al., 2018; Schefuß et al., 2016; Tao et al., 2015; Xue et al., 2017), the stock and corresponding age of OC stored in river corridors (Harvey and Gooseff, 2015) has yet to be quantified on broad scales.

OC that enters the fluvial network can either be stored, commonly as downed wood or soil (Sutfin et al., 2016), or exported. If not stored, OC can be respired by microbial activity (Falloon et al., 2011; Jobbágy and Jackson, 2000) or exported to a long-term sedimentary sink, such as the ocean (Blair and Aller, 2012). Erosion of OC-bearing sediment strongly regulates the fate of OC and whether that OC is stored long-term or respired to the atmosphere (Doetterl et al., 2016; Hilton, 2017; Wang et al., 2017). Modeling indicates that sedimentation dynamics should regulate the age of OC in floodplain soils (Torres et al., 2017), complementary to the idea that geomorphic processes regulate OC concentrations in those soils (Lininger et al., 2018; Sutfin and Wohl, 2017; Wohl et al., 2017a; Chapter 3) as well as wood loads in valley bottoms (Chapter 2).

Despite the importance of erosion and the transport of wood and soil in determining the fate of OC in river networks, there is still a need for extensive quantification of the valley bottom OC stock and its residence time. Here, I quantify the OC stock in downed wood and floodplain soil in four mountain river basins across the western United States. I complement this quantification of stock with an expansive sample of radiocarbon dates of floodplain soil bulk carbon to quantify the residence time of OC in mountain river floodplain soils. In doing so, I present a novel characterization of an important component of the terrestrial carbon pool and

determine the role of mountain river basins in terrestrial carbon dynamics. I contextualize this characterization in terms of the geomorphic and geologic history of the study basins to draw broad, testable inferences regarding the interactions between climate, geomorphology, and OC dynamics in valley bottoms.

4.3 Methods

I stratified and randomly sampled four disparate basins to quantify the valley bottom OC stock in wood and soil (Figure 4-1). The Middle Fork Snoqualmie, in the central Cascade Range of Washington, has a mean annual precipitation of 3.04 m (Oregon State University, 2004), 2079 m of relief, a 407 km^2 drainage area, and erosion rates ranging from 0.05 to 0.33 mm/yr (Reiners et al., 2003). The MF Snoqualmie exhibits glaciogenic topography with small glaciers still evident in headwaters and dominantly thick forests of fir and hemlock, with thinner, younger forests lower in the basin where clearcut logging was widespread over the last century. The Big Sandy, in the Wind River Range of Wyoming, exhibits a mean annual precipitation of 0.72 m (Oregon State University, 2004), 1630 m of relief, a 114 km^2 drainage area, and erosion rates that are likely significantly lower than those in basins studied in Washington, based on erosion rates generally < 0.1 mm/yr in nearby ranges (Garber, 2013; Kirchner et al., 2001). Similar to the MF Snoqualmie, the Big Sandy exhibits broad, glacially carved valleys and recently extensive glaciers (with remnants near summits), but generally sparse, parkland forests(Fall, 1994) of pine, spruce, and fir with broad grassy meadows. The Sitkum and South Fork Calawah basins, in the Olympic Mountains of Washington, exhibit similar precipitation (3.61 and 3.67 m, respectively (Oregon State University, 2004)), drainage area (112 and 85 km^2, respectively), identical 1024 m relief, and exhumation rates between 0.3 and 0.7 mm/yr (Brandon et al., 1998). Both basins

exhibit deeply incised fluvial canyons, likely due to a lack of glacial erosion. Despite their similarity, the Sitkum has been extensively clearcut since the 1940s, whereas the SF Calawah is relatively pristine, residing in Olympic National Park (designated in 1938).

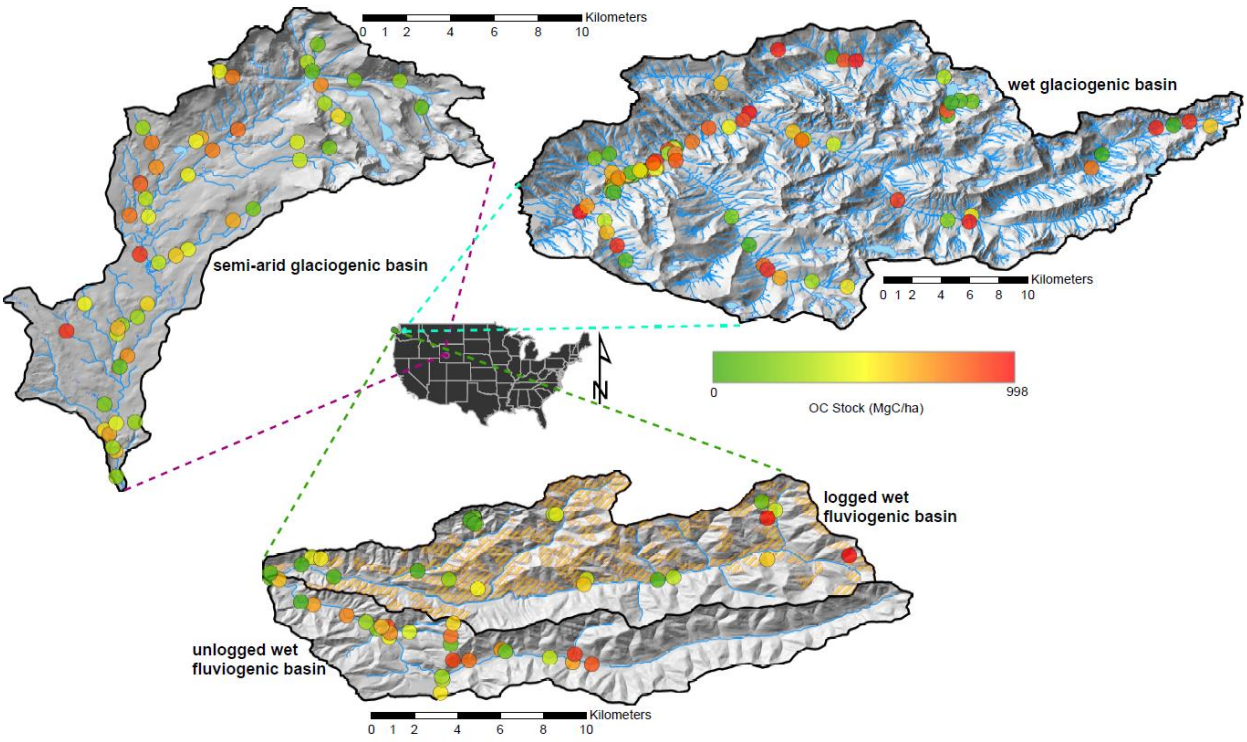

Figure 4-1: Map showing the location, topography, sampling sites, and stream network of the sampled basins. Clockwise, from upper left: Big Sandy watershed, Wyoming; MF Snoqualmie watershed, Washington; Sitkum (north) and SF Calawah (south) watersheds, Washington. Circles represent sampling locations, colored by total OC stock (wood and soil). The orange overlay in the Sitkum basin represents areas that have experienced recorded clearcut timber harvest.

To simplify my presentation of results, I categorize these basins by climate and erosion rate (which generally relate to an order of magnitude) and geomorphic legacy, or whether the valley bottoms display dominantly glaciogenic or fluviogenic topography. I term the MF Snoqualmie, with its moderate erosion rate, wet climate, and glaciogenic lakes and broad valley bottoms as the *glaciogenic, wet* basin. In contrast, I term the Big Sandy, with its low erosion rate,

semi-arid climate, and glaciogenic broad valley bottoms as the *glaciogenic, semi-arid* basin. Finally, I term the Sitkum and SF Calawah, which exhibit the highest erosion rate, wettest climate, but most fluvially incised, narrow valley bottoms as the *fluviogenic, wet* basins. I further subset the Sitkum as the *logged* fluviogenic, wet basin and the SF Calawah as the *unlogged* fluviogenic, wet basin.

I sampled field basins in summer 2016 (Sitkum, SF Calawah, and Big Sandy) and summer 2017 (MF Snoqualmie). In the fluviogenic, wet basins, I randomly located five samples along each of five stream order strata in each basin. Due to accessibility issues, I surveyed 34 of the original 50 randomly sampled locations, which I supplemented with 16 subjectively chosen sites, for a total of 50 measured reaches. In the Big Sandy, I was able to utilize a 10 m DEM and high-resolution aerial imagery to stratify the river network by confinement (unconfined if the channel width occupied less than half the valley bottom, and confined otherwise) and then into five drainage area strata. I then randomly sampled five reaches in each of these ten strata. My eventual sample included 48 out of 50 randomly sampled sites, supplemented by 4 subjectively chosen sites, for a total of 52 samples. In the MF Snoqualmie, I stratified the stream network by bed slope (from a 10 m DEM) into four strata, within which I randomly located ten sample sites. The large width of the floodplain in the lower portion of this basin necessitated separate stratification of that floodplain into individual geomorphic units (fill, point bar, oxbow lake, wetland, and undifferentiated floodplain). Within each of these units, I randomly sampled six points to take soil cores to supplement my soil sampling throughout the rest of the basin. This resulted in a total of 30 randomly sampled sites within the MF Snoqualmie stratified by floodplain type in addition to 38 randomly sampled and eight subjectively sampled sites stratified by slope throughout the basin.

At each sample site in all four basins, I measured the total channel and floodplain wood load in jams and individual pieces within a reach surrounding the site defined as either 100 m or 10 channel widths, whichever was shorter (see Chapter 1 for detailed wood load measurement methodology). I converted total wood volume per unit area to wood OC mass per unit area (stock) by assuming a density based on estimated decay classes assigned to wood pieces and jams in the field (Harmon et al., 2011) and the approximation that half of the wood mass is carbon (Lamlom and Savidge, 2003). I also took a single soil core at a location on the floodplain of each site judged to be representative of the floodplain as a whole, if soil was present. I did not observe floodplain soils in the Sitkum or SF Calawah basins that were sufficiently fine textured to core, and as such, I consider those basins to store negligible soil OC. MF Snoqualmie sites stratified by floodplain type were not explicitly associated with a reach, so I did not measure wood load at those sites.

At all sites where floodplain soil was present, cores were collected to refusal or 1 m depth, with a few exceptions slightly over 1 m in the Big Sandy. Five cores in the Big Sandy, 12 cores in the MF Snoqualmie sites stratified by slope, and 11 cores in the MF Snoqualmie sites stratified by floodplain type did not reach refusal. Samples were refrigerated within 1 – 48 hours after collection, then frozen until analysis. I used loss-on-ignition (Hoogsteen et al., 2015) (LOI) of bulk soil samples (including coarse organic matter, such as buried wood pieces) after drying at 105 °C (to determine moisture) to estimate organic matter concentration, which I converted to OC concentration using a clay-held water correction (Hoogsteen et al., 2015) based on soil texture estimated by feel (Thien, 1979). I used a pedotransfer function (Adams, 1973) to estimate soil bulk density from organic matter (De Vos et al., 2005), allowing us to calculate OC stock at

each site as the average OC concentration multiplied by bulk density, weighted by the proportion of the total core depth occupied by each sample.

I randomly sampled across individual soil samples in the MF Snoqualmie and Big Sandy basins (the only two with floodplain soil) to select samples to be analyzed for ^{14}C age. I randomly selected 11 soil samples in each of the four MF Snoqualmie slope strata that had soil samples (the highest gradient stratum had so few samples that exhibited floodplain soil that I excluded it). I randomly selected four samples from each of the MF Snoqualmie floodplain type strata as well. In the Big Sandy, I randomly selected six samples from each of the unique combinations of drainage area class and confinement strata. If too little soil was left after LOI analysis, I replaced the random sample with one of similar characteristics, if possible. This resulted in a total of 121 samples split between the Middle Fork Snoqualmie and Big Sandy basins that I analyzed for radiocarbon age.

I dried each radiocarbon sample in an oven at 100 °C for 24 hours before sending samples to DirectAMS (Zoppi et al., 2007) for radiocarbon dating of bulk sediment, integrating all carbonaceous sources in the sample and providing an estimate of the distribution of age of all carbon that would be measured in a process such as LOI. I used OxCal 4.3 (Ramsey, 2001) to calibrate samples using both the IntCAL13 (Reimer et al., 2013) and Bomb13NH1 (Hua et al., 2013) calibration curves, depending on the uncalibrated radiocarbon age. My modeling and data reporting utilize the best estimate of the median age of the bulk carbon in each sample, based on the most appropriate calibration curve. This allowed us to estimate the distribution of age of the carbon stock measured in each study basin.

Field measurements (listed in Table 4-1) were inconsistent across basins because field protocol evolved during the course of the study. I measured confinement and channel bed slope

in all basins. I estimated a proxy for stream power by multiplying the drainage area, bed slope, and average basin-wide annual precipitation (Oregon State University, 2004) at each reach. I also measured bankfull width and depth in the MF Snoqualmie, bankfull width in the Sitkum and SF Calawah (generally equivalent to valley bottom width, since almost all reaches were tightly confined by their valley walls), and valley bottom width in the Big Sandy. In the MF Snoqualmie, I classified dominant bedform (Montgomery and Buffington, 1997), classified streams as being either multithread or single thread, and noted whether grasses, shrubs, or trees were present at each soil core site. I also visually classified the dominant channel bed material as either sand (< 2mm), pebble (2-64 mm), cobble (64-256 mm), boulder (> 256 mm), or bedrock. I did not measure channel-specific variables for floodplain-stratified sites in the MF Snoqualmie, since such sites were not clearly associated with a specific reach. I used a 10 m DEM and National Land Cover Database data (Homer et al., 2015) to measure elevation, the mean slope of the basin draining to each reach (including hillslopes and channels), canopy cover, and land cover classification, and drainage area.

Table 4-1: Matrix of variables measured in each basin and model group (note the MF Snoqualmie is split by samples stratified by floodplain type and those stratified by channel slope). Variables in italics are relevant response variables for comparisons or models presented in this study. Y indicates the variable was measured, N indicates that it was not measured, and NA indicates that it does not apply to the particular basin or model group. For soil-specific variables in the Sitkum and SF Calawah, NA is listed because soil retention in those basins is negligible.

Model Group	**Variables Measured**																										
	Wood Load	*Soil OC Stock*	*Soil Depth*	*^{14}C Age*	Confinement	Bedform	Channel Slope	Bed Material	Multithread	Valley Width	Bankfull Width	Bankfull Depth	Stream Power	Floodplain Type	Standing Water	Clay Content	Moisture	Grasses Present	Shrubs Present	Trees Present	Elevation	Basin Slope	Canopy Cover	NLCD	OC %	OC Peak	Drainage Area
MF Snoqualmie stratified by slope	Y	Y	Y	Y	Y	Y	Y	Y	Y	Y	Y	Y	Y	NA	NA	Y	Y	Y	Y	Y	Y	Y	Y	Y	Y	Y	Y
MF Snoqualmie stratified by floodplain type	N	Y	Y	Y	NA	NA	NA	NA	NA	NA	NA	NA	NA	Y	Y	Y	Y	Y	Y	Y	Y	NA	Y	Y	Y	Y	NA
Big Sandy	Y	Y	Y	Y	Y	N	Y	N	N	Y	N	N	Y	NA	NA	Y	Y	N	N	N	Y	Y	Y	Y	Y	Y	Y
Sitkum	Y	NA	NA	NA	Y	N	Y	N	N	Y	N	N	Y	NA	NA	NA	NA	N	N	N	Y	Y	Y	Y	NA	NA	Y
SF Calawah	Y	NA	NA	NA	Y	N	Y	N	N	Y	N	N	Y	NA	NA	NA	NA	N	N	N	Y	Y	Y	Y	NA	NA	Y

I compared my measured OC stocks to upland OC stocks in downed wood and soil using data from Smithwick et al. (2002), who measured those OC pools for the Washington Cascades. The MF Snoqualmie was the only basin with sufficient data to perform this comparison. I performed this comparison both in terms of the total mass of OC stored and the mass of OC stored per unit area. To determine total OC mass in the MF Snoqualmie, I first estimated stream length for the entire network by sampling strata. I used my maps of unconfined floodplain surfaces and estimates of valley width for each stratum to compute a total valley bottom area for each stratum and for the entire basin, in addition to the total surface area (uplands and valley bottoms) for the basin (Table 4-2). The OC mass in each stratum was computed by multiplying the OC stock in both wood and soil for that stratum as appropriate. The OC mass for uplands was computed by multiplying estimates of the soil and downed wood OC stock data of Smithwick et al. (2002) for the Washington Cascades by the total non-valley bottom area of the basin. Using these estimates, I was able to compute the proportion of OC mass stored in valley bottoms as well as the proportion of total basin area taken up by valley bottoms. Uncertainty in these estimates was computed by redoing calculations with the low and high end of the 95% confidence intervals on the median estimates for OC stock and valley width.

Table 4-2: All estimates used in computing total OC mass and surface area in valley bottoms, and uplands for the Middle Fork Snoqualmie basin. Value refers to a measured value in GIS (stream lengths, area of floodplain strata, area of entire basin) with no estimated uncertainty, or a median value computed from a set of values. Low refers to the low end of the 95% confidence interval on the median, where appropriate. High refers to the high end of the 95% confidence interval on the median, where appropriate.

Estimate	**Units**	**Value**	**Low**	**High**
stream length in pool-riffle strata for floodplain stratified portion of basin	m	30625		
stream length in plane-bed strata for floodplain stratified portion of basin	m	7253		
stream length in step-pool strata for floodplain stratified portion of basin	m	9695		
stream length in cascade strata for floodplain stratified portion of basin	m	2539		
stream length in pool-riffle strata for whole basin	m	72091		
stream length in plane-bed strata for whole basin	m	28963		
stream length in step-pool strata for whole basin	m	117942		
stream length in cascade strata for whole basin	m	362688		
stream length in pool-riffle strata for slope stratified portion of basin	m	41467		
stream length in plane-bed strata for slope stratified portion of basin	m	21710		
stream length in step-pool strata for slope stratified portion of basin	m	108247		
stream length in cascade strata for slope stratified portion of basin	m	360149		
valley width in pool-riffle strata	m	181	94	327
valley width in plane-bed strata	m	110	41	584
valley width in step-pool strata	m	40	19	121
valley width in cascade strata	m	10	7	18
area of undifferentiated floodplain for floodplain-stratified part of basin	ha	296.78		
area of fill for floodplain-stratified part of basin	ha	6.03		
area of oxbow lakes for floodplain-stratified part of basin	ha	7.40		
area of point bars for floodplain-stratified part of basin	ha	45.17		
area of wetlands for floodplain-stratified part of basin	ha	9.56		
area of fill for floodplain-stratified part of basin	Mg C / ha	11.58	0.21	94.58
wood OC stock in plane-bed strata	Mg C / ha	9.90	0.16	90.08

wood OC stock in step-pool strata	Mg C / ha	41.98	5.24	149.52
wood OC stock in cascade strata	Mg C / ha	20.24	6.86	66.36
soil OC stock in pool-riffle strata for slope-stratified part of basin	Mg C / ha	540.78	52.67	883.23
soil OC stock in plane-bed strata for slope-stratified part of basin	Mg C / ha	464.02	115.16	579.05
soil OC stock in step-pool strata for slope-stratified part of basin	Mg C / ha	263.14	0.00	679.34
soil OC stock in cascade strata for slope-stratified part of basin	Mg C / ha	0.00	0.00	129.73
soil OC stock in undifferentiated floodplain strata for floodplain-stratified part of basin	Mg C / ha	336.69	188.74	393.21
soil OC stock in fill strata for floodplain-stratified part of basin	Mg C / ha	196.06	21.76	285.41
soil OC stock in oxbow lake strata for floodplain-stratified part of basin	Mg C / ha	120.39	82.05	321.06
soil OC stock in point bar strata for floodplain-stratified part of basin	Mg C / ha	142.97	112.07	380.92
soil OC stock in wetland strata for floodplain-stratified part of basin	Mg C / ha	166.07	28.73	708.15
area of entire basin (uplands and valley bottoms)	ha	40979.80		
area of valley bottoms throughout basin	ha	2158.84	1280.46	4953.85
Smithwick et al. (2002) soil OC to 1 m upland stock for Washington Cascades	Mg C / ha	102.45	59.90	204.80
Smithwick et al. (2002) coarse downed wood logs upland stock for Washington Cascades	Mg C / ha	42.60	16.60	84.90

Statistical analyses were performed using the R statistical package (R Core Team, 2017). I modeled OC stock and OC radiocarbon age to quantify the variability in the magnitude and age of the floodplain soil OC pool. Modeling soil depth allowed us to determine controls on soil retention. Using multiple linear regression, I modeled the OC stock, soil depth, and median radiocarbon age in the Big Sandy and MF Snoqualmie, with individual sample sites (reaches) used as sample units for models of OC stock and soil depth, and individual, dated soil samples used as sample units for modeling radiocarbon age. I separate the MF Snoqualmie into slope and floodplain stratified sites for the purpose of modeling, due to differences in measured variables

for each of those strata. I first performed univariate analysis between each hypothesized predictor and response, filtering out variables that appear to have a completely random relationship with the response, based on visual examination, Wilcoxon rank-sum tests (Wilcoxon, 1945), and/or Spearman correlation coefficients. I model each response variable using all subsets multiple linear regression with a corrected Akaike Information Criterion as a model selection criteria (Wagenmakers and Farrell, 2004). I iteratively transformed response variables to ensure homoscedasticity of error terms. To determine variable importance, I also consider sample size, p values, and effect magnitudes. I performed comparisons using Wilcoxon rank-sum tests (Wilcoxon, 1945) due to the generally skewed distributions of my data, with a Holm multiple-comparison correction (Holm, 1979) when appropriate. All uncertainties presented represent 95% confidence intervals (CI) on estimates. To test for buried, high-OC concentration layers at depth, I compared each buried soil sample to the sample above it using the criterion that a peak in OC at depth should have an OC concentration 1.5 times that of the overlying sample and be above 0.5% (Appling et al., 2014).

4.4 Results

Both wet, fluviogenic basins store only wood, with negligible soil. In the two glaciogenic basins that store OC in soil and wood, the proportion of OC stored in soil is significantly different ($p < 0.0001$) between the semi-arid glaciogenic basin ($n = 52$, 95% CI on median between 0.95 and 1.00) and wet glaciogenic basin ($n = 44$, 95% CI on median between 0.00 and 0.90). Figure 4-2A shows OC stocks in wood and soil for each basin. Variability in wood load (linearly related to wood OC stock) in all three basins is discussed in detail in Chapter 2.

Soil OC stock across both glaciogenic basins is dominantly controlled by soil moisture and soil depth. In wet glaciogenic basin sites stratified by slope, soil OC stock ($n = 44$, adjusted $R^2 = 0.87$, $p < 0.0001$, cube root transform) is controlled by moisture content ($\beta = 0.014 \pm 0.0057$), soil depth ($\beta = 0.069 \pm 0.011$), and whether the reach is multithread ($\beta = 1.59 \pm 0.97$). Soil OC stock in wet glaciogenic basin sites stratified by floodplain type ($n = 30$, adjusted $R^2 = 0.67$, $p < 0.0001$, no transform) is controlled by soil depth ($\beta = 3.35 \pm 1.15$) and moisture ($\beta = 1.17 \pm 0.37$). Soil OC stock in semi-arid glaciogenic basin sites ($n = 52$, adjusted $R^2 = 0.81$, $p < 0.0001$, cube root transform) is similarly controlled by soil depth ($\beta = 0.26 \pm 0.0066$) and moisture ($\beta = 0.0093 \pm 0.0024$). All modeling results are summarized in Table 4-3.

Table 4-3: Matrix of all models, listed by model group, response variable, and scale. Grey fill indicates that a variable was included in model selection. A minus (−) indicates that the variable was selected as important in predicting the response, and denotes an indirect correlation, while a plus (+) indicates a direct correlation. For Confinement, a plus indicates that unconfined streams display a higher magnitude response variable. OC Peak refers to whether the sample was classified as a peak in the vertical OC profile. NA indicates that the variable is not applicable as a predictor for the model. [1]No significant results were observed for this model.

Model Group	**Response**	**Variables**																						
		Confinement	Bedform	Channel Slope	Bed Material	Multithread	Valley Width	Bankfull Width	Bankfull Depth	Stream Power	Floodplain Type	Standing Water	Soil Depth	Clay Content	Moisture	Grasses Present	Shrubs Present	Trees Present	Elevation	Basin Slope	Canopy Cover	NLCD	OC %	OC Peak	Drainage Area
MF Snoqualmie stratified by slope	OC (MgC/ha)					+					NA	NA	+		+								NA	NA	
	Soil Depth (cm)	−		+							NA	NA	NA											NA	
	Median ^{14}C age (yr BP)										NA	NA	+											+	
MF Snoqualmie stratified by floodplain type	OC (MgC/ha)	NA	NA	NA	NA	NA	NA	NA	NA	NA			+		+								NA	NA	NA
	Soil Depth (cm)[1]	NA	NA	NA	NA	NA	NA	NA	NA	NA			NA											NA	NA
	Median ^{14}C age (yr BP)	NA	NA	NA	NA	NA	NA	NA	NA	NA			+												NA
Big Sandy	OC (MgC/ha)		NA		NA	NA		NA	NA		NA	NA	+		+	NA	NA	NA					NA	NA	
	Soil Depth (cm)	−	NA	+	NA	NA		NA	NA		NA	NA	NA			NA	NA	NA	−					NA	
	Median ^{14}C age (yr BP)	+	NA		NA	NA		NA	NA		NA	NA	+			NA	NA	NA							

Soil depth, a primary control on OC stock, is dominantly controlled by confinement and channel bed slope. Modeling soil depth as a proxy for soil retention in wet glaciogenic basin sites stratified by floodplain type yielded no significant results. Soil depth in wet glaciogenic basin sites stratified by slope (n = 44, adjusted $R^2 = 0.56$, $p < 0.0001$, cube root transform) is controlled by channel bed slope ($\beta = -4.79 \pm 2.14$) and whether the stream is unconfined ($\beta = 1.05 \pm 0.64$). Soil depth in semi-arid glaciogenic basin sites (n = 52, adjusted $R^2 = 0.56$, $p < 0.0001$, cube root transform) is controlled by elevation ($\beta = -0.00073 \pm 0.00080$), channel bed slope ($\beta = -1.68 \pm 1.20$), and whether the stream is unconfined ($\beta = 0.48 \pm 0.49$).

Comparing wet glaciogenic basin sites (n = 74, 95% CI on median between 123.37 and 263.14) to comparable upland sites (n = 10, 95% CI on median between 59.90 and 204.80) measured by Smithwick et al. (2002), I find that floodplain soils may store higher OC stocks than uplands ($p = 0.11$) Using estimates of valley bottom area and the total area of my wet, glaciogenic study basin, I find that valley bottoms (2159^{+2795}_{-878} ha) take up only 5^{+7}_{-2} % of the total land surface area, but store 12^{+14}_{-9} % ($0.79^{+2.89}_{-0.69}$ Tg OC) of the total OC mass in the basin, indicating that valley bottoms, at least in this basin, are disproportionately important in storing OC compared to their surface area. However, I note that uncertainties in these estimates are large and overlapping, indicating that more data is necessary to fully evaluate this finding. I was unable to find comparable upland data for other study basins.

Floodplain soil OC is moderately old (10^2 yr) in these study basins, and its age is dominantly controlled by sample depth below the ground surface, confinement, and whether the sample is a peak in the vertical profile of OC (Figure 4-2). I found no significant difference in median radiocarbon age of floodplain OC between the two study basins. Bulk carbon in soils sampled in the semi-arid glaciogenic basin (median age 126 yr BP) and wet glaciogenic basin

(age 425 yr BP) ranges in age from modern (≤ 0 years before 1950) to 6179 yr BP, and the median OC age across both basins is 185 yr BP (Figure 4-2). In wet glaciogenic basin soil samples stratified by slope (n = 44, adjusted $R^2 = 0.57$, $p < 0.0001$, no transformation), sample depth below ground surface ($\beta = 15.39 \pm 6.26$) and whether the sample exhibited a peak in the vertical profile of OC ($\beta = 665.76 \pm 500.87$) controlled median radiocarbon age. In wet glaciogenic basin soil samples stratified by floodplain type (n = 20, no transformation), only depth below ground surface was found to directly correlate to radiocarbon age (Spearman $\rho = 0.41$, 95% CI between 0.22 and 0.58). In semi-arid glaciogenic basin soil samples (n = 57, adjusted $R^2 = 0.47$, $p < 0.0001$, no transformation), sample depth below ground surface ($\beta = 21.32 \pm 8.20$) and whether the reach was unconfined ($\beta = 392.98 \pm 337.09$) controlled median radiocarbon age.

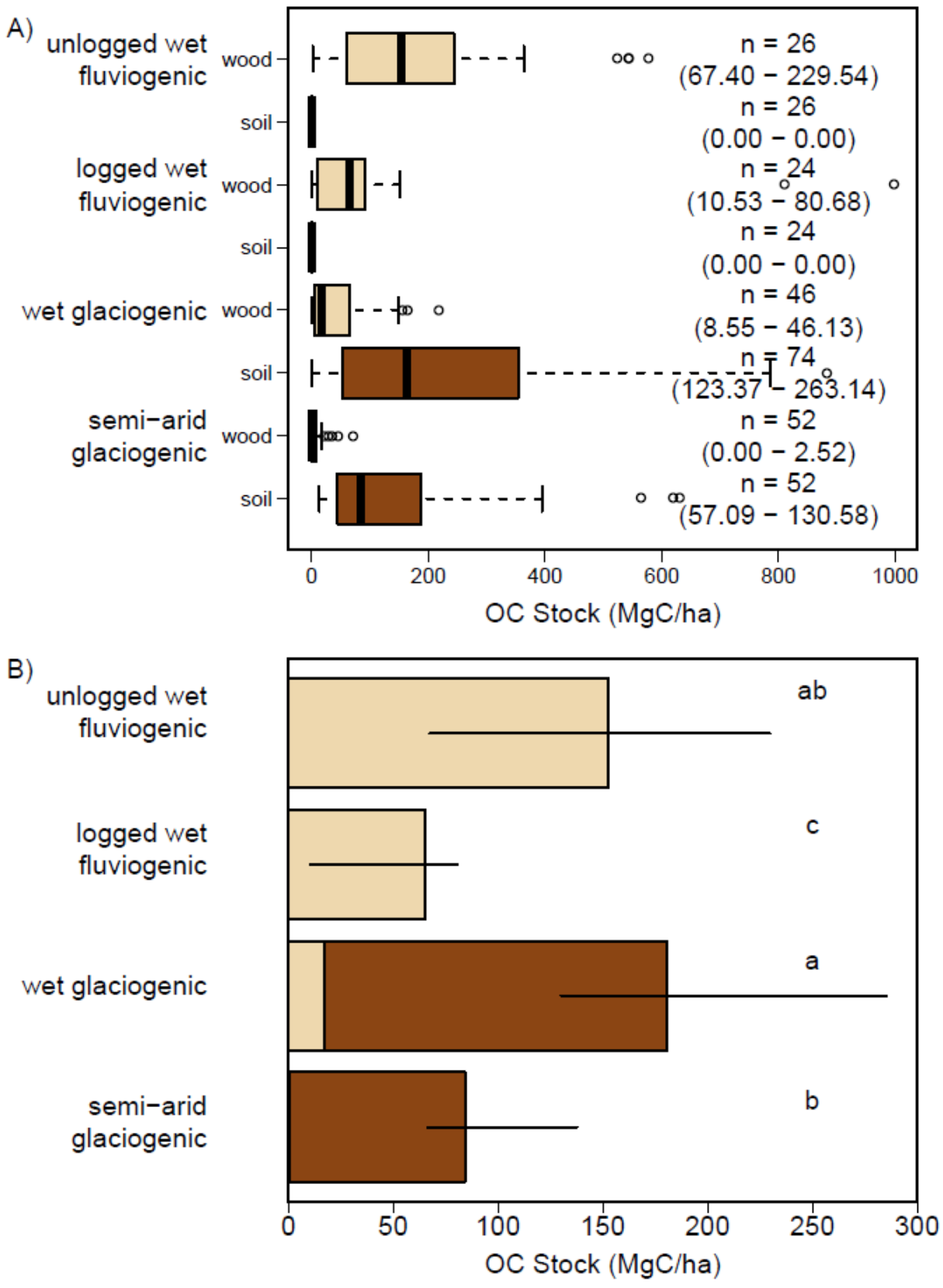
A)
unlogged wet fluviogenic
wood
soil
logged wet fluviogenic
wood
soil
wet glaciogenic
wood
soil
semi−arid glaciogenic
wood
soil
n = 26
(67.40 − 229.54)
n = 26
(0.00 − 0.00)
n = 24
(10.53 − 80.68)
n = 24
(0.00 − 0.00)
n = 46
(8.55 − 46.13)
n = 74
(123.37 − 263.14)
n = 52
(0.00 − 2.52)
n = 52
(57.09 − 130.58)
0
200
400
600
800
1000
OC Stock (MgC/ha)
B)
unlogged wet fluviogenic
logged wet fluviogenic
wet glaciogenic
semi−arid glaciogenic
ab
c
a
b
0
50
100
150
200
250
300
OC Stock (MgC/ha)

Figure 4-2: Boxplot of OC stock in wood (tan) and soil (brown) for each basin. Boxplots (A) show distribution of data, including the lack of soil in the SF Calawah and Sitkum (unlogged and logged wet fluviogenic basins, respectively). Bold lines represent median, box represents interquartile range, dashed lines represent 1.5 times the interquartile range, and circles represent outliers. Sample size (n) and 95% confidence interval on median estimates (shown in parentheses) are given for each group. Stacked bar plots (B) show the median total OC stock for each basin, separated into wood (tan) and soil (brown). Error bars represent the 95% CI on the median. Letters a-c represent significant differences based on combined examination of 95% CI and pairwise wilcoxon rank-sum tests. Note that the unlogged and logged wet fluviogenic basins contain negligible floodplain soil, and hence a zero value for soil OC stock.

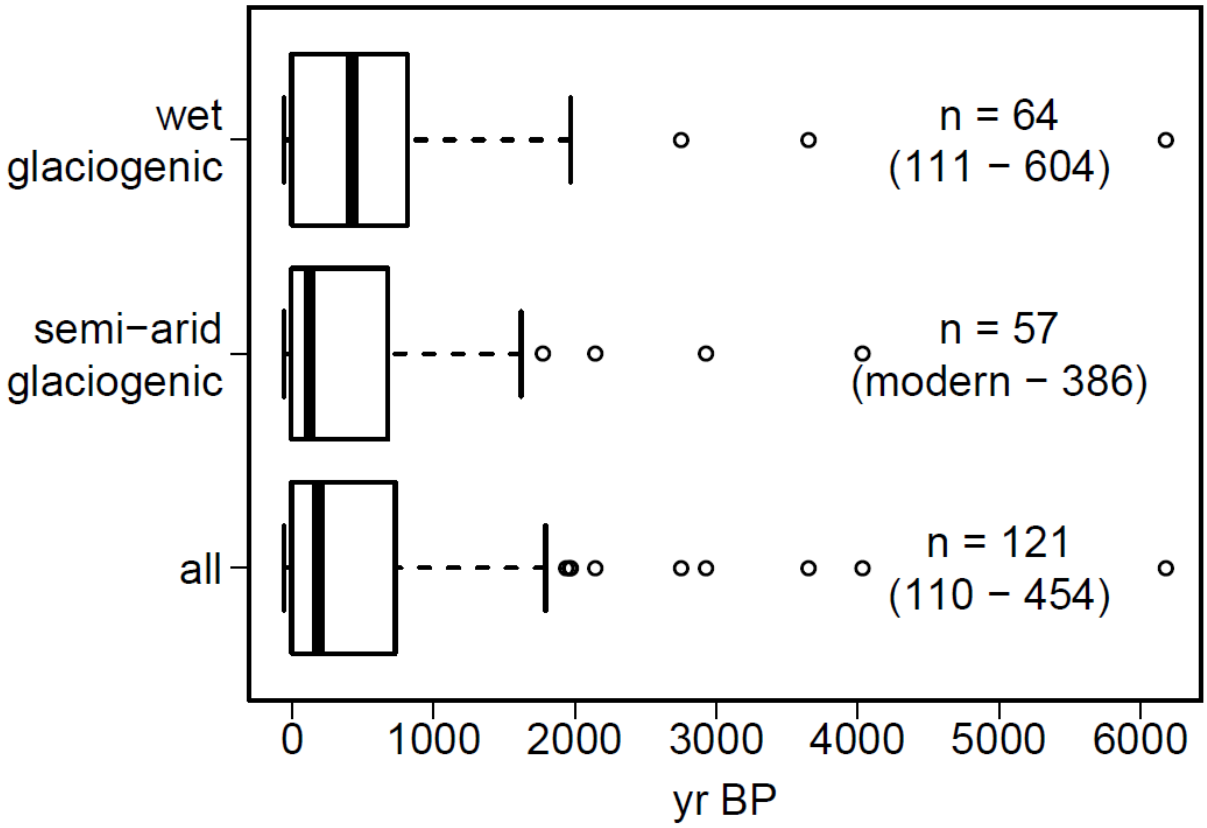

Figure 4-3: Boxplot of floodplain soil OC sample median radiocarbon age. Bold lines represent median, box represents interquartile range, dashed lines represent 1.5 times the interquartile range, and circles represent outliers. Sample size (n) and 95% confidence interval on median estimates (shown in parentheses) are given for each group.

4.5 Discussion

Increased soil retention (both in terms of valley width and soil depth) leads to a higher mass of OC by storing more deep soil over a larger area and to the preservation of older OC. Along with likely storing more soil OC than uplands (Lininger et al., 2018; Wohl et al., 2012), a nearly 200 yr BP median age shows that floodplain soils store OC over moderate timescales, preventing fast respiration to the atmosphere. In addition, deep burial in floodplain deposits where microbial respiration is likely inhibited can lead to biospheric OC storage on timescales of up to 10^3 years (median age of buried OC peaks is 1056 yr BP, with a 95% CI ranging from modern to 2750 yr BP), even in these mountainous rivers. Modeling of floodplain soil OC age indicates that buried samples tend to be significantly older than samples near the surface, and buried OC-rich layers (preserved OC peaks in the vertical soil profile) in the wet glaciogenic basin tend to be older than other samples. (I was unable to test this for the semi-arid glaciogenic basin due to a lack of preserved OC peaks at depth.) In the semi-arid glaciogenic basin, OC from unconfined streams is generally older than that from confined streams, indicating that unconfined streams likely have a longer floodplain turnover time, allowing buried OC to be preserved. Essentially, packets of soil OC that are more shielded from the atmosphere (deeply buried) and from rapid lateral migration (in reaches with wider valleys and presumably slower floodplain turnover times) can be preserved longer than shallower soils in confined valleys that are eroded more rapidly. This indicates that burial of soil OC in wide, retentive valley bottoms is the dominant process in preserving old OC in these basins, a trend that fits with both modeling (Torres et al., 2017) and field observations (Barnes et al., 2018).

Net changes in wood and soil retention due to activities such as grazing in the semi-arid glaciogenic basin or forest harvest in the wet glaciogenic basin have likely caused substantial

redistribution of OC and potential sequestration lower in the network (Wohl et al., 2017a, 2017c; Wohl and Scott, 2016). A century-scale turnover of the majority of the substantial floodplain soil OC pool indicates that changes in soil retention and resulting storage of OC (e.g., due to land use change) should be tightly linked to OC respiration rate to the atmosphere over moderate timescales. Although OC likely turns over more rapidly in the mountainous basins studied here, it may be stored for longer periods of time lower in the river network after being eroded (Doetterl et al., 2016; Van Oost et al., 2012; Schook et al., 2017; Wang et al., 2017), depending on sedimentation dynamics (Torres et al., 2017). Changes in retention of the mountain river valley bottom OC stock may have rapid (due to generally short turnover times) and substantial (due to its high magnitude) effects on the distribution of OC between the atmosphere and terrestrial storage. My modeling indicates that soil depth, a proxy for retention, is largely a function of erosivity (the efficiency of soil erosion and transport downstream), with wider, lower gradient valley bottoms storing deeper soils and more OC. Wood load in these basins is likely a function of wood supply, governed by climate and land use, and spatial heterogeneity, which regulates how efficiently valley bottoms can trap wood (Chapter 1).

My comparison of disparate basins shows that where there is an abundant source of wood (e.g., wet basins with dense forests), wood acts as a substantial OC pool (Chapter 1). However, where forests are sparse (e.g., the semi-arid glaciogenic basin), soil is by far the dominant valley bottom OC pool. When taken in the context of radiocarbon analyses of OC in larger rivers (Barnes et al., 2018; Schefuß et al., 2016; Xue et al., 2017), my results indicate substantially faster soil OC cycling in mountainous, headwater basins, in contrast to sites lower in river networks, where burial of OC may lead to longer OC preservation (Blazejewski et al., 2009; Ricker et al., 2013). However, soil burial in any portion of the network can lead to long OC

residence time (on the order of 10^3 yr). It is uncertain how the residence time of wood varies with basin size, but burial of wood in floodplains, which can lead to exceptionally long-term preservation, likely only occurs in unconfined, wider reaches. Wood retention is also likely easier and more commonly managed (Roni et al., 2015) than soil (Bullinger-Weber et al., 2014), as wood trapping structures or direct wood placement can both enhance wood loads. The partitioning of OC between wood and soil has direct implications for best management practices in terms of restoring OC stocks to anthropogenically influenced valley bottoms. For instance, my results imply that attempting to increase soil OC stock in wet, fluviogenic basins such as the Sitkum would likely be ineffective due to the naturally low soil retention in such a basin with deeply incised, narrow valleys. Restoring wood there, however, would likely increase the OC stock substantially, if the unlogged wet, fluviogenic basin in this study is representative of potential wood OC stocks.

Climate, by influencing forest characteristics and resulting litter input rates to soils and wood supply to channels, acts as a first-order control on the partitioning of OC between floodplain soil and wood as well as the total valley bottom OC stock. In both the wet and semi-arid glaciogenic basins, floodplain soils store more OC stock than downed wood. However, if I take the unlogged wet fluviogenic basin as an example of wood loads in a pristine basin in the Pacific Northwest, it appears possible that wood OC stock can be of comparable magnitude to soil OC stock (in the wet glaciogenic basin). This implies a strong potential for increasing the OC stock in wood in the wet glaciogenic basin, in which wood loads are likely decreased as a result of logging (Chapter 2). It is also important to note the significant difference between soil OC stocks in the wet versus semi-arid glaciogenic basin. Both of these basins have similar soil retention, as measured by soil depth ($p = 0.85$), but OC concentrations in the wetter basin can be

substantially higher than those in the semi-arid basin, potentially due to difference in OC inputs resulting from differing rates of litter input (Chapter 3).

Comparing the distribution of OC between wood and soil in these basins reveals a strong impact of basin morphology, which is a result of uplift rate, erosion rate and style, and climate. Where valley bottoms are narrow, likely due to a high precipitation rate and accompanying rates of fluvial incision, valleys store negligible amounts of soil, but forests grow dense and wood OC stock can be extremely high, as long as trees go unharvested and can be recruited to channels, as in the two study basins in the Olympics (Chapter 2). In the semi-arid glaciogenic basin, low uplift rate, glaciogenic valleys, and dry climate correspond to broad valley bottoms but sparse forests, resulting in almost negligible wood OC stock (Chapter 2) and only moderate soil OC storage, likely due to low rates of litterfall input (Chapter 3). Where the climate is wet, uplift is moderately high, but valleys are widened by recent glaciation, I observe both broad valley bottoms and dense forests, leading to substantial OC stocks in soil in the wet glaciogenic basin. Given that the wet glaciogenic basin has been extensively logged, it is likely that total OC stocks there were much higher than either the wet fluviogenic or semi-arid glaciogenic basins until the last century. Valley bottoms of the wet glaciogenic basin represent a peak in potential OC stock due to dense forests; wide, retentive valley bottoms; and high rates of OC input from vegetation.

4.6 Conclusion

The legacies of glaciation and tectonics, combined with geomorphic processes, determine the distribution, magnitude, and age of the OC stock in mountain river valley bottoms. Here, I show through extensive field observation that this OC pool is highly variable both spatially and temporally, but that geomorphic processes can explain that variation. Burial and preservation of

OC-rich soil is essential to preserving soil OC past the median age in these floodplains of around 200 years. Deeper soils in unconfined valleys, especially those that were unusually OC-rich, reaches ages up to a few thousand years. Valley bottom geometry, forest stand characteristics (directly affected by land use), and climate interact to regulate the retention of both wood (Chapter 2) and soil. This implies that managing the substantial valley bottom OC stock necessitates a careful consideration of geomorphic process and form. Future examination of carbon sequestration efforts in river corridors (e.g., Bullinger-Weber et al., 2014) will test this inference by determining the rate and magnitude at which OC can be restored to floodplain soils in varying environments.

The century-scale turnover time of much of the soil OC measured in these basins implies a close coupling between soil retention and the distribution of OC across the landscape and between the land and atmosphere. The alteration of valley bottom morphology and resulting changes in soil OC retention likely influence the fate of OC sequestered in high primary productivity (Schimel and Braswell, 2005) mountain ranges over short (Wohl et al., 2017a, 2017c) and long (Berner, 1990; Molnar and England, 1990) timescales. Changes in soil retention likely alter how much OC reaches downstream water bodies that may sequester OC over longer timescales, thus altering the respiration of that OC to the atmosphere. Future work to quantify the residence time and decay rate of wood in valley bottoms and its eventual fate when exported, in addition to examination of the sources and fate of soil OC, will further constrain and illuminate this feedback.

4.7 Data Availability

Data to support analyses presented here are available in the CSU Digital Repository (Scott and Wohl, 2018b).

Chapter 5 : Conclusion

In this dissertation, I quantify OC storage in wood and soil across the entirety of four disparate mountain river basins that span three distinct mountain ranges across the western United States. My results indicate that OC storage in mountain river valley bottoms is a function of processes acting on multiple spatial scales, from individual packets of soil to reaches and entire watersheds. At the broadest, inter-basin scale, climate and land use regulate forest stand and vegetation characteristics, thereby regulating OC inputs to valley bottoms in the form of both large wood and decaying plant material that may eventually become floodplain soil OC (Chapters 2 and 3). Similarly, basin morphology reflects the legacy of past broad-scale geomorphic processes; glaciation in two of the study basins has left them with broad valley bottoms that retain soil and associated OC. The interaction between geomorphic legacy at the basin to valley scale and climate regulates the partitioning of OC between soil and wood in valley bottoms (Chapter 4). At the valley to reach scale, modern geomorphic processes regulate the transport and storage of wood and soil. Energy level, valley morphology, and wood and sedimentation dynamics regulate the retention of soil and wood within valley bottoms, exerting a direct control on the magnitude of OC stock stored in those valley bottoms. At the scale of individual packets of soil, geomorphic processes that set soil texture and hydrologic processes that set soil moisture dominantly regulate OC concentration.

Importantly, geomorphologic processes influence OC storage at all scales, whether by setting basin morphology via erosion style (glacial versus fluvial), setting the dynamics between retention and transport at the reach scale, or setting grain size at the scale of individual packets of soil. These geomorphic processes are not well accounted for in either management of the valley

bottom carbon pool or predictions of terrestrial carbon storage in the context of a changing climate.

My research implies that management of the valley bottom OC pool should take into account both the partitioning of OC between wood and soil at the basin scale as well as the highly variable spatial distribution of OC between reaches within a basin. For a given basin, management should prioritize the OC storage mechanisms that are dominant in the basin. For example, attempting to restore high wood loads in the Big Sandy to levels comparable to basins in the Pacific Northwest may be ineffective due to a lack of natural wood supply in that basin. At the reach scale, valley bottom morphology, hydrology, and geomorphic processes must be taken into account to effectively manage the retention of soil and reach-scale wood trapping efficiency. For example, wood restoration will likely be more effective in reaches that are already spatially heterogeneous and have the morphological complexity needed to retain wood in transport.

From the perspective of OC dynamics and fundamental processes, my research implies that geomorphology matters in regulating terrestrial OC storage in mountain river valley bottoms. One of the primary objectives of Earth system models is to understand how carbon moves and resides on the land, before either being stored for long periods of time in the ocean or respired to the atmosphere where it can impact climate. The heterogeneous distribution of carbon on the land hampers estimates of the potential for human activities such as land use change to influence carbon respiration and global climate. My research has shown that although broad-scale processes that regulate primary productivity (e.g., climate) have some influence on OC storage, estimates of OC stock and the residence time of that OC stock in floodplain soil should reflect spatial variability in geomorphic process to better represent the magnitude and dynamics

of the likely substantial valley bottom OC stock. Although it may be unfeasible for global models to take intra-basin variability into account, accounting for geomorphic legacy and regional trends in valley bottom morphology (i.e., retentiveness) may significantly improve estimates of the spatial distribution of OC across the landscape.

This research has numerous caveats. First, I do not fully situate wood OC storage in a temporal context. Ideally, I would have conducted paired radiocarbon and dendrochronology studies on a broad sample of logs in each basin to quantify their residence time in the basin. Such an analysis would allow me to compare wood and floodplain soil in terms of residence time, understand the spatial distribution of wood residence time, and provide a better conceptualization of how the wood component of the valley bottom OC stock fits into terrestrial OC dynamics. Second, my methods are approximate, leading to both unquantifiable uncertainty (e.g., in bulk density estimates used to calculate OC stocks) as well as quantified variability in both OC- and morphology-related measurements used in my modeling. One instance in which a greater sample size and higher precision may have led to more definitive conclusions is in my comparison of the wood piece sizes in the Sitkum and SF Calawah. Although the Sitkum has consistently smaller pieces, there is too much variability to make a definitive conclusion on whether piece size actually differs between basins, and as such, I cannot fully evaluate the hypothesis that logging impacted wood loads in the Sitkum primarily by removing the largest trees that tend to form wood jams. Finally, as with many observational studies, this one suffers from an incomplete understanding of the human legacy in each study basin. While I was unable to find records that would show this, it remains possible that wood loads in the Big Sandy could have been impacted by forest harvest over the past two centuries. Similarly, records for surrounding regions show that Native Americans had a significant impact on the forest structure of the Olympic Peninsula,

but I was unable to locate any information on their use of the SF Calawah basin. No study basin is pristine, but having a more detailed record of human activities would certainly allow for a more rigorous examination of the relatively sensitive processes studied here.

Future work aimed at better understanding terrestrial OC dynamics should focus on the fate of OC as it moves from mountain environments to lowlands and eventually to large marine reservoirs. As noted above, quantifying wood residence time within basins at a broad scale that would permit a powerful estimate of variability in residence time would provide a temporal context for the importance of the wood OC pool. Another major knowledge gap is determining what happens to wood when it is exported to oceans. Export to oceans may result in preferential respiration or preservation of OC in wood, depending on factors such as off-shore transport, wood density and waterlogging, and wood species. However, there has yet to be a study that tracks wood from rivers, through estuaries, and to the coastal environment that quantifies wood breakdown and decay throughout this transition. Although I have shown the importance of wood jams in affecting wood loads, wood jam dynamics are poorly understood. I am not yet able to predict where in a river network wood jams are most stable, and how they behave over multi-year timescales.

With regard to floodplain soil OC, future work could examine floodplain sediment residence times and compare them to the soil OC ages I measured in this study, which could provide insight into whether OC is dominantly being exported via respiration or erosion. This would also provide more evidence to evaluate the source of OC in floodplains, as OC older than the sediment it resides in must have come from upstream. Finally, although I and other researchers have made significant progress in this regard, constraining the spatial distribution of the terrestrial OC sink requires massive, extensive sampling of OC stocks. My work, combined

with the work of others, provides a context for understanding OC spatial distribution in valley bottoms. This will hopefully benefit future work to quantify the mass of OC stored in different components of the landscape (i.e., valley bottoms versus hillslopes) across entire continents, which will eventually be necessary to fully quantify the terrestrial carbon sink and place it in the context of the global carbon cycle.

References

Aberle J, Smart GM. 2003. The influence of roughness structure on flow resistance on steep slopes. Journal of Hydraulic Research **41**: 259–269.

Adams WA. 1973. The Effect of Organic Matter on the Bulk and True Densitites of Some Uncultivated Podzolic Soils. Journal of Soil Science **24**: 10–17.DOI: 10.1111/j.1365-2389.1973.tb00737.x

Appling AP, Bernhardt ES, Stanford JA. 2014. Floodplain biogeochemical mosaics: A multi-dimensional view of alluvial soils. Journal of Geophysical Research: Biogeosciences **119**: 1538–1553.DOI: 10.1002/2013JG002543

Aufdenkampe AK, Mayorga E, Raymond PA, Melack JM, Doney SC, Alin SR, Aalto RE, Yoo K. 2011. Riverine coupling of biogeochemical cycles between land, oceans, and atmosphere. Frontiers in Ecology and the Environment **9**: 53–60.DOI: 10.1890/100014

Ballantyne AP, Alden CB, Miller JB, Tans PP, White JWC. 2012. Increase in observed net carbon dioxide uptake by land and oceans during the past 50 years. Nature **488**: 70–73.DOI: 10.1038/nature11299

Bao H, Kao S, Lee T, Zehetner F, Huang J, Chang Y, Lu J, Lee J. 2017. Distribution of organic carbon and lignin in soils in a subtropical small mountainous river basin. Geoderma **306**: 81–88.DOI: 10.1016/j.geoderma.2017.07.011

Barnes RT, Butman DE, Wilson H, Raymond PA. 2018. Riverine export of aged carbon driven by flow path depth and residence time. Environmental Science and Technology DOI: 10.1021/acs.est.7b04717

Battin TJ, Kaplan L a., Findlay S, Hopkinson CS, Marti E, Packman AI, Newbold JD, Sabater F. 2008. Biophysical controls on organic carbon fluxes in fluvial networks. Nature Geoscience **1**: 95–100.DOI: 10.1038/ngeo602

Battin TJ, Luyssaert S, Kaplan LA, Aufdenkampe AK, Richter A, Tranvik LJ. 2009. The boundless carbon cycle. Nature Geoscience **2**: 598–600.DOI: 10.1038/ngeo618

Beckman ND, Wohl E. 2014. Effects of forest stand age on the characteristics of logjams in mountainous forest streams. Earth Surface Processes and Landforms **39**: 1421–1431.DOI: 10.1002/esp.3531

Beechie TJ, Sibley TH. 1997. Relationships between Channel Characteristics , Woody Debris , and Fish Habitat in Northwestern Washington Streams. Transactions of the American Fisheries Society **126**: 217–229.DOI: 10.1577/1548-8659(1997)1262.3.CO

Benda L. 1990. The influence of debris flows on channels and valley floors in the Oregon Coast Range, U.S.A. Earth Surface Processes and Landforms **15**: 457–466.DOI: 10.1002/esp.3290150508

Benda L, Bigelow P. 2014. On the patterns and processes of wood in northern California streams. Geomorphology **209**: 79–97.DOI: 10.1016/j.geomorph.2013.11.028

Benda L, Miller D, Sias J, Martin D, Bilby R, Veldhuisen C, Dunne T. 2003a. Wood Recruitment Processes and Wood Budgeting. American Fisheries Society Symposium **37**: 49–73.

Benda L, Veldhuisen C, Black J. 2003b. Debris flows as agents of morphological heterogeneity at low-order confluences, Olympic Mountains, Washington. Bulletin of the Geological Society of America **115**: 1110–1121.DOI: 10.1130/B25265.1

Benfield EF. 1997. Comparison of Litterfall Input to Streams. Journal of the North American

Benthological Society **16**: 104–108.DOI: 10.2307/1468242

Benke AC, Wallace B. 2003. Influence of Wood on Invertebrate Communities in Streams and Rivers Wood-Created Habitat. American Fisheries Society Symposium **37**: 149–177.

Berhe AA, Harte J, Harden JW, Torn MS. 2007. The significance of the erosion-induced terrestrial carbon sink. BioScience **57**: 337–346.DOI: 10.1641/B570408

Berner RA. 1990. Global biogeochemical cycles of carbon and sulfur and atmospheric O2 over phanerozoic time. Chemical Geology **84**: 159.

Bertoldi W, Gurnell AM, Welber M. 2013. Wood recruitment and retention: The fate of eroded trees on a braided river explored using a combination of field and remotely-sensed data sources. Geomorphology **180**–**181**: 146–155.DOI: 10.1016/j.geomorph.2012.10.003

Bilby RE. 1984. Removal of Woody Debris May Affect Stream Channel Stability. Journal of Forestry : 609–613.

Bilby RE, Ward JW. 1989. Changes in Characteristics and Function of Woody Debris with Increasing Size of Streams in Western Washington. Transactions of the American Fisheries Society **118**: 368–378.DOI: 10.1577/1548-8659(1989)118<0368:CICAFO>2.3.CO;2

Bilby RE, Ward JW. 1991. Characteristics and Function of Large Woody Debris in Streams Draining Old-Growth, Clear-Cut, and Second-Growth Forests in Southwestern Washington. Canadian Journal of Fisheries and Aquatic Sciences **48**: 2499–2508.DOI: 10.1139/f91-291

Blair N, Leithold EL. 2014. Impacts of watershed processes on exported riverine organic carbon. In Biogeochemical Dynamics at Major River-Coastal Interfaces, Linkages with Global Change , Bianchi TS, Allison MA, and Cai W-J (eds). Cambridge University Press; 174–199.

Blair NE, Aller RC. 2012. The Fate of Terrestrial Organic Carbon in the Marine Environment.

Annual Review of Marine Science **4**: 401–423.DOI: 10.1146/annurev-marine-120709-142717

Blazejewski GA, Stolt MH, Gold AJ, Gurwick N, Groffman PM. 2009. Spatial Distribution of Carbon in the Subsurface of Riparian Zones. Soil Science Society of America Journal **73**: 1733.DOI: 10.2136/sssaj2007.0386

Bocchiola D, Rulli MC, Rosso R. 2006. Transport of large woody debris in the presence of obstacles. Geomorphology **76**: 166–178.DOI: 10.1016/j.geomorph.2005.08.016

Bocchiola D, Rulli MC, Rosso R. 2008. A flume experiment on the formation of wood jams in rivers. Water Resources Research **44**: 1–17.DOI: 10.1029/2006WR005846

Boye K, Noël V, Tfaily MM, Bone SE, Williams KH, Bargar JR, Fendorf S. 2017. Thermodynamically controlled preservation of organic carbon in floodplains. Nature Geoscience DOI: 10.1038/NGEO2940

Brandon KA, Roden-Tice TM, Garver JI. 1998. Late Cenozoic exhumation of the cascadia accretionnary wedge in the Olympic montains, northwest Washington State. Geological Society of America Bulletin **110**: 985–1009.DOI: 10.1130/0016-7606(1998)110<0985:LCEOTC>2.3.CO;2

Braudrick CA, Grant GE. 2000. When do logs move in rivers? Water Resources Research **36**: 571–583.DOI: 10.1029/1999WR900290

Braudrick CA, Grant GE, Ishikawa Y, Ikeda H. 1997. Dynamics of Wood Transport in Streams: A Flume Experiment. Earth Surface Processes and Landforms **22**: 669–683.

Brooks AP, Brierley GJ, Millar RG. 2003. The long-term control of vegetation and woody debris on channel and flood-plain evolution: Insights from a paired catchment study in southeastern Australia. Geomorphology **51**: 7–29.DOI: 10.1016/S0169-555X(02)00323-9

Bullinger-Weber G et al. 2014. Carbon storage and soil organic matter stabilisation in near-natural, restored and embanked Swiss floodplains. Geoderma **228**–**229**: 122–131.DOI: 10.1016/j.geoderma.2013.12.029

Burton JI, Olson DH, Puettmann KJ. 2016. Effects of riparian buffer width on wood loading in headwater streams after repeated forest thinning. Forest Ecology and Management **372**: 247–257.DOI: 10.1016/j.foreco.2016.03.053

Cadol D, Wohl E, Goode JR, Jaeger KL. 2009. Wood distribution in neotropical forested headwater streams of La Selva, Costa Rica. Earth Surface Processes and Landforms **34**: 1198–1215.DOI: 10.1002/esp.1800

Carah JK, Blencowe CC, Wright DW, Bolton LA. 2014. Low-Cost Restoration Techniques for Rapidly Increasing Wood Cover in Coastal Coho Salmon Streams. North American Journal of Fisheries Management **34**: 1003–1013.DOI: 10.1080/02755947.2014.943861

Clarke BA, Burbank DW. 2010. Bedrock fracturing, threshold hillslopes, and limits to the magnitude of bedrock landslides. Earth and Planetary Science Letters **297**: 577–586.DOI: 10.1016/j.epsl.2010.07.011

Collins BD, Montgomery DR, Fetherston KL, Abbe TB. 2012. The floodplain large-wood cycle hypothesis: A mechanism for the physical and biotic structuring of temperate forested alluvial valleys in the North Pacific coastal ecoregion. Geomorphology **139**–**140**: 460–470.DOI: 10.1016/j.geomorph.2011.11.011

D'Elia AH, Liles GC, Viers JH, Smart DR. 2017. Deep carbon storage potential of buried floodplain soils. Scientific Reports **7**: 8181.DOI: 10.1038/s41598-017-06494-4

Davidson SL, MacKenzie LG, Eaton BC. 2015. Large wood transport and jam formation in a

series of flume experiments. Water Resources Research **51**: 10065–10077.DOI: 10.1002/2015WR017446

Dixon SJ, Sear DA. 2014. The influence of geomorphology on large wood dynamics in a low gradient headwater stream. Water Resources Research **50**: 9194–9210.DOI: 10.1002/2014WR015947

Doetterl S et al. 2015. Soil carbon storage controlled by interactions between geochemistry and climate. Nature Geoscience **8**: 780–783.DOI: 10.1038/NGEO2516

Doetterl S, Berhe AA, Nadeu E, Wang Z, Sommer M, Fiener P. 2016. Erosion, deposition and soil carbon: A review of process-level controls, experimental tools and models to address C cycling in dynamic landscapes. Earth-Science Reviews **154**: 102–122.DOI: 10.1016/j.earscirev.2015.12.005

Dunkerley D. 2014. Nature and hydro-geomorphic roles of trees and woody debris in a dryland ephemeral stream: Fowlers Creek, arid western New South Wales, Australia. Journal of Arid Environments **102**: 40–49.DOI: 10.1016/j.jaridenv.2013.10.017

Elosegi A, Díez J, Pozo J. 2007. Contribution of dead wood to the carbon flux in forested streams. Earth Surface Processes and Landforms **32**: 1219–1228.DOI: 10.1002/esp.1549

Fall PL. 1994. Modern Pollen Spectra and Vegetation in the Wind River Range, Wyoming, U.S.A. Arctic and Alpine Research **26**: 383–392.

Falloon P, Jones CD, Ades M, Paul K. 2011. Direct soil moisture controls of future global soil carbon changes: An important source of uncertainty. Global Biogeochemical Cycles **25**: 1–14.DOI: 10.1029/2010GB003938

Fetherston KL, Naiman RJ, Bilby RE. 1995. Large woody debris, physical process, and riparian

forest development in montane river networks of the Pacific Northwest. Geomorphology **13**: 133–144.DOI: 10.1016/0169-555X(95)00033-2

Garber J. 2013. Using in situ cosmogenic radionuclides to constrain millenial scale denudation rates and chemical weathering rates on the Colorado Front Range, Colorado State University

Gerstel WJ, Lingley Jr. WS. 2000. Geologic Map of the Forks 1:100,000 Quadrangle, Washington

Gomi T, Sidle RC, Woodsmith RD, Bryant MD. 2003. Characteristics of channel steps and reach morphology in headwater streams, southeast Alaska. Geomorphology **51**: 225–242.DOI: 10.1016/S0169-555X(02)00338-0

Gran KB, Czuba JA. 2017. Sediment pulse evolution and the role of network structure. Geomorphology **277**: 17–30.DOI: 10.1016/j.geomorph.2015.12.015

Gurnell AM. 2013. Wood in Fluvial Systems. In Treatise on Geomorphology , Schroder J and Wohl E (eds). Elsevier Ltd.: San Diego, CA; 163–188.

Gurnell AM, Petts GE, Harris N, Ward J V., Tockner K, Edwards PJ, Kollmann J. 2000. Large wood retention in river channels: The case of the Fiume Tagliamento, Italy. Earth Surface Processes and Landforms **25**: 255–275.DOI: 10.1002/(SICI)1096-9837(200003)25:3<255::AID-ESP56>3.0.CO;2-H

Gurnell AM, Piegay H, Swanson FJ, Gregory S V. 2002. Large wood and fluvial processes. Freshwater Biology **47**: 601–619.DOI: 10.1046/j.1365-2427.2002.00916.x

Guthrie RH. 2002. The effects of logging on frequency and distribution of landslides in three watersheds on Vancouver Island, British Columbia. Geomorphology **43**: 273–292.DOI: 10.1016/S0169-555X(01)00138-6

Guyette RP, Cole WG, Dey DC, Muzika R-M. 2002. Perspectives on the age and distribution of large wood in riparian carbon pools. Canadian Journal of Fisheries and Aquatic Sciences **59**: 578–585.DOI: 10.1139/f02-026

Guyette RP, Dey DC, Stambaugh MC. 2008. The Temporal Distribution and Carbon Storage of Large Oak Wood in Streams and Floodplain Deposits. Ecosystems **11**: 643–653.DOI: 10.1007/s10021-008-9149-9

Hanberry BB, Kabrick JM, He HS. 2015. Potential tree and soil carbon storage in a major historical floodplain forest with disrupted ecological function. Perspectives in Plant Ecology, Evolution and Systematics **17**: 17–23.DOI: 10.1016/j.ppees.2014.12.002

Harmon ME, Woodall CW, Sexton J. 2011. Standing and Downed Dead Tree Wood Density Reduction Factors : A Comparison Across Decay Classes and Tree Species

Harvey JW, Gooseff M. 2015. River corridor science: Hydrologic exchange and ecological consequences frombedforms to basins. Water Resources Research **51**: 6893–6922.DOI: 10.1002/2015WR017617

Hilton RG. 2017. Climate regulates the erosional carbon export from the terrestrial biosphere. Geomorphology **277**: 118–132.DOI: 10.1016/j.geomorph.2016.03.028

Hilton RG, Galy A, Hovius N, Horng MJ, Chen H. 2011. Efficient transport of fossil organic carbon to the ocean by steep mountain rivers: An orogenic carbon sequestration mechanism. Geology **39**: 71–74.DOI: 10.1130/G31352.1

Hoffmann T, Glatzel S, Dikau R. 2009. A carbon storage perspective on alluvial sediment storage in the Rhine catchment. Geomorphology **108**: 127–137.DOI: 10.1016/j.geomorph.2007.11.015

Holm S. 1979. A Simple Sequentially Rejective Multiple Test Procedure. Scandinavian Journal of Statistics **6**: 65–70.

Homer CG, Dewitz JA, Yang L, Jin S, Danielson P, Xian G, Coulston J, Herold ND, Wickham JD, Megown K. 2015. Completion of the 2011 National Land Cover Database for the conterminous United States-Representing a decade of land cover change information. Photogrammetric Engineering and Remote Sensing **81**: 345–354.

Hoogsteen MJJ, Lantinga EA, Bakker EJ, Groot JCJ, Tittonell PA. 2015. Estimating soil organic carbon through loss on ignition: Effects of ignition conditions and structural water loss. European Journal of Soil Science **66**: 320–328.DOI: 10.1111/ejss.12224

Hough-Snee N, Kasprak A, Rossi RK, Bouwes N, Roper BB, Wheaton JM. 2015. Hydrogeomorphic and Biotic Drivers of Instream Wood Differ Across Sub-basins of the Columbia River Basin, USA. River research and applications **32**: 1302–1315.DOI: 10.1002/rra.2968

Houston DB. 1973. Wildfires in Northern Yellowstone National Park. Ecology **54**: 1111–1117.DOI: 10.2307/1935577

Howard DM, Howard PJA. 1993. Relationships between CO2 evolution, moisture content and temperature for a range of soil types. Soil Biology and Biochemistry **25**: 1537–1546.DOI: 10.1016/0038-0717(93)90008-Y

Hua Q, Barbetti M, Rakowski AZ. 2013. Atmospheric Radiocarbon for the Period 1950–2010. Radiocarbon **55**: 2059–2072.DOI: 10.2458/azu_js_rc.v55i2.16177

Hyatt T, Naiman RJ. 2001. The residence time of large woody debris in the Queets River, Washington, USA. Ecological Applications **11**: 191–202.

IPCC. 2014. Climate Change 2014: Synthesis Report . Pachauri RK and Meye LA (eds). IPCC: Geneva, Switzerland

Iroumé A, Mao L, Andreoli A, Ulloa H, Ardiles MP. 2015. Large wood mobility processes in low-order Chilean river channels. Geomorphology **228**: 681–693.DOI: 10.1016/j.geomorph.2014.10.025

Jakob M. 2000. The impacts of logging on landslide activity at Clayoquot Sound, British Columbia. Catena **38**: 279–300.

Jobbágy EG, Jackson RB. 2000. The vertical distribution of soil organic carbon and its relation to climate and vegetation. Ecological applications **10**: 423–436.DOI: 10.1890/1051-0761(2000)010[0423:TVDOSO]2.0.CO;2

Jones KK, Anlauf-Dunn K, Jacobsen PS, Strickland M, Tennant L, Tippery SE. 2014. Effectiveness of Instream Wood Treatments to Restore Stream Complexity and Winter Rearing Habitat for Juvenile Coho Salmon. Transactions of the American Fisheries Society **143**: 334–345.DOI: 10.1080/00028487.2013.852623

Kaiser K, Guggenberger G. 2000. The role of DOM sorption to mineral surfaces in the preservation of organic matter in soils. Organic Geochemistry **31**: 711–725.DOI: 10.1016/S0146-6380(00)00046-2

Kirchner JWJWJW, Finkel RCRCRC, Riebe CSCCSCCSCS, Granger DE, Clayton JL, King JG, Megahan WF, Sites F. 2001. Mountain erosion over 10 yr , 10 k.y., and 10 m.y. time scales. Geology **29**: 591–594.DOI: 10.1130/0091-7613(2001)029<0591:MEOYKY>2.0.CO;2

Kramer N, Wohl E. 2016. Rules of the road: A qualitative and quantitative synthesis of large wood transport through drainage networks. Geomorphology **279**: 74–97.DOI:

10.1016/j.geomorph.2016.08.026

Lamlom SH, Savidge RA. 2003. A reassessment of carbon content in wood: Variation within and between 41 North American species. Biomass and Bioenergy **25**: 381–388.DOI: 10.1016/S0961-9534(03)00033-3

Larsen IJ, Montgomery DR. 2012. Landslide erosion coupled to tectonics and river incision. Nature Geoscience **5**: 468–473.DOI: 10.1038/ngeo1479

Leithold EL, Blair NE, Wegmann KW. 2016. Source-to-sink sedimentary systems and global carbon burial: A river runs through it. Earth-Science Reviews **153**: 30–42.DOI: 10.1016/j.earscirev.2015.10.011

Lininger KB, Wohl E, Rose JR. 2018. Geomorphic Controls on Floodplain Soil Organic Carbon in the Yukon Flats, Interior Alaska, From Reach to River Basin Scales. Water Resources Research DOI: 10.1002/2017WR022042

Lininger KB, Wohl E, Sutfin NA, Rose JR. 2017. Floodplain downed wood volumes: a comparison across three biomes. Earth Surface Processes and Landforms DOI: 10.1002/esp.4072

Loope LL, Gruell GE. 1973. The ecological role of fire in the Jackson Hole area, northwestern Wyoming. Quaternary Research **3**: 425–443.DOI: 10.1016/0033-5894(73)90007-0

Manners RB, Doyle MW, Small MJ. 2007. Structure and hydraulics of natural woody debris jams. Water Resources Research **43**: 1–17.DOI: 10.1029/2006WR004910

Marcus WA, Marston RA, Colvard CR, Gray RD. 2002. Mapping the spatial and temporal distributions of woody debris in streams of the Greater Yellowstone Ecosystem, USA. Geomorphology **44**: 323–335.DOI: Pii S0169-555x(01)00181-7\rDoi 10.1016/S0169-555x(01)00181-7

Martin DJ, Benda L. 2001. Patterns of Instream Wood Recruitment and Transport at the Watershed Scale. Transactions of the American Fisheries Society **130**: 940–958.DOI: 10.1577/1548-8659(2001)130<0940:POIWRA>2.0.CO;2

Molnar P, England P. 1990. Late Cenozoic uplift of mountain ranges and global climate change: chicken or egg? Nature **346**: 29–34.DOI: 10.1038/346029a0

Montgomery DR, Abbe TB, Buffington JM, Peterson NP, Schmidt KM, Stock JD. 1996. Distribution of bedrock and alluvial channels in forested mountain drainage basins. Nature **381**: 587–589.DOI: 10.1038/381587a0

Montgomery DR, Buffington JM. 1997. Channel-reach morphology in mountain drainage basins. Bulletin of the Geological Society of America **109**: 596–611.DOI: 10.1130/0016-7606(1997)109<0596:CRMIMD>2.3.CO

Montgomery DR, Massong TM, Hawley SCS. 2003. Influence of debris flows and log jams on the location of pools and alluvial channel reaches, Oregon Coast Range. Bulletin of the Geological Society of America **115**: 78–88.DOI: 10.1130/0016-7606(2003)115<0078:IODFAL>2.0.CO;2

Mulholland PJ, Elwood JW. 1982. The role of lake and reservoir sediments as sinks in the perturbed global carbon cycle. Tellus **34**: 490–499.DOI: 10.3402/tellusa.v34i5.10834

Nagayama S, Nakamura F, Kawaguchi Y, Nakano D. 2012. Effects of configuration of instream wood on autumn and winter habitat use by fish in a large remeandering reach. Hydrobiologia **680**: 159–170.DOI: 10.1007/s10750-011-0913-z

Naiman RJ, Melillo JM, Lock MA, Ford TE, Reice SR. 1987. Longitudinal patterns of ecosystem processes and community structure in a subarctic river continuum. Ecology **68**: 1139–

1156.DOI: 10.2307/1939199

Nanson GC, Barbetti M, Taylor G. 1995. River stabilisation due to changing climate and vegetation during the late Quaternary in western Tasmania, Australia. Geomorphology **13**: 145–158.DOI: 10.1016/0169-555X(95)00040-C

Omengo FO, Geeraert N, Bouillon S, Govers G. 2016. Deposition and fate of organic carbon in floodplains along a tropical semiarid lowland river (Tana River, Kenya). Journal of Geophysical Research G: Biogeosciences **121**: 1131–1143.DOI: 10.1002/2015JG003288

Van Oost K, Verstraeten G, Doetterl S, Notebaert B, Wiaux F, Broothaerts N, Six J. 2012. Legacy of human-induced C erosion and burial on soil-atmosphere C exchange. Proceedings of the National Academy of Sciences of the United States of America **109**: 19492–19497.DOI: 10.1073/pnas.1211162109

Opperman JJ, Meleason M, Francis R a., Davies-Colley R. 2008. "Livewood": Geomorphic and Ecological Functions of Living Trees in River Channels. BioScience **58**: 1069.DOI: 10.1641/B581110

Oregon State University. 2004. PRISM Climate Group

Osei NA, Gurnell AM, Harvey GL. 2015. The role of large wood in retaining fine sediment, organic matter and plant propagules in a small, single-thread forest river. Geomorphology **235**: 77–87.DOI: 10.1016/j.geomorph.2015.01.031

Pacific District Olympic National Forest. 2012. Sitkum Watershed Restoration Action Plan

Pfeiffer A, Wohl E. 2018. Where Does Wood Most Effectively Enhance Storage? Network-Scale Distribution of Sediment and Organic Matter Stored by Instream Wood. Geophysical Research Letters **45**: 194–200.DOI: 10.1002/2017GL076057

Piégay H, Moulin B, Hupp CR. 2017. Assessment of transfer patterns and origins of in-channel wood in large rivers using repeated field surveys and wood characterisation (the Isère River upstream of Pontcharra, France). Geomorphology **279**: 27–43.DOI: 10.1016/j.geomorph.2016.07.020

R Core Team. 2017. R: A Language and Environment for Statistical Computing

Ralph SC, Poole GC, Conquest LL, Naiman RJ. 1994. Stream Channel Morphology and Woody Debris in Logged and Unlogged Basins of Western Washington. Canadian Journal of Fisheries and Aquatic Sciences **51**: 37–51.DOI: 10.1139/f94-006

Ramsey CB. 2001. Development of the radiocarbon calibration program. Radiocarbon **43**: 355–363.DOI: papers2://publication/uuid/5B399323-3576-4144-BF98-497069142583

Rasmussen C et al. 2018. Beyond clay: towards an improved set of variables for predicting soil organic matter content. Biogeochemistry DOI: 10.1007/s10533-018-0424-3

Rathburn S., Bennett GL, Wohl E, Briles C, McElroy B, Sutfin N. 2017. The fate of sediment, wood, and organic carbon eroded during an extreme flood, Colorado Front Range, USA. Geology **45**: 1–14.DOI: 10.1130/G38935.1

Reimer PJ et al. 2013. IntCal13 and Marine13 Radiocarbon Age Calibration Curves 0–50,000 Years cal BP. Radiocarbon **55**: 1869–1887.DOI: 10.2458/azu_js_rc.55.16947

Reiners PW, Ehlers TA, Mitchell SG, Montgomery DR. 2003. Coupled spatial variations in precipitation and long-term erosion rates across the Washington Cascades. Nature **426**: 645–647.DOI: 10.1038/nature02111

Richard GA, Julien PY, Baird DC. 2005. Statistical analysis of lateral migration of the Rio Grande, New Mexico. Geomorphology **71**: 139–155.DOI: 10.1016/j.geomorph.2004.07.013

Ricker MC, Stolt MH, Donohue SW, Blazejewski GA, Zavada MS. 2013. Soil Organic Carbon Pools in Riparian Landscapes of Southern New England. Soil Science Society of America Journal **77**: 1070–1079.DOI: 10.2136/sssaj2012.0297

Roberts B, Ward B, Rollerson T. 2004. A comparison of landslide rates following helicopter and conventional cable-based clear-cut logging operations in the Southwest Coast Mountains of British Columbia. Geomorphology **61**: 337–346.DOI: 10.1016/j.geomorph.2004.01.007

Roni P, Beechie T, Pess G, Hanson K, Jonsson B. 2015. Wood placement in river restoration: fact, fiction, and future direction. Canadian Journal of Fisheries and Aquatic Sciences **72**: 466–478.DOI: 10.1139/cjfas-2014-0344

Ruffing CM, Daniels MD, Dwire KA. 2015. Disturbance legacies of historic tie-drives persistently alter geomorphology and large wood characteristics in headwater streams, southeast Wyoming. Geomorphology **231**: 1–14.DOI: 10.1016/j.geomorph.2014.10.029

Ruiz-Villanueva V, Wyżga B, Mikuś P, Hajdukiewicz H, Stoffel M. 2016. The role of flood hydrograph in the remobilization of large wood in a wide mountain river. Journal of Hydrology **541**: 330–343.DOI: 10.1016/j.jhydrol.2016.02.060

Schefuß E, Eglinton TI, Spencer-Jones CL, Rullkötter J, De Pol-Holz R, Talbot HM, Grootes PM, Schneider RR. 2016. Hydrologic control of carbon cycling and aged carbon discharge in the Congo River basin. Nature Geoscience **9**: 687–690.DOI: 10.1038/ngeo2778

Schimel DS, Braswell BH. 2005. The role of mid-latitude mountains in the carbon cycle: Global perspective and a Western U.S. case study. In Global Change and Mountain Regions , Huber UM, Bugmann HKM, and Reasoner MA (eds). Springer; 449–456.

Schmidt MWII et al. 2011. Persistence of soil organic matter as an ecosystem property. Nature

478: 49–56.DOI: 10.1038/nature10386

Schook DM, Rathburn SL, Friedman JM, Wolf JM. 2017. A 184-year record of river meander migration from tree rings, aerial imagery, and cross sections. Geomorphology **293**: 227–239.DOI: 10.1016/j.geomorph.2017.06.001

Schwabe E et al. 2015. Wood-associated fauna collected during the KuramBio expedition in the North West Pacific. Deep-Sea Research Part II: Topical Studies in Oceanography **111**: 376–388.DOI: 10.1016/j.dsr2.2014.08.001

Scott D, Wohl E. 2018a. Dataset for Geomorphic regulation of floodplain soil organic carbon concentration in watersheds of the Rocky and Cascade Mountains, USA

Scott D, Wohl E. 2018b. Dataset for Geomorphology and Climate Interact to Control Organic Carbon Stock and Age in Mountain River Valley Bottoms. DOI: https://hdl.handle.net/10217/187763

Scott DN, Brogan DJ, Lininger KB, Schook DM, Daugherty EE, Sparacino MS, Patton AI. 2016. Evaluating survey instruments and methods in a steep channel. Geomorphology **273**: 236–243.DOI: 10.1016/j.geomorph.2016.08.020

Scott DN, Montgomery DR, Wohl E. 2014. Log step and clast interactions in mountain streams in the central Cascade Range of Washington State, USA. Geomorphology **216**: 180–186.DOI: 10.1016/j.geomorph.2014.04.004

Scott DN, Wohl E. 2017. Evaluating Carbon Storage on Subalpine Lake Deltas. Earth Surface Processes and Landforms DOI: 10.1002/esp.4110

Scott DN, Wohl E. 2018c. Dataset for Natural and Anthropogenic Controls on Wood Loads in River Corridors of the Rocky, Cascade, and Olympic Mountains, USA. DOI:

https://hdl.handle.net/10217/186057

Shields FD, Knight SS, Stofleth JM. 2006. Large wood addition for aquatic habitat rehabilitation in an incised, sand-bed stream, Little Topashaw Creek, Mississippi. River Research and Applications **22**: 803–817.DOI: 10.1002/rra.937

Sidle RC, Ziegler AD, Negishi JN, Nik AR, Siew R, Turkelboom F. 2006. Erosion processes in steep terrain - Truths, myths, and uncertainties related to forest management in Southeast Asia. Forest Ecology and Management **224**: 199–225.DOI: 10.1016/j.foreco.2005.12.019

Simenstad CA, Wick A, Van de Wetering S, Bottom DL. 2003. Dynamics and ecological functions of wood in estuarine and coastal marine ecosystems. 265–277 pp.

Smithwick E, Harmon ME, Remillard SM, Acker SA, Franklin JF. 2002. Potential upper bounds of carbon stores in forests of the Pacific Northwest. Ecological Applications **12**: 1303–1317.DOI: 10.1890/1051-0761(2002)012[1303:PUBOCS]2.0.CO;2

Sparks DL. 1996. Methods of Soil Analysis. Part 3, Chemical Methods . Sparks DL, Page AL, Helmke PA, Loeppert RH, Soltanpour PN, Tabatabai MA, Johnston CT, Sumber ME, Bartels JM, and Bingham JM (eds). Soil Science Society of America, Inc.: Madison, Wisconsin

Stallard RF. 1998. Terrestrial sedimentation and the carbon cycle: Coupling weathering and erosion to carbon burial. Global Biogeochemical Cycles **12**: 231–257.DOI: 10.1029/98GB00741

Strahler AN. 1957. Quantitative classification of watershed geomorphology. Transactions, American Geophysical Union **38**: 915–920.

Sun OJ, Campbell J, Law BE, Wolf V. 2004. Dynamics of carbon stocks in soils and detritus across chronosequences of different forest types in the Pacific Northwest, USA. Global Change Biology **10**: 1470–1481.DOI: 10.1111/j.1365-2486.2004.00829.x

Sutfin NA, Wohl E. 2017. Substantial soil organic carbon retention along floodplains of mountain streams. Journal of Geophysical Research: Earth Surface **122**: 1325–1338.DOI: 10.1002/2016JF004004

Sutfin NA, Wohl E, Dwire KA. 2016. Banking carbon: A review of organic carbon storage and physical factors influencing retention in floodplains and riparian ecosystems. Earth Surface Processes and Landforms **60**: 38–60.DOI: 10.1002/esp.3857

Tao S, Eglinton TI, Montluçon DB, McIntyre C, Zhao M. 2015. Pre-aged soil organic carbon as a major component of the Yellow River suspended load: Regional significance and global relevance. Earth and Planetary Science Letters **414**: 77–86.DOI: 10.1016/j.epsl.2015.01.004

Thien SJ. 1979. A flow diagram for teaching texture-by-feel analysis. Journal of Agronomic Education **8**

Torres MA, Limaye AB, Ganti V, Lamb MP, Joshua West A, Fischer WW. 2017. Model predictions of long-lived storage of organic carbon in river deposits. Earth Surface Dynamics **5**: 711–730.DOI: 10.5194/esurf-5-711-2017

De Vos B, Van Meirvenne M, Quataert P, Deckers J, Muys B. 2005. Predictive Quality of Pedotransfer Functions for Estimating Bulk Density of Forest Soils. Soil Science Society of America Journal **69**: 500–510.DOI: 10.2136/sssaj2005.0500

Wagenmakers E-J, Farrell S. 2004. AIC model selection using Akaike weights. Psychonomic bulletin & review **11**: 192–196.DOI: 10.3758/BF03206482

Van Wagner CE. 1968. The line intersect method in forest fuel sampling. Forest Science **14**: 20–26.

Wallace JB, Benke AC. 1984. Quantification of Wood Habitat in Subtropical Coastal Plain

Streams. Canadian Journal of Fisheries and Aquatic Sciences **41**: 1643–1652.DOI: 10.1139/f84-203

Wang Z, Hoffmann T, Six J, Kaplan JO, Govers G, Doetterl S, Van Oost K. 2017. Human-induced erosion has offset one-third of carbon emissions from land cover change. Nature Climate Change **7**: 345–349.DOI: 10.1038/nclimate3263

Warren DR, Keeton WS, Kraft CE. 2008. A comparison of line-intercept and census techniques for assessing large wood volume in streams. Hydrobiologia **598**: 123–130.DOI: 10.1007/s10750-007-9144-8

Webb AA, Erskine WD. 2003. Distribution, recruitment, and geomorphic significance of large woody debris in an alluvial forest stream: Tonghi Creek, southeastern Australia. Geomorphology **51**: 109–126.DOI: 10.1016/S0169-555X(02)00327-6

Wickert AD, Martin JM, Tal M, Kim W, Sheets B, Paola C. 2013. River channel lateral mobility: Metrics, time scales, and controls. Journal of Geophysical Research: Earth Surface **118**: 396–412.DOI: 10.1029/2012JF002386

Wilcoxon F. 1945. Individual Comparisons by Ranking Methods. Biometrics Bulletin **1**: 80–83.DOI: 10.2307/3001946

Wohl E. 2013. Floodplains and wood. Earth-Science Reviews **123**: 194–212.DOI: 10.1016/j.earscirev.2013.04.009

Wohl E. 2014. A legacy of absence: Wood removal in US rivers. Progress in Physical Geography **38**: 637–663.DOI: 10.1177/0309133314548091

Wohl E, Cadol D, Pfeiffer A, Jackson K, Laurel D. 2018. Distribution of Large Wood Within River Corridors in Relation to Flow Regime in the Semiarid Western US. Water Resources

Research : 1–15. DOI: 10.1002/2017WR022009

Wohl E, Dwire K, Sutfin N, Polvi L, Bazan R. 2012. Mechanisms of carbon storage in mountainous headwater rivers. Nature communications **3**: 1263.DOI: 10.1038/ncomms2274

Wohl E, Goode JR. 2008. Wood dynamics in headwater streams of the Colorado Rocky Mountains. Water Resources Research **44**: 1–14.DOI: 10.1029/2007WR006522

Wohl E, Hall RO, Lininger KB, Sutfin NA, Walters DM. 2017a. Carbon dynamics of river corridors and the effects of human alterations. Ecological Monographs **87**: 379–409.DOI: 10.1002/ecm.1261

Wohl E, Lininger KB, Fox M, Baillie BR, Erskine WD. 2017b. Instream large wood loads across bioclimatic regions. Forest Ecology and Management **404**: 370–380.DOI: 10.1016/j.foreco.2017.09.013

Wohl E, Lininger KB, Scott DN. 2017c. River beads as a conceptual framework for building carbon storage and resilience to extreme climate events into river management. Biogeochemistry DOI: 10.1007/s10533-017-0397-7

Wohl E, Scott DN. 2016. Wood and sediment storage and dynamics in river corridors. Earth Surface Processes and Landforms : n/a-n/a. DOI: 10.1002/esp.3909

Wohl E, Scott DN, Lininger KB. n.d. Spatial distribution of channel and floodplain large wood in forested river corridors of the Northern Rockies. In Review. Water Resources Research

Wolter A, Ward B, Millard T. 2010. Instability in eight sub-basins of the Chilliwack River Valley, British Columbia, Canada: A comparison of natural and logging-related landslides. Geomorphology **120**: 123–132.DOI: 10.1016/j.geomorph.2010.03.008

Wondzell SM, Bisson PA. 2003. Influence of Wood on Aquatic Biodiversity. American

Fisheries Society Symposium **37**: 249–263.

Wyżga B, Mikuś P, Zawiejska J, Ruiz-villanueva V, Kaczka RJ, Czech W. 2017. Log transport and deposition in incised , channelized , and multithread reaches of a wide mountain river : Tracking experiment during a 20-year fl ood. Geomorphology **279**: 98–111.DOI: 10.1016/j.geomorph.2016.09.019

Xue Y, Zou L, Ge T, Wang X. 2017. Mobilization and export of millennial-aged organic carbon by the Yellow River. Limnology and Oceanography **13**DOI: 10.1002/lno.10579

Zhao B, Li Z, Li P, Xu G, Gao H, Cheng Y, Chang E, Yuan S, Zhang Y, Feng Z. 2017. Spatial distribution of soil organic carbon and its influencing factors under the condition of ecological construction in a hilly-gully watershed of the Loess Plateau, China. Geoderma **296**: 10–17.DOI: 10.1016/j.geoderma.2017.02.010

Zoppi U, Crye J, Song Q. 2007. Performance evaluation of the new AMS system at Accium BioSciences. Radiocarbon **49**: 171–180.

Appendix A : Searching for Evidence of European Settlement Influence on Soil Organic Carbon Concentration in Soils of the Quileute River Floodplain

After finding a lack of floodplain soil in the Sitkum and SF Calawah, I attempted to constrain the effects of logging on soil OC storage (roughly coincident with extensive European settlement of the area) by examining soils at the far downstream end of the Quileute River, to which the Sitkum and SF Calawah drain. The mouth of the Quileute River represents the last terrestrial storage zone for soil eroded from the Quileute Basin before it reaches the marina at the town of La Push, where sediment is either dredged by the Army Corp. of Engineers for boat passage or transported off-shore in the Pacific Ocean. I hypothesized that soil being deposited at the mouth of the Quileute in the extensive side-channels, floodplains, and mid-channel islands in that reach would reflect land use signals from upstream and that clearcut logging would impact soil OC concentrations upstream in the basin, which would then be reflected in a soil chronosequence at the Quileute mouth.

This assumes: 1) that logging would be the dominant impact on soil OC concentrations over the last century in the greater Quileute basin, 2) that soils deposited at the Quileute mouth would be deposited at a rate sufficient to resolve upstream signals, and 3) that soils at the Quileute mouth uniformly reflect the entire Quileute basin, as opposed to being biased towards parts that were more anthropogenically impacted than others. Assumption 1 is justified by the lack of other basin-wide disturbances (e.g., fire, urbanization) since European settlement. With the exception of Forks, a small logging town, there has been no urban development or natural resource extraction in the basin other than logging. Assumption 2 is justified by the relatively high exhumation rate (implying high sediment transport downstream; Brandon et al., 1998) and

the high rate of lateral mobility of the Quileute at its mouth, which implies active deposition across the floodplain (observed from Google Earth historical imagery).

To test this hypothesis, I collected soil cores along transects of floodplain surfaces near the Quileute mouth. Transects were subjectively placed based on aerial imagery and 10 m DEM mapping conducted prior to fieldwork (Figure A-1) with the aim of capturing soil cores that would span a range of depositional ages, as sediment was laterally accreted across the floodplain. Sampling was performed in two stages, first in summer 2016 and again in winter 2016/2017. During the first sampling period, cores were collected in increments that filled the sampling bucket. During the second sampling period, cores were collected in 20 cm increments to facilitate more uniform depth analysis across multiple cores. Cores were collected either to refusal (i.e., coarse sediment or wood that prevented further sampling) or a maximum depth of 2.4 m during the first sampling period or approximately 1.2 m during the second sampling period. I collected a total of 19 cores across 4 transects (including an island, lateral bar, point bar, and former point bar now surrounded by an oxbow lake).

Figure A-1: Google Earth map of Quileute mouth, with study sites labeled. Sites starting with "Q" were sampled during the initial sampling phase (summer 2016) and site starting with "2Q" were sampled during the second sampling phase (winter 2016/2017). For "2Q" sites, "I" stands for "island", "NPB" stands for "north point bar", and "OB" stands for "oxbow".

Soil samples were analyzed for total OC by the CSU soil testing laboratory using a CHN furnace (Sparks, 1996; J. Self, Colorado State University, pers. comm., 2016). To test my hypothesis, I had planned to look for a threshold-based relationship between soil age and soil OC content, whereby modern or relatively young (<50 yr BP, or years before 1950) samples would display significantly different OC concentrations than older samples. Samples from the bottoms of 3 cores were sent to DirectAMS (Zoppi et al., 2007) for radiocarbon dating of humins, the soil carbon fraction that is least likely to be mobilized from the soil (i.e., most resistant to respiration or transport).I used OxCal 4.3 (Ramsey, 2001) to calibrate samples using the IntCAL13 (Reimer et al., 2013) calibration curve. Sample ages were interpreted from probability density plots of calibrated radiocarbon age for each sample (Figure A-2).

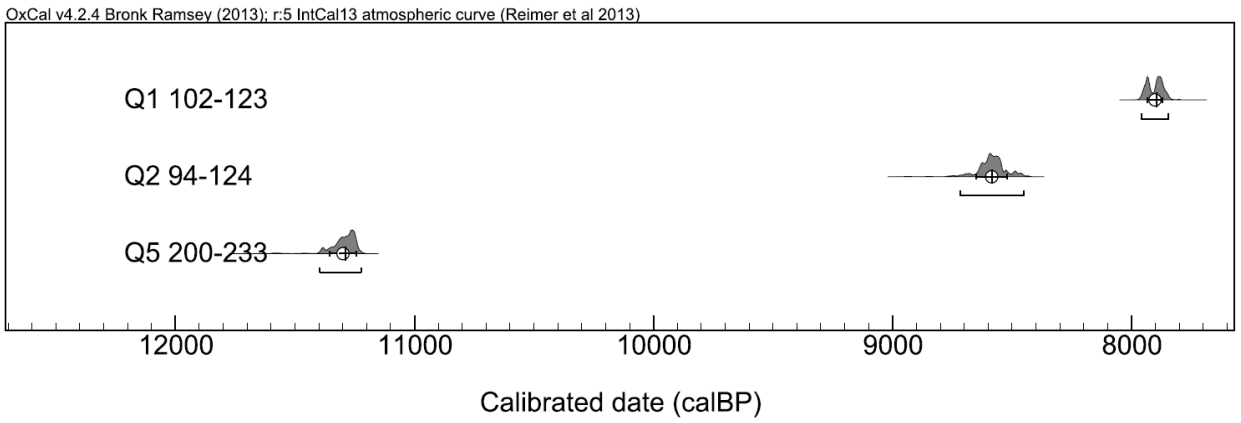

Figure A-2: Probability density functions plotted for the three cores (Q1, Q2, and Q5) whose deepest sample was radiocarbon dated to constrain the age of deposition of the core.

Sample ages for the bottoms of cores were interpreted as maximum ages of the oldest sediment in that core. Assuming dominantly lateral accretion in this system, I needed to find both recently deposited floodplain soils as well as older floodplain soils that had been deposited before European settlement. The calibrated ages of the sampled cores (all over 1000 yr BP, Figure A-2) indicated that all dated cores were potentially too old to evaluate my hypothesis, motivating the second stage of sampling that included what were obviously younger packets of floodplain soil (recently deposited point bars and islands, observed to be deposited within the last 50 years from aerial imagery in Google Earth).

OC concentrations generally declined with depth in each core. However, after analyzing vertical trends in the OC content of the cores taken during the second phase of sampling (Figure A-3), I found that many of the cores displayed OC peaks in the vertical depth profile (i.e., samples of abnormally high OC content compared to samples above, or breaks in the expected decreasing trend of OC with depth (Jobbágy and Jackson, 2000)). These discrete peaks in OC content likely indicate abrupt vertical accretion (see Chapter 3 for more detail), as opposed to lateral accretion. This indicates that to test for a signal of European settlement, it would be necessary to obtain a date for each individual soil sample, as opposed to grouping all samples

within each core together as being of a similar depositional age. Given the number of samples (117) and the limited funds available for this part of the project (each radiocarbon date costs approximately $300), I judged it imprudent to obtain the necessary radiocarbon analysis to fully test my hypothesis that logging had impacted OC concentrations in floodplain soils of the Quileute basin.

To fully accomplish this objective, it would be necessary to obtain a radiocarbon date that indicated a depositional age, or an age of the OC in the sample, for each sample. After completing planning for radiocarbon analysis for Chapter 4, I also realized that humin dating, representing the maximum age of carbon in the soil, is likely a poor tool for evaluating the depositional age of soils or the age of the carbon within the soil (hence justifying a switch to bulk sediment dating for samples analyzed in Chapter 4). A better tool would be to either date depositional markers, such as wood or charcoal fragments, or to do bulk sediment radiocarbon dating to obtain bulk carbon age. Another complication in this study is that the source of OC in these samples is not known. Obtaining carbon isotope data to constrain the source of OC (i.e., from autochthonous vegetation or vegetation higher in the basin) would allow for better inference of the cause of OC variability between samples (i.e., upstream land use versus other confounding factors such as how the OC was input to the soil).

Data for samples taken from the Quileute mouth is available in Table A-1. Radiocarbon data for the three samples that were dated are available in Table A-2.

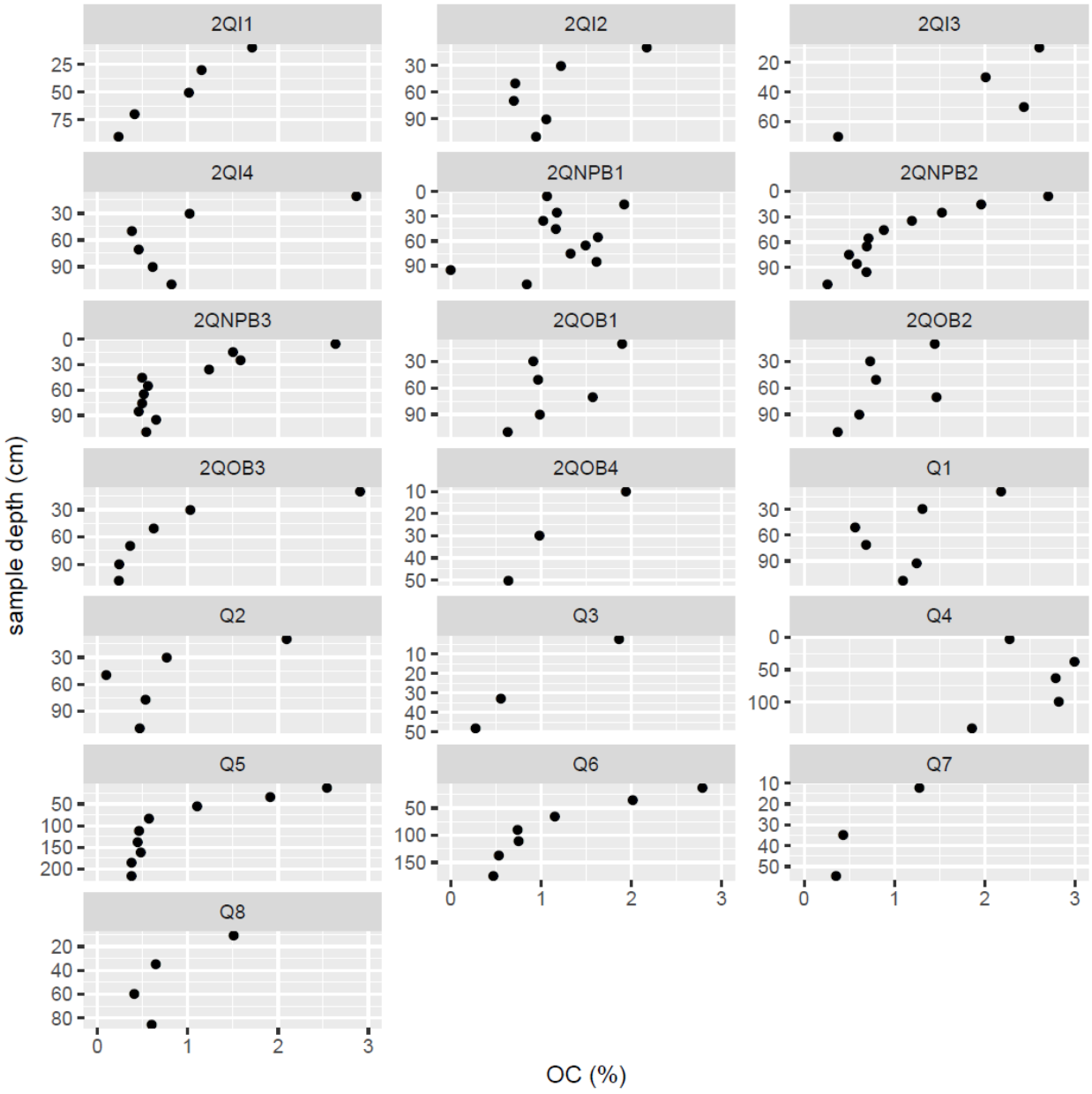

Figure A-3: OC content (% by mass) for samples collected at the Quileute mouth. Note that y axes are of variable scale, but x axes are of fixed scale.

Table A-1: Data for each sample collected at the Quileute Mouth. All values given as percentages refer to percentages by dry sample mass. Type refers to the geomorphic feature from which the core was taken (PB = point bar, ISL = island, and OB = oxbow). Average OC is calculated for each core as the sum of the OC (%) for each sample weighted by the proportion of the total core depth occupied by that sample (bottom depth minus top depth). Latitude and Longitude are given in decimal degrees. C refers to carbon, IC refers to inorganic carbon, and OC refers to organic carbon.

Sample ID	Calcium Carbonate (%)	Total C (%)	IC (%)	OC (%)	Type	Latitude	Longitude	Top Depth (cm)	Bottom Depth (cm)	Mean OC (%)
2QNPB1 0-10	0.59	1.14	0.07	1.07	PB	47.914801	-124.605703	0	10	1.16
2QNPB1 10-20	0.74	2.01	0.09	1.92	PB	47.914801	-124.605703	10	20	1.16
2QNPB1 20-30	0.43	1.23	0.05	1.17	PB	47.914801	-124.605703	20	30	1.16
2QNPB1 30-40	0.81	1.12	0.10	1.03	PB	47.914801	-124.605703	30	40	1.16
2QNPB1 40-50	0.23	1.19	0.03	1.16	PB	47.914801	-124.605703	40	50	1.16
2QNPB1 50-60	1.09	1.76	0.13	1.63	PB	47.914801	-124.605703	50	60	1.16
2QNPB1 60-70	0.76	1.59	0.09	1.49	PB	47.914801	-124.605703	60	70	1.16
2QNPB1 70-80	1.13	1.46	0.14	1.32	PB	47.914801	-124.605703	70	80	1.16
2QNPB1 80-90	0.67	1.70	0.08	1.62	PB	47.914801	-124.605703	80	90	1.16
2QNPB1 90-100	1.17	0.14	0.14	0.00	PB	47.914801	-124.605703	90	100	1.16
2QNPB1 100-125	0.95	0.96	0.11	0.84	PB	47.914801	-124.605703	100	125	1.16
2QNPB2 0-10	0.93	2.81	0.11	2.70	PB	47.914561	-124.602369	0	10	1.00

2QNPB2 10-20	1.07	2.09	0.13	1.96	PB	47.914561	-124.602369	10	20	1.00
2QNPB2 20-30	0.96	1.64	0.11	1.53	PB	47.914561	-124.602369	20	30	1.00
2QNPB2 30-40	0.95	1.31	0.11	1.19	PB	47.914561	-124.602369	30	40	1.00
2QNPB2 40-50	1.12	1.02	0.13	0.88	PB	47.914561	-124.602369	40	50	1.00
2QNPB2 50-60	0.90	0.82	0.11	0.71	PB	47.914561	-124.602369	50	60	1.00
2QNPB2 60-70	0.92	0.81	0.11	0.69	PB	47.914561	-124.602369	60	70	1.00
2QNPB2 70-80	0.98	0.61	0.12	0.50	PB	47.914561	-124.602369	70	80	1.00
2QNPB2 80-90	0.82	0.68	0.10	0.58	PB	47.914561	-124.602369	80	90	1.00
2QNPB2 90-100	1.25	0.84	0.15	0.69	PB	47.914561	-124.602369	90	100	1.00
2QNPB2 100-120	2.12	0.51	0.25	0.26	PB	47.914561	-124.602369	100	120	1.00
2QNPB3 0-10	0.95	2.75	0.11	2.63	PB	47.913677	-124.596714	0	10	0.93
2QNPB3 10-20	0.73	1.59	0.09	1.50	PB	47.913677	-124.596714	10	20	0.93
2QNPB3 20-30	1.74	1.79	0.21	1.58	PB	47.913677	-124.596714	20	30	0.93
2QNPB3 30-40	1.26	1.39	0.15	1.24	PB	47.913677	-124.596714	30	40	0.93
2QNPB3 40-50	1.02	0.62	0.12	0.49	PB	47.913677	-124.596714	40	50	0.93
2QNPB3 50-60	0.96	0.67	0.11	0.56	PB	47.913677	-124.596714	50	60	0.93
2QNPB3 60-70	0.82	0.61	0.10	0.51	PB	47.913677	-124.596714	60	70	0.93

2QNPB3 70-80	0.91	0.60	0.11	0.50	PB	47.913677	-124.596714	70	80	0.93
2QNPB3 80-90	1.05	0.58	0.13	0.46	PB	47.913677	-124.596714	80	90	0.93
2QNPB3 90-100	0.98	0.77	0.12	0.65	PB	47.913677	-124.596714	90	100	0.93
2QNPB3 100-120	1.30	0.69	0.16	0.54	PB	47.913677	-124.596714	100	120	0.93
2QI1 0-20	0.87	1.82	0.10	1.71	ISL	47.920088	-124.62857	0	20	0.90
2QI1 20-40	0.79	1.25	0.09	1.15	ISL	47.920088	-124.62857	20	40	0.90
2QI1 40-60	0.83	1.11	0.10	1.01	ISL	47.920088	-124.62857	40	60	0.90
2QI1 60-80	1.14	0.55	0.14	0.41	ISL	47.920088	-124.62857	60	80	0.90
2QI1 80-100	0.89	0.34	0.11	0.23	ISL	47.920088	-124.62857	80	100	0.90
2QI2 0-20	0.95	2.28	0.11	2.17	ISL	47.919917	-124.627528	0	20	1.13
2QI2 20-40	0.91	1.33	0.11	1.22	ISL	47.919917	-124.627528	20	40	1.13
2QI2 40-60	1.09	0.84	0.13	0.71	ISL	47.919917	-124.627528	40	60	1.13
2QI2 60-80	0.89	0.80	0.11	0.70	ISL	47.919917	-124.627528	60	80	1.13
2QI2 80-100	1.00	1.18	0.12	1.06	ISL	47.919917	-124.627528	80	100	1.13
2QI2 100-120	0.80	1.04	0.10	0.94	ISL	47.919917	-124.627528	100	120	1.13
2QI3 0-20	1.32	2.76	0.16	2.60	ISL	47.919827	-124.6248	0	20	1.85
2QI3 20-40	0.75	2.10	0.09	2.01	ISL	47.919827	-124.6248	20	40	1.85
2QI3 40-60	0.76	2.52	0.09	2.43	ISL	47.919827	-124.6248	40	60	1.85
2QI3 60-80	0.79	0.47	0.09	0.37	ISL	47.919827	-124.6248	60	80	1.85
2QI4 0-20	0.71	2.95	0.08	2.87	ISL	47.9199	-124.622514	0	20	1.03
2QI4 20-40	0.83	1.12	0.10	1.02	ISL	47.9199	-124.622514	20	40	1.03
2QI4 40-60	0.89	0.49	0.11	0.38	ISL	47.9199	-124.622514	40	60	1.03
2QI4 60-80	0.74	0.54	0.09	0.46	ISL	47.9199	-124.622514	60	80	1.03
2QI4 80-100	0.77	0.70	0.09	0.61	ISL	47.9199	-124.622514	80	100	1.03
2QI4 100-120	0.58	0.89	0.07	0.82	ISL	47.9199	-124.622514	100	120	1.03

2QOB1 0-20	0.87	2.00	0.10	1.90	OB	47.907713	-124.577705	0	20	1.16
2QOB1 20-40	0.89	1.02	0.11	0.91	OB	47.907713	-124.577705	20	40	1.16
2QOB1 40-60	0.84	1.07	0.10	0.97	OB	47.907713	-124.577705	40	60	1.16
2QOB1 60-80	0.67	1.65	0.08	1.57	OB	47.907713	-124.577705	60	80	1.16
2QOB1 80-100	0.97	1.10	0.12	0.98	OB	47.907713	-124.577705	80	100	1.16
2QOB1 100-120	1.24	0.78	0.15	0.63	OB	47.907713	-124.577705	100	120	1.16
2QOB2 0-20	1.18	1.59	0.14	1.44	OB	47.906345	-124.578979	0	20	0.90
2QOB2 20-40	0.63	0.81	0.08	0.73	OB	47.906345	-124.578979	20	40	0.90
2QOB2 40-60	1.01	0.92	0.12	0.80	OB	47.906345	-124.578979	40	60	0.90
2QOB2 60-80	0.77	1.56	0.09	1.47	OB	47.906345	-124.578979	60	80	0.90
2QOB2 80-100	0.97	0.72	0.12	0.61	OB	47.906345	-124.578979	80	100	0.90
2QOB2 100-120	0.87	0.48	0.10	0.37	OB	47.906345	-124.578979	100	120	0.90
2QOB3 0-20	1.13	3.05	0.14	2.91	OB	47.904828	-124.581847	0	20	0.93
2QOB3 20-40	0.84	1.13	0.10	1.03	OB	47.904828	-124.581847	20	40	0.93
2QOB3 40-60	0.82	0.72	0.10	0.62	OB	47.904828	-124.581847	40	60	0.93
2QOB3 60-80	1.04	0.49	0.12	0.36	OB	47.904828	-124.581847	60	80	0.93
2QOB3 80-100	0.92	0.35	0.11	0.24	OB	47.904828	-124.581847	80	100	0.93
2QOB3 100-115	0.95	0.35	0.11	0.24	OB	47.904828	-124.581847	100	115	0.93
2QOB4 0-20	1.18	2.08	0.14	1.94	OB	47.90229	-124.578807	0	20	1.19
2QOB4 20-40	0.89	1.09	0.11	0.98	OB	47.90229	-124.578807	20	40	1.19
2QOB4 40-60	1.15	0.77	0.14	0.64	OB	47.90229	-124.578807	40	60	1.19
Q1 0-18	1.09	2.31	0.13	2.18	OB	47.908922	-124.57558	0	18	1.15
Q1 18-40	0.55	1.38	0.07	1.31	OB	47.908922	-124.57558	18	40	1.15

Q1 40-60	0.44	0.62	0.05	0.56	OB	47.908922	-124.57558	40	60	1.15
Q1 60-83	0.43	0.74	0.05	0.69	OB	47.908922	-124.57558	60	83	1.15
Q1 83-102	0.24	1.27	0.03	1.25	OB	47.908922	-124.57558	83	102	1.15
Q1 102-123	0.19	1.12	0.02	1.10	OB	47.908922	-124.57558	102	123	1.15
Q2 0-20	0.18	2.12	0.02	2.09	OB	47.905291	-124.580385	0	20	0.73
Q2 20-39	0.24	0.80	0.03	0.77	OB	47.905291	-124.580385	20	39	0.73
Q2 39-61	5.53	0.76	0.66	0.10	OB	47.905291	-124.580385	39	61	0.73
Q2 61-94	2.88	0.88	0.35	0.53	OB	47.905291	-124.580385	61	94	0.73
Q2 94-124	1.95	0.70	0.23	0.47	OB	47.905291	-124.580385	94	124	0.73
Q3 0-25	2.03	2.11	0.24	1.86	OB	47.902962	-124.582729	0	5	0.39
Q3 25-40	1.61	0.75	0.19	0.56	OB	47.902962	-124.582729	25	40	0.39
Q3 40-56	1.10	0.41	0.13	0.27	OB	47.902962	-124.582729	40	56	0.39
Q4 0-27	0.95	2.39	0.11	2.27	PB	47.91022	-124.62602	0	7	2.22
Q4 27-49	0.91	3.10	0.11	2.99	PB	47.91022	-124.62602	27	49	2.22
Q4 49-77	0.50	2.85	0.06	2.78	PB	47.91022	-124.62602	49	77	2.22
Q4 77-120	0.61	2.89	0.07	2.82	PB	47.91022	-124.62602	77	120	2.22
Q4 120-160	0.61	1.93	0.07	1.86	PB	47.91022	-124.62602	120	160	2.22
Q5 0-22	0.43	2.59	0.05	2.54	PB	47.912361	-124.620809	0	22	0.85
Q5 22-44	0.39	1.96	0.05	1.91	PB	47.912361	-124.620809	22	44	0.85
Q5 44-67	0.18	1.12	0.02	1.10	PB	47.912361	-124.620809	44	67	0.85
Q5 67-100	0.38	0.61	0.05	0.57	PB	47.912361	-124.620809	67	100	0.85
Q5 100-124	0.31	0.50	0.04	0.46	PB	47.912361	-124.620809	100	124	0.85
Q5 124-149	0.22	0.47	0.03	0.45	PB	47.912361	-124.620809	124	149	0.85
Q5 149-172	0.15	0.50	0.02	0.48	PB	47.912361	-124.620809	149	172	0.85
Q5 172-200	0.20	0.40	0.02	0.38	PB	47.912361	-124.620809	172	200	0.85
Q5 200-233	0.27	0.41	0.03	0.38	PB	47.912361	-124.620809	200	233	0.85
Q6 0-24	0.27	2.82	0.03	2.79	PB	47.915427	-124.617094	0	24	1.11

Q6 24-47	0.15	2.03	0.02	2.01	PB	47.915427	-124.617094	24	47	1.11
Q6 47-82	0.15	1.17	0.02	1.15	PB	47.915427	-124.617094	47	82	1.11
Q6 82-96	0.25	0.77	0.03	0.74	PB	47.915427	-124.617094	82	96	1.11
Q6 96-124	0.30	0.79	0.04	0.75	PB	47.915427	-124.617094	96	124	1.11
Q6 124-150	0.12	0.55	0.01	0.53	PB	47.915427	-124.617094	124	150	1.11
Q6 150-200	0.08	0.48	0.01	0.47	PB	47.915427	-124.617094	150	200	1.11
Q7 0-24	0.16	1.30	0.02	1.28	PB	47.917837	-124.617589	0	24	0.73
Q7 24-45	0.06	0.44	0.01	0.43	PB	47.917837	-124.617589	24	45	0.73
Q7 45-64	0.01	0.35	0.00	0.35	PB	47.917837	-124.617589	45	64	0.73
Q8 0-21	0.07	1.52	0.01	1.51	PB	47.918579	-124.618023	0	21	0.76
Q8 21-48	0.10	0.66	0.01	0.65	PB	47.918579	-124.618023	21	48	0.76
Q8 48-72	0.24	0.44	0.03	0.41	PB	47.918579	-124.618023	48	72	0.76
Q8 72-98	0.12	0.62	0.01	0.60	PB	47.918579	-124.618023	72	98	0.76

Table A-2: Radiocarbon data for Quileute mouth samples dated by DirectAMS. 95.4% low and high values refer to the low and high values of the 95.4% probability distribution for the calibrated age. F14C refers to the 14C fraction of the sample. 14C BP refers to the uncalibrated radiocarbon age provided by DirectAMS. 1 sigma errors represent uncertainty estimates for various values.

Sample ID	**95.4% low (yr BP)**	**95.4% high (yr BP)**	**mean (yr BP)**	**1 sigma error mean (yr BP)**	**median (yr BP)**	**DirectAMS sample code**	**F14C**	**1 sigma F14C**	**14C BP**	**1 sigma error 14C BP**
Q1 102-123	7959	7845	7902	33	7896	D-AMS 018936	0.4147	0.0015	7071	29
Q2 94-124	8716	8451	8585	63	8583	D-AMS 018937	0.3784	0.0022	7806	47
Q5 200-233	11395	11224	11299	56	11287	D-AMS 018938	0.2917	0.0014	9897	39